Grid Integration of Variable Renewable Energies in Ghana: Assessment of the Impact on System Stability

A thesis approved for the academic degree of

Doktor der Ingenieurwissenschaften (Dr.-Ing.)

at the

Faculty of Electrical Engineering and Information Technology

TU Dortmund University

by

Marilyn Winifred Asmah, M.Sc.
Dortmund

Supervisor:	Univ.-Prof. Dr.-Ing. Johanna Myrzik, Universität Bremen
Co-Advisor:	Univ.-Prof. Dr.-Ing. Christian Rehtanz, TU Dortmund University

Day of Oral Examination: 12.06.2023

Kurzfassung

Der Anteil an thermischer Stromerzeugung in Ghana beträgt derzeit mehr als 70% der gesamten installierten Leistung. Dies führt zu einem erhöhten Einsatz fossiler Brennstoffe, was den Staatshaushalt angesichts des derzeitigen Anstiegs der Stromerzeugung belastet. Um die Abhängigkeit des Landes von fossilen Brennstoffen zu verringern, wird der Stromerzeugungsmix durch erneuerbare Energien (EE) diversifiziert. Zu den laufenden Maßnahmen gehört das nationale Ziel, bis zum Jahr 2020 den Anteil an EE (hauptsächlich Photovoltaik und Windkraft) auf 10 % zu erhöhen.

Dennoch bringt die EE-Integration neue Herausforderungen (betrieblich und infrastrukturell) für das ghanaische Stromnetz mit sich, für die neuartige Maßnahmen erforderlich sind. In dieser Arbeit wird daher untersucht, welche Auswirkungen die EE-Integration auf das ghanaische Verbundnetz hat und inwiefern dessen Stabilität beeinflusst wird.

Die Analyse in dieser Arbeit beginnt mit der Entwicklung eines Modells des ghanaischen Übertragungsnetzes. Für dieses Modell werden Simulationsszenarien erstellt, welche verschiedenen Netzbedingungen für drei Jahre erfassen. Als erstes wird der aktuelle Zustand des Netzes und dessen Bereitschaft EE-Erzeugung aufzunehmen anhand statische Berechnungsmethoden bewertet.

Der Schwerpunkt dieser Dissertation ist die Untersuchung der Stabilität des ghanaischen Netzes bei zukünftigem Ausbau der EE. Um den Einfluss auf die Netzstabilität zu bewerten, werden Methoden zur Transienten und Spannung Stabilitätsanalyse eingesetzt. Außerdem werden durch Optimierungsmethoden die blindleistungsarmen Knoten im Netz festgestellt, die als Ausgangspunkte für die Stabilitätsverbesserungsmaßnahmen dienen.

Die Simulationsergebnisse zeigen, dass das Zielszenario (10% EE) das größte Risiko für sowohl statische als auch dynamische Spannungsstabilität darstellt. Die Transiente Stabilitätsanalyse belegt, dass das Netz über das Zieljahr hinaus instabil sein wird. Zudem weisen die Simulationsergebnisse daraufhin, dass eine Verbesserung der Systemstabilität durch die implementierten Maßnahmen erreicht wird. Schließlich kann mit dieser Arbeit gezeigt werden, dass die Integration von EE in Ghana „technisch“ machbar ist, solange die erforderlichen Netzverstärkungen und betrieblichen Änderungen entsprechend berücksichtigt werden.

Abstract

Thermal power generation in Ghana constitutes over 70% of the total installed capacity. This translates into an increased use of fossil fuel, which constrains the national budget considering the current rise in electricity production. To reduce the nation's dependence on fossil fuel, power generation mix is being diversified to include renewable energy (RE) sources. Efforts to achieve this involved a national target to attain 10% RE penetration (mainly PV and wind) by the year 2020.

Despite this ambition, the RE integration introduces new challenges (operational and infrastructural) in Ghana's network, to which novel measures are required. This research thus analyses the impact of RE generation on the national interconnected transmission system (NITS) and how its stability is affected.

The analysis in this dissertation begins with the development of a model of Ghana's transmission network using the DIgSILENT PowerFactory simulation tool. Simulation scenarios are created to capture diverse network conditions like different RE penetration levels, load demand and infrastructural expansion for three separate years. As one of the main objectives of this research, the current state of the network and its readiness to accommodate generation from RE is assessed using steady-state analyses.

Another focus of this work is the investigation of the stability of the NITS with RE. To this, transient stability analysis techniques in addition to static and dynamic voltage stability analysis techniques are used to evaluate the extent to which system stability is affected by the RE generation. Furthermore, methods of optimization are used to determine the reactive power deficient nodes in the NITS, which serve as the basis for the stability enhancement measures. The 'optimum' penetration level of RE in the NITS considering voltage and loading limits is also identified using optimization techniques.

The simulation results show that the target scenario is the most prone to both static and dynamic voltage instability. The transient stability analysis however reveals the post-target scenario to be unstable. The simulations and analysis additionally indicate that implementing the proposed measures indeed enhances the stability of the NITS. Finally, this research shows that RE integration is 'technically' feasible in Ghana as long as the required network reinforcements and operational changes are accordingly considered.

Dedication

To my grandmother, in loving memory

Acknowledgement

The six years of working on my PhD have been a very exciting and challenging part of my career (PhD) and personal life. I am convinced that it is the good Lord of Host who thus has sustained me and brought me this far. For these and all others, I am thankful for the breath and strength to complete this dissertation.

I would like to thank the Reiner Lemoine Foundation for the financial support in the first three years of my doctoral studies. I am utterly grateful also for the knowledge exchange and networking opportunities you offered me.

My appreciation goes to Prof. Dr.-Ing. Johanna Myrzik, whose supervision led to the completion of this doctoral dissertation. Thank you also for the opportunity you offered me to work in your team. To Prof. Dr.-Ing. Christian Rehtanz, I am not only grateful that you accepted to assess the thesis, but also for introducing me to a network of engineers and opportunities. It has really been a great time working under your supervision in the latter years of my PhD.

Sincere and profound gratitude goes to Dr.-Ing. Yuven Yerima (DIgSILENT GmbH) who not only served as a coach but a personal mentor during my doctoral studies. Thank you for the pep talks, family times and the countless modelling and scripting sessions. Special thanks also go to Dr. Joseph Essandoh-Yeddu (formerly of the Ghana Energy Commission), Ings. Rasheed Baisie and Benjamin Ahunu (of the Ghana Grid Company) for giving me access to valuable data on the Ghanaian power system. Thank you also for the fruitful discussions on Ghana's power system during and beyond my research stay in Ghana.

To my colleagues and friends at the ie3 institute, your comments, reviews, criticisms, and suggestions to the dissertation are no less underscored. To Baktash, Desmond, Rajkumar and all - this is a profound gratitude for your friendship and immense support during my PhD.

To my mother, sister, family members and friends, the social support you rendered has been immense and strong to carry me through challenging times. Lastly, to my husband Richard and kids Roi and Eli, you have always been great sources of inspiration for me while completing this work. Special thanks to you, Richard, for your unflinching role in keeping our home and taking care of the 'kiddies' for the many days and nights you spent without your Mama.

Contents

1 Introduction

1.1 The Ghanaian Power System

Electricity demand growth in Ghana is projected to increase beyond the estimated 10% annual load growth in the coming years. For instance, a coincident peak demand of approximately 2,800 MW was recorded for the year 2019, which represents a 12% increase in the 2018 peak demand value (2,500 MW) [1]. Similarly, the 2018 peak demand of 2,500 MW represented approximately 15.1% and 14.2% percentage increase over the peak demands for 2017 and 2016 respectively [2]. Power generation[1] in Ghana is mainly from hydro and thermal (crude oil, natural gas and diesel) sources, with respective percentage shares of 37.7% and 61.4% as at the end of 2018 [3]. The generation mix at the end of the year 2019 comprised 40.5% and 58.8% of hydro and thermal generation respectively [4]. The remaining percentage share accounts for imports and renewable power generation, which is currently only from photovoltaic (PV). Based on current generation expansion plans, thermal power generation is expected to increase to more than 66% of the projected total generation, while generation from hydro and PV reduce to 33% and 0.3% from the year 2020 onwards [3].

The current thermal-biased power generation in a developing country like Ghana increases the risks of economic adversities that challenge the viability and sustainability of local utility companies as well as general commercial operations in the country. A report from the Ghana Energy Commission indicates that approximately US$ 1.04 billion [2], which represents 1.6% of the 2019 national GDP[2] [5, 6], was the estimated annual cost of fossil fuels for thermal power generation [3]. Furthermore, about 20% of the required gas and 100% of all other fuels (light crude oil, LCO, heavy fuel oil, HFO and diesel) are imported [7], which increases the dependency of thermal generation on diverse external factors. Disruptions in fuel supply either locally or from imports increase the likelihood of power crisis, which hitherto has had damaging effects on the nation's economic growth. Fuel supply for thermal generation has been erratic in previous years due

[1] Power generation in Ghana was hydro-based until 2015. Due to sporadic rainfall patterns and the reduction in the annual rainfall for hydro generation which led to power crisis, several thermal plants have been commissioned into operation since 2016. The result is the current 'thermal-biased' power generation in the country.

[2] The GDP for the year 2019 was US$ 67.08 Billion

to damaged pipelines and uncleared financial agreements between trading parties (indebtedness to fuel suppliers) [3]. This has therefore affected the reliability of power supply and the efficiency of the entire power system since 2011. The availability of the hydro plants has also been lesser than expected due to insufficient water levels in the water reservoirs. The dependence on the nation's hydrological pattern results in seasonal changes in generation such as more hydro generation in the rainy season and more thermal generation in the dry season, when there is low water for hydro generation. Although Ghana boasts of sufficient installed generation, its dependence on only hydro and thermal sources [8] coupled with existing fuel supply unreliability, which renders most of the thermal units non-operational [1–3], [9] leaves only about 50% of the installed generation available for power generation [7].

Available generation in the national interconnected transmission system (NITS) is thus barely enough to meet the nation's demand, which in many cases has resulted in load shedding. To simultaneously deal with this problem and reduce the nation's dependence on fossil fuels, a Renewable Energy Act (Act 832) was passed in 2011 to govern "the development, management, utilisation, sustainability and adequate supply of renewable energy for generation of heat and power and for related matters." [10]. The forms of energy considered in the Act include wind, solar, hydro (less than 100 MW [11]), biomass and biogas [10].

In relation to power supply from renewable energies (RE), a national target was set to increase the share of RE in the national energy mix to 10% of the total installed capacity by the year 2020 [11, 12]. To achieve this target, diverse projects such as the development of grid-connected PVs and wind farm, mini-hydro and bio-fuel projects etc were proposed by both the government and private investors. More specifically, the government has put in place measures such as tax 'holidays', import duty exemptions, Feed-In-Tariff (FIT) scheme, Renewable Energy Purchase Obligations (REPO), etc [11] for RE projects in order to attract investors and foster the development of RE. A total of 785 MW PV and wind projects (see table 1-1) have therefore been proposed for integration into the Ghanaian power system till the year 2023. These will however be integrated directly into the transmission network due to the limited infrastructure and technical constraints in the distribution networks.

The Ghanaian power system, just like any other power system, is divided into the generation, transmission and distribution sectors managed by both government and private institutions. The power sector reform, which began in the early 1980s fostered major transformations by removing proprietorship barriers in all sectors

of the power system. The power sector reform introduced and allowed the participation of independent power producers (IPP) in a sector, which hitherto was solely owned and managed by the state. Through this reform, power transmission has been separated from the main power generation institution to allow fairness and introduce competition into Ghana's power market [13, 14].

1.1.1 The Generation Sector

The fossil fuel requirements of the thermal-based power generation in Ghana influence the location of the thermal power stations in the network. Most of the generating units are located along the coast in the south due to the proximity to fuel sources or fuel reception points for the ease of fuel transportation [15]. The location of the major load centres in the south also impacts the placement of generating stations in the network. Table 1-1 provides a summary of the generation units with their respective installed capacities, unit types, fuel used and locations in the country. A pictorial view of the sizes and locations of the generation units in the NITS is presented in Figure 1-1. Two modes of operation – combined and simple cycle operations are used for thermal generation in the NITS. The combined cycle (CC) plants (marked with asterix* in Table 1-1) employ a heat recovery steam generator (HRSG) to capture the exhaust gas to produce steam for power generation.

As seen from the table all conventional power plants except for the Bui generating station (GS) are located in the south. The Bui GS, which is the second largest hydro plant is currently the only available generation in the north. This generation unit is also a peaking plant which means it is only operational during the peak period or when system demand is high. Resultingly, there is no available generation in the north during the off-peak period. Existing loads in the north of the NITS are thus supplied with power from the south using long transmission lines. More than 70% of the proposed PV units will be located in the north due to higher solar irradiation and the availability of large expanses of land in the north.

The Volta River Authority (VRA), a state-owned institution, is currently the largest power producer in Ghana with 47% share of the total installed capacity. [3] The remaining 53% of the installed capacity is managed by the Bui Power Authority, BPA (with about 8% share) and other IPP.

[3] The share is made of approximately 52% and 48% hydro and thermal generation respectively

Table 1-1: Power Plants in the Ghanaian NITS [1, 2, 7]

Generating Unit	*Installed Capacity (MW)*	*Unit Type*	*Fuel Required*	*Location*
Akosombo GS	1,020	Hydro	Water	South-East
Bui GS	404	Hydro	Water	North-West
Kpong GS	160	Hydro	Water	South-East
*Takoradi Thermal Power Plant, T1**[4]	330	Thermal	Oil/Natural Gas	South-West
*Takoradi Thermal Power Plant, (T2)**	340	Thermal	Oil/Natural Gas	South-West
CENIT	110	Thermal	LCO/Natural Gas	South-East
Tema Thermal Plant 1, TT1PP	110	Thermal	Oil/Natural Gas	South-East
Tema Thermal Plant 2, TT2PP	80	Thermal	Oil/Natural Gas	South-East
*Sunon Asogli Power Plant (SAPP) I**	200	Thermal	Natural Gas	South-East
*Sunon Asogli Power Plant (SAPP) II**	360	Thermal	Natural Gas	South-East
CENPower	330	Thermal	LCO	South-East
Ameri	250	Thermal	Natural Gas	South-West
KTPP	220	Thermal	Oil/DFO	South-East
Karpower[5]	470	Thermal	HFO	South-East
Aksa	260	Thermal	HFO	South-East
Early Power	200	Thermal	Natural Gas	South-East
Total Generation	**4844**			
Proposed Plants to attain the 10% RE Penetration by the year 2020				
Ayitepa Wind	225	Wind	Wind	South-East
Ada Wind	50	Wind	Wind	South-East
GIC	50	PV	Solar	North-East
Green Electric	40	PV	Solar	North-East
Sankana	100	PV	Solar	North-West
Savanah	100	PV	Solar	North-East
Signik	50	PV	Solar	North-West
WhiteCap	100	PV	Solar	North-East
Windiga	20	PV	Solar	North-East
Ayitepa Solar	20	PV	Solar	South-East
TFI Solar	30	PV	Solar	South-East

[4] *: Combined Cycle Plants

[5] : The Karpower ship was originally (and at the time of modelling) located in the south-east but is currently located in the south-west.

1.1.2 The Transmission Sector

Power transmission in Ghana is realized through the NITS (see figure 1-1), which is connected to the transmission systems of the three neighbouring countries: Ivory Coast to the West, Burkina Faso to the North and Togo/Benin to the East.

The NITS consists of approximately 6,500 km [1] of transmission lines at three voltage levels; 330 kV, 161 kV, and 69 kV[6] (see figure 1-1). Although 161 kV is currently the main transmission voltage in the NITS, plans are underway to make 330 kV the main transmission voltage. The existing 330 kV lines are currently used to transport power from the generating units in the west to the load centres in the east. The 69 kV is used in the extreme east of the NITS due to the low demand and sparse nature of the loads in that part. The 225 kV transmission lines currently serve as the tie-line between Ghana and Ivory Coast. Interconnections from Ghana to Togo and Burkina Faso which are currently through 161 kV transmission lines, are being upgraded to 330 kV and 225 kV respectively under the West African Power Pool (WAPP)[7] [16, 17] scheme. The NITS is also equipped with 65 substations (bulk supply points, BSPs), which are used to distribute power to local consumers [1]. The transformer capacity as at the end of year 2019 amounts to approximately 9,000 MVA with a total of 123 transformers [1] at operating voltages of 330/161 kV; 161/69 kV; 161/34.5 kV; 161/11.5 kV.

The NITS is characterised by a longitudinal structure based on the country's geography and landscape. Owing to the location of thermal generating units mostly in the south and the uneven population density across the country coupled with its longitudinal structure, large distances are covered during power transmission with lines longer than 80 km. The transmission capacity (line loading limit) of such lines (lengths between 80 km and 320 km) is no more limited by the thermal capacity but by the voltage maintenance (voltage drop limits) [18]. Voltage maintenance therefore becomes very important in the efficient operation of the Ghanaian power system, which is currently managed using diverse reactive compensation devices.

[6] A peculiar feature of the NITS is the use of 69 kV voltages in the transmission network. These lines were originally intended to be 161 kV lines but are now operated at 69 kV due to the light loading in the part of the network.

[7] The West African Power Pool (WAPP) is an institution created by 14 of the 15 member States of the ECOWAS (Economic Community of West African States) to amalgamate the individual national power systems into a regional power system with the aim of fostering and easing electricity trade in the west-African sub-region.

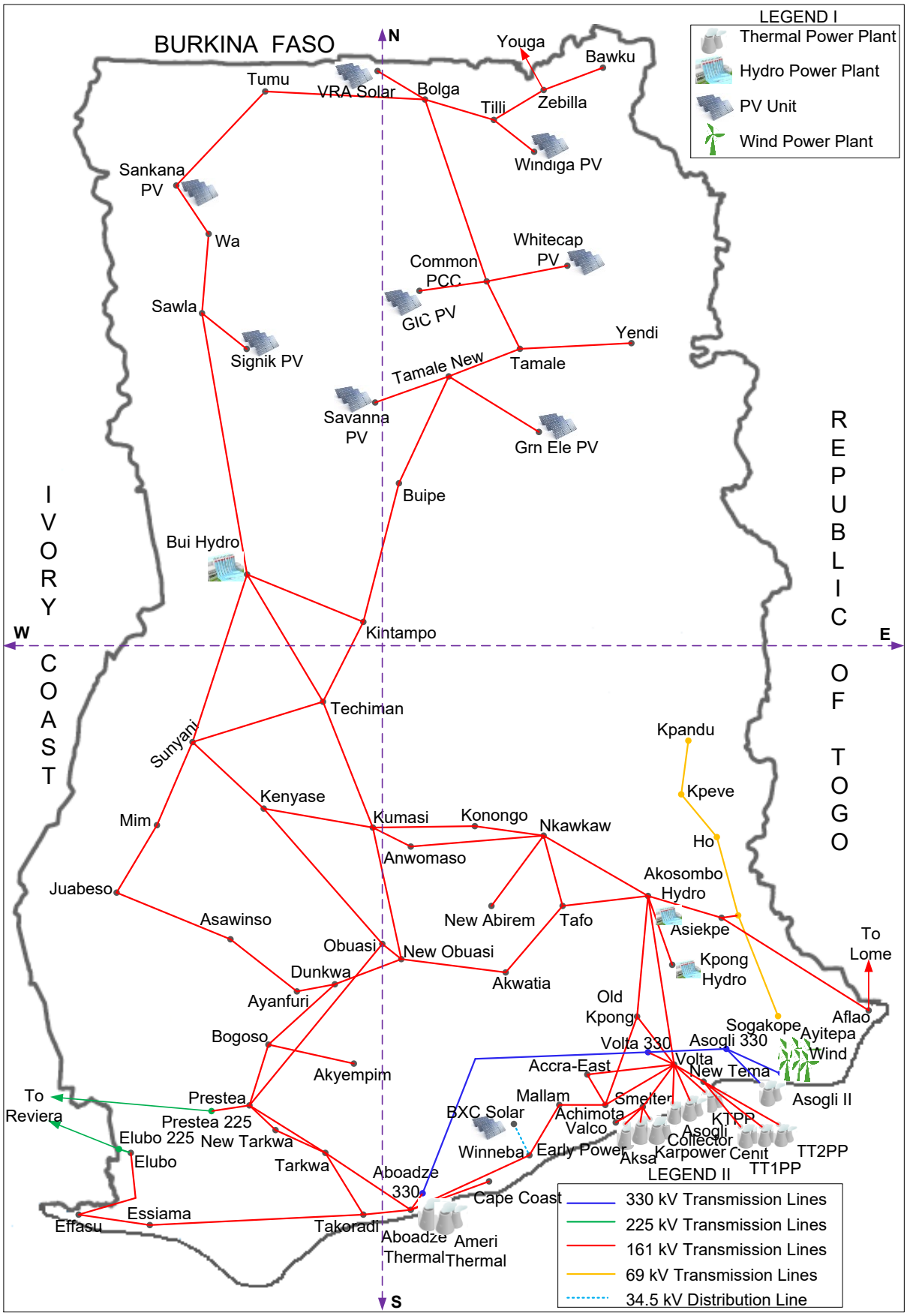

Figure 1-1: The National Interconnected Transmission System (NITS) of Ghana

Reactive power compensation in the NITS thus range from classic compensation devices such as fixed capacitors and shunt reactors with total capacities of 310 MVAr and 230 MVAr respectively to FACTS devices, which is currently only a 40 MVAr Static Synchronous Compensator - STATCOM [1].

1.1.3 The Distribution Sector

Power distribution in Ghana is managed by two state distribution companies - the Electricity Company of Ghana (ECG) and the Northern Electricity Distribution Company (NEDCo) – and a private-owned distribution company, the Enclave Power Company (EPC), which has been in operation since 2009 [19]. ECG operates and manages the distribution networks in nine of the 16 regions in the country; Ashanti, Ahafo, Central, Eastern, Greater Accra, Volta, Western, Western North and Oti Regions with a net demand of 62.4% of the total system peak [1]. The distribution networks in the remaining seven regions; Bono East, Bono Region, Upper East, North East, Upper West, Northern and Savannah [1] and the northern parts of the Ashanti, Oti, and Western North Regions [20] are managed and operated by the NEDCo with a total demand of 7.5% [1]. The EPC, with a demand of 1.5% of the total system peak is responsible for power distribution in the Tema Free Zone Enclave in the Greater Accra region [7, 19]. The remaining 28.6% accounts for power exports to Togo/Benin and Burkina Faso, loads in the mines and VALCO[8] as well as losses [1]. The distribution network demand accounts for about 80% of the total system demand [1].

1.1.4 Institutional Framework

Ghana's power system comprises diverse bodies that play various roles in its management and day-to-day operations. Nine different institutions under the office of the president as presented in figure 1-2 are currently involved in the power sector with functions such as policy making, planning and daily grid operations. The institutions include the Ministry of Energy, Energy Commission, Public Utility Regulatory Commission, Independent Power Producers, Volta River Authority, Bui Power Authority, Ghana Grid Company, Electricity Company of Ghana and the Northern Electricity Distribution Company [21]. All institutions are state-owned except the IPPs, which consist of several private-owned generating companies with and without government shares.

[8] VALCO, the Volta Aluminium Company is a government owned aluminium smelter in Ghana with an estimated demand of 3% of the total system demand.

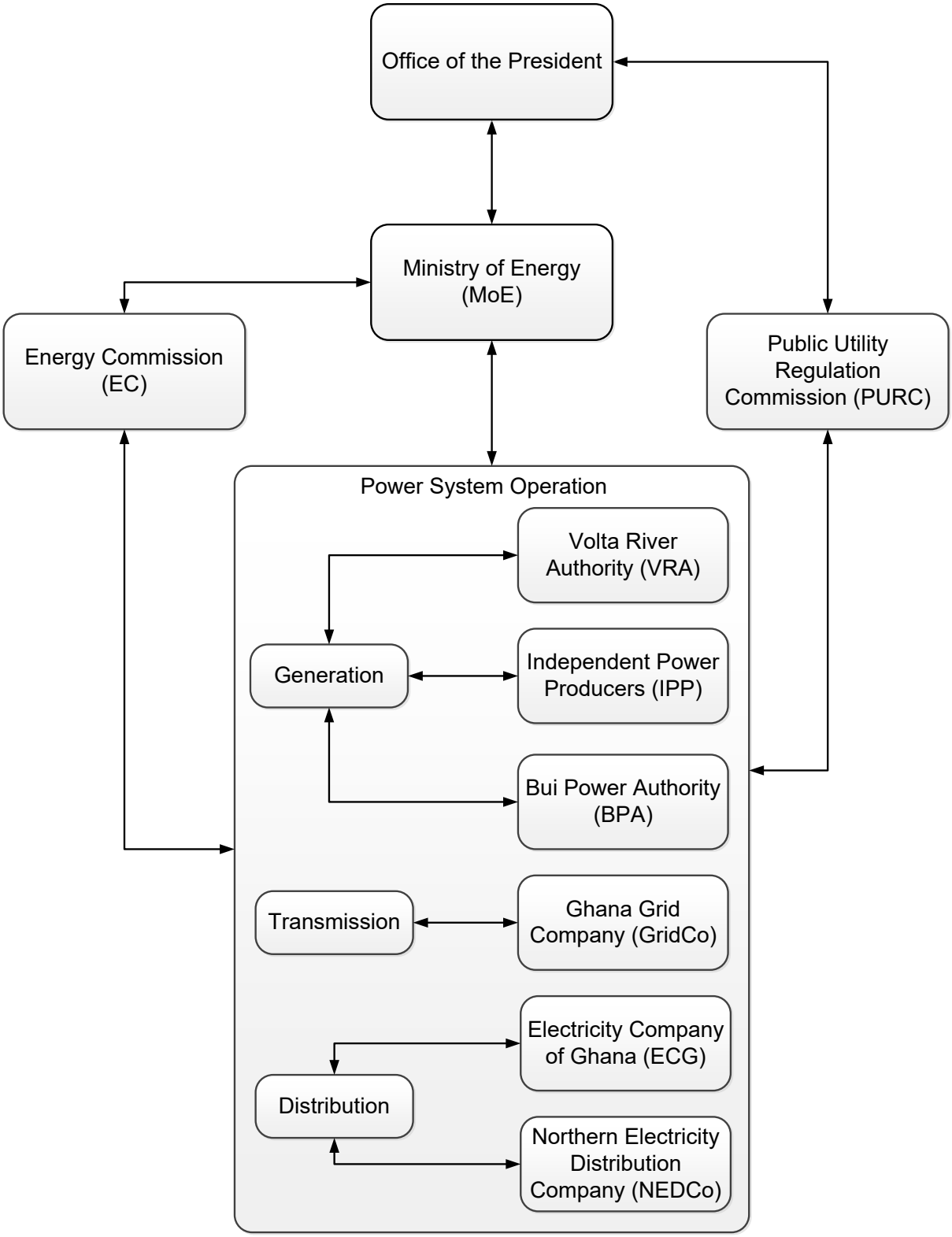

Figure 1-2: Overview of the Organisational Structure of Ghana's Power Sector

Ministry of Energy: The Ministry of Energy (MoE) is a Government of Ghana ministry created for the sole responsibility of policy formulation, implementation, monitoring and evaluation. It is also responsible for supervising and coordinating activities in all energy sub-sectors [22]. The MoE has an additional function of serving as the liaison between the Government and people of Ghana [21].

Energy Commission: Ghana's Energy Commission (EC), set up in 1997 under the Energy Commission Act (Act 541) is mandated with the regulation, management, development and utilization of energy resources in the country. The EC serves as the government advisor on energy related issues [23] and is thus known as the nation's technical regulator and energy policy advisor. The EC is also responsible for issuing licenses to developers of energy in the country [24].

Public Utility Regulatory Commission (PURC): The PURC is an independent state institution that regulates utility services such as water and electricity. It provides guidelines for electricity rates and other utility charges. Pricing and charges in the generation, transmission and distribution sectors are regulated by the PURC.

Volta River Authority (VRA): The Volta River Authority was instituted by the Government of Ghana in 1961 to solely generate, transmit and distribute power in the country. Through the power sector reform however, this mandate is now restricted to only power generation [25]. Approximately 47% of the country's installed generation capacity (2,260 MW) is operated by the VRA [1].

Bui Power Authority (BPA): The BPA operates the Bui Hydro GS, one of the three main hydro generating stations in the country [26], with about 26% share of the total hydro generation capacity and 8% of the total installed generation capacity. The Bui hydro generating station is the second largest hydro generating unit in the country.

Independent Power Producers (IPP): The power sector reform in 2005 allowed the introduction of IPPs into Ghana's power system. The IPPs are private owned companies that generate and sell power to the public. About ten IPPs exist in the country, which currently only operate thermal generating units, which make up about 45% of the total installed generation capacity.

Ghana Grid Company (GridCo): GridCo was established in accordance with the requirements of the power sector reform to be an independent entity responsible for the transmission of power in the country. The exclusive operation, planning and management of the NITS remains the responsibility of GridCo [27].

Electricity Company of Ghana (ECG): The ECG is an entity responsible for the distribution of electricity to consumers in the southern electricity distribution zone (SEDZ) of the country [1]. It is the nation's largest distribution company serving more than 60% of the total system demand.

Northern Electricty Distribution Company (NEDCo): NEDCo was originally established by the VRA to distribute power in the northern regions. However, through the power sector reform, it is now a wholly owned subsidiary of the VRA [28]. NEDCo's current operational area covers about 64% of the national geographic area [1, 28] and about 7.5% of the total demand [1].

1.2 Research Background

The longitudinal structure of Ghana's power system, the country's landscape and natural distribution of resources present diverse challenges, which adversely affect power system operations. The longitudinal structure and the non-uniform distribution of load and generation (see Figure 1-3), creates the need for long transmission lines from the generation units to the various load centres. As the transmission capacity of such long lines is not limited by the thermal capacity of the lines but by the voltage drop limits [18], the part of the network with the longer transmission lines is often plagued with voltage problems such as higher voltages in less populated areas and low voltages in dense areas. During light load conditions, as is the case in the north [29], (due to lower economic activities), the capacitances on the line increase more than the inductance resulting in high voltages at the end of the line. This is reflected in the extreme high voltages at the end of the long transmission lines in the north [29], which require additional reactive compensation to deal with. On the other hand, the fast-pace economic and industrial activities in the south of the country have contributed to increased loads with very high demand and utilization of the transmission lines in the south resulting in low voltages. The high utilization in the dense part of the network again leads to transmission line and equipment overloads, which are recorded on regular bases in the network. Violations of both the upper and lower voltage limits are therefore recorded even during normal operation of the NITS. Existing poor customer-end power factors and insufficient reactive power compensation contribute to worsening the existing voltage violations [2]. Maintaining voltages within the prescribed voltage range is important in the day-to-day operation of the NITS. Figure 1-3 illustrates the location of the major loads and the generating units in the NITS.

Although some measures have been put in place to manage the constraints in the NITS, these have not been adequate to fulfil the operational requirements specified by the national grid code. Frequent load shedding and disconnection of loads with long-term effects on system stability and potential system-wide blackout are the consequences of these operational constraints, which are regularly experienced in the NITS.

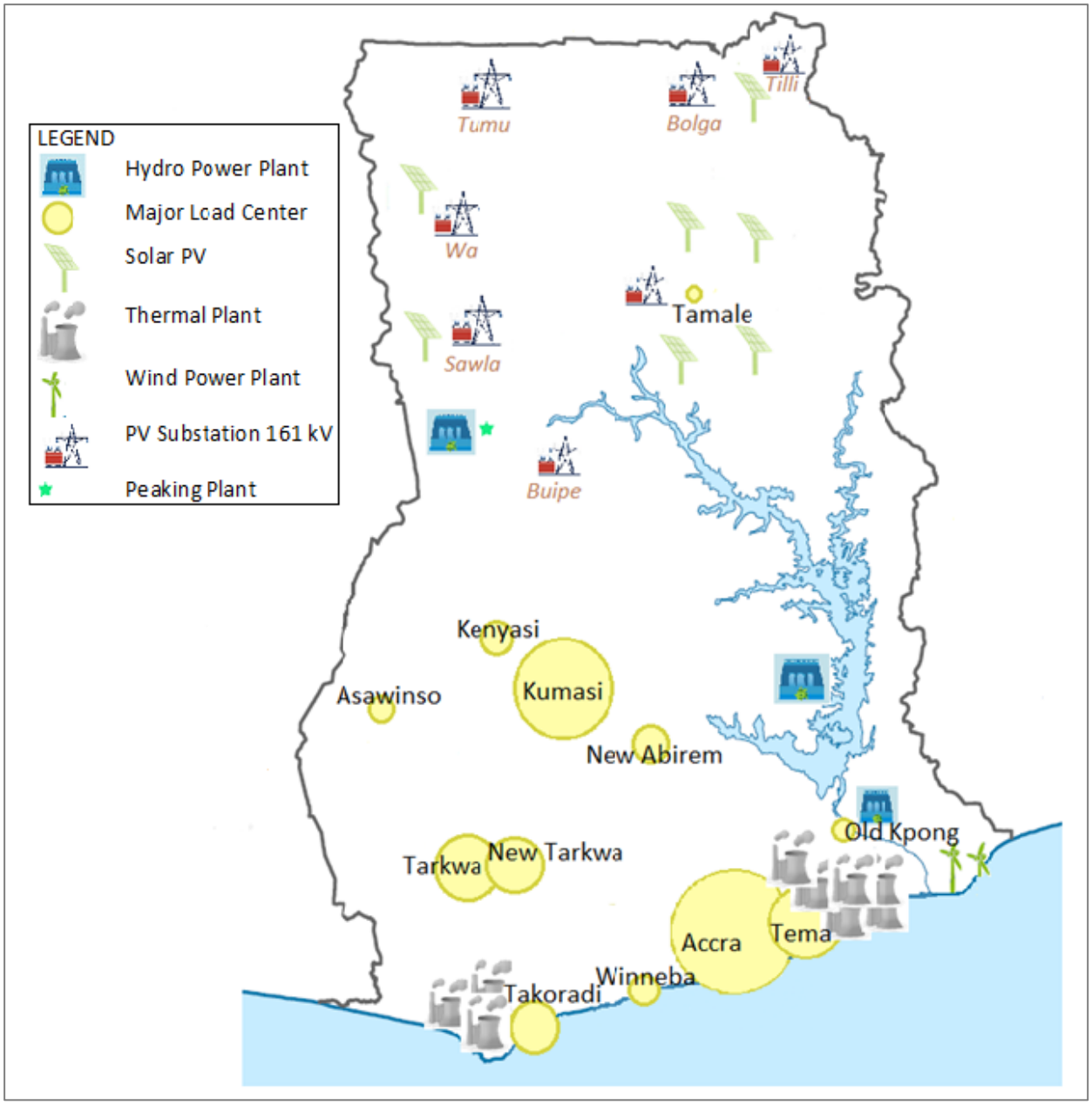

Figure 1-3: Generation and Demand Distribution in NITS

Furthermore, based on the natural distribution of resources in Ghana, higher solar irradiation is available in the north of the country where the existing demand is low (largest load is estimated to be only about 3% of the largest load in the NITS).

Despite, the availability of large expanse of lands in the north makes the north suitable for the installation of the PV units. The introduction of PV units in the north therefore creates an opportunity also for loads in the north to be served locally. However, with majority of the load concentrated in the south (see Figure 1-3), power generation from PVs in the north will require an increased percentage of PV generated power to be transported to the load centres in the south, where demand is higher. This alters the original unidirectional power flow from the 'south to the other parts of the network' to a bidirectional flow, where power flow is not only from generation units in the south but also from the north. The bidirectional flow raises concerns on the reliability and quality of the transmission infrastructure especially in the north, which hitherto had less and underdeveloped transmission infrastructure.

RE integration in the NITS is enabled by various sections of Ghana's RE Act 832. Sections 26 and 30 of the Act for instance describe respectively the 'Renewable Energy Purchase Obligation, (REPO)' and "connection to transmission and distribution system" [10]. These offer connection priority to RE generators in the power system and mandate distribution utilities and bulk customers to procure a specified percentage of RE generated energy. The fulfilment of these sections requires a reduction in power generation from the conventional units during periods of 'high' PV generation in order to safely meet the demand without the risk of over-generation, which has detrimental effects on system stability. A reduction in power generation from the conventional units results in a reduced system inertia and the reactive power contribution of such units, which leads to a decrease in the available reactive power with a subsequent effect on voltage and transient stability.

The operational challenges introduced by the RE integration require a thorough investigation of their effects on system stability. This is particularly important because the RE units will be directly connected in the transmission system, where faults generally have greater impacts than in the distribution system [30]. The extent to which renewable power generation affects the grid will be evaluated in this thesis with the aid of network simulations. The appropriate mitigation measures, which will ensure the secure and stable operation of the NITS with a higher share of RE will also be investigated. To this, scenarios will be developed to consider changes in the network such as new generating units, load increase and transmission infrastructure upgrade, etc for specific study years.

1.3 Research Questions

As part of measures to ensure the successful integration of RE into Ghana's NITS, this research seeks to evaluate the impacts of the renewable power generation on the stability of the NITS. This research work thus aims at answering the following research questions:

1. **To what extent can the current power system accommodate renewable power generation?**
    a. What is the operating condition of the current network?
    b. What potential bottlenecks exist in Ghana's NITS?
    c. What measures can be taken to improve the identified bottlenecks?
    d. What operational and structural changes are required in the network for the RE integration?
2. **How does the RE integration affect grid stability?**
    a. To what extent does the RE integration lead to instability?
    b. What is the optimum RE penetration level required to maintain grid stability?
    c. What measures need to be taken to enhance grid stability?

1.4 Research Contributions

This research brings to light new evidence on existing issues in Ghana's power system. The results of the thesis provide valuable information to power system operators and stakeholders in Ghana's energy sector on the effective integration of RE in the power system. The proposed strategies for the successful grid integration of RE in Ghana will also be beneficiary to other countries in the early stages of the RE integration especially in the sub-Saharan Africa as well as countries with comparable network features. The analyses presented in this research offer insights into the operational changes the grid integration of RE introduces in the Ghanaian power system. The outcome of this research also forms part of the technical documentation of the RE integration in the NITS as part of the RE development in Ghana. More specifically, the results of this work are expected to provide valuable contributions in the following aspects:

- The development of a network model of Ghana's transmission system, which is suitable for both static and dynamic analysis. The network model serves as a benchmark for diverse research (presently and in the future) involving the modelling and analysis of Ghana's NITS as well as other networks with similar characteristics (longitudinal structure, uneven load distribution, limited network infrastructure, voltage issues and also in the early stages of the RE integration, etc.). The developed model and the analysis carried out make this research the first of its kind in the country.
- Assessment of the technical feasibility of the RE integration in the NITS. Through various analysis, this research determines clearly whether or not the network is able to accommodate RE. The research also provides a framework of measures to be taken to enhance the network for the RE integration. The results of the research have already contributed to the changes in the RE project allocations in Ghana. New RE capacities in Ghana are now procured through renewable energy auctions and competitive bidding programmes.
- Optimization methods are proposed for identification of the optimal placement and sizing of reactive power compensation devices as well as the optimum share of RE the network can accommodate considering the current technical constraints such as voltage limits, transmission line loadings and power losses.
- Proposal of novel measures for the improvement of system stability, which suits the characteristics of the NITS and are tailored to fit the economic and technical constraints in the Ghanaian network.

1.5 Thesis Outline

The introduction to the dissertation in chapter 1 offered an overview of Ghana's power system with the corresponding sectors. The research motivation, which highlights the research background and serves as the foundation of the research was also presented. The research questions and scientific contribution of the thesis conclude chapter 1. Chapter 2 presents the literature review with a detailed current state of the art of research and a brief research gap analysis.

The modelling of the NITS with its components is presented in chapter 3. The network model is developed using real data of Ghana's power system. The

national electricity grid code and the renewable energy sub-code for NITS connected renewable energy power plants are introduced and briefly reviewed in this chapter to highlight the allowed limits for voltages, loadings, etc. The development of the study scenarios that consider different network conditions is also presented in this chapter.

Chapter 4 focuses on the steady-state analysis performed in this research. Load flow analysis is performed to identify the bottlenecks that exist in the NITS. The appropriate and prospective corrective measures for the bottlenecks are further proposed. The contingency analysis is subsequently carried out to ascertain the (n-1) reliability of the network and also identify the critical transmission lines. The effects of different combinations of RE generation (as a result of weather changes) are further investigated in this chapter.

The stability analysis is presented in chapter 5. Voltage and transient stability analysis are considered preceded by a brief overview of the concept of power system stability. P-V and Q-V curves are used to assess the static voltage stability of the NITS with different RE penetration levels. The dynamic voltage stability analysis is carried out using time-domain analysis (RMS simulations) for the loss of load, generation and transmission line. The network's ability to respond to large disturbances is also investigated in the transient stability analysis. Novel measures to enhance the stability of the NITS are discussed in chapter 6. The optimum location and sizing of FACTS devices as well as the optimum RE penetration level are determined using the genetic algorithm method of solving optimization. Chapter 7 concludes the dissertation with a brief summary of the research and also highlights the limitations of the thesis. Suggestions and recommendations for future research work, which fall within the scope of this thesis are also presented.

2 Research Gap Analysis

With increasing shares of RE being integrated into power systems world-wide, the need to address the challenges associated with the RE integration also increases. Due to its complexity and comprehensiveness however, the topic of grid integration of RE has been investigated focussing on aspects such as the impacts on power system parameters as well as implementation strategies for individual countries.

This chapter reviews some existing literature and identifies the gaps in research, which will be addressed in this thesis. Aspects of the topic considered include the grid integration of RE in sub-Saharan Africa, the methods of analysing stability and the effects of RE on system stability as well as measures to improve system stability. The deductions made from the research gap analysis are summarised at the end of the chapter.

2.1 Grid Integration of RE in Sub-Saharan Africa

The researches of Elombo et al. [31, 32] review the grid integration of wind energy in Namibia. The impacts of penetration levels and the point of connection of wind generators in the sub-transmission network are investigated. To this, the characteristics of two wind generator technologies: the direct-driven synchronous generator (DDSG) and doubly-fed induction generator (DFIG) are compared to ascertain their relative performances. The review of the wind generator technologies reveals that DDSGs have higher voltage stability limits than DFIGs due to their peculiar characteristics. While the DDSG is equipped with external excitation for additional reactive power control, the DFIG generally absorbs reactive power from the network, which reduces the available reactive power and leads to voltage instability. The use of DFIG thus creates the need for additional reactive power compensation within the vicinity of the wind generator. Simulation results indicate that wind generators positioned closer to conventional generating units have severe impacts on the transient stability of the network than wind generators farther away. This leads to the conclusion that wind generators farther away from conventional generating units is beneficial for the stability of the network. The researches further investigate the impact of automatic voltage regulators (AVR) and recommend them for improving the transient instability that arise from the increasing penetration levels of wind generators.

The research of Bello et al. [33] reviews the planning process for RE integration in South Africa and proposes a standardized concept for the planning, design and operation of distribution networks in the country using the SMART Grid approach. Expected planning limitations and technical issues associated with the RE integration in the South-African network are highlighted. Violation of the steady-state voltage limits, increased equipment thermal ratings, increased faults levels from RE generating units, rapid voltage change and transient instability are reviewed, to which standardized approaches using smart grid are proposed.

The German experience of the grid integration of RE sources is discussed in the research of Buchholz and Sassnick [34]. The research highlights various plans to integrate different percentages of RE in the German power system with different timelines. The economic incentives and legalities of network connections and operation required for the RE integration are presented in the research. The authors emphasize that the high financial gain derived from RE power generation in Germany through the diverse incentives offered by the state is among the main factors for the rapid expansion of the RE sector. Challenges associated with the integration of large-scale wind power in the German transmission network are identified to be the variability of wind energy, the need for additional transmission capacity and the behaviour of wind generators during faults. Precise weather forecasts and special wind energy prediction tools are proposed to help deal with the variability of wind energy. Grid expansion, which is proposed for the transmission system is for instance also restricted by legal difficulties and prolonged processes in obtaining the appropriate permissions. As solutions currently exist for all possible challenges of the RE integration in Germany, the authors conclude that unlimited shares of RE can be integrated as long as given guidelines are adhered to.

The research of Cochran et al. [35] reviews the integration of variable RE (VRE) sources (solar and wind) in different countries across the globe with different markets and power systems. The research summarises the approaches used in countries like Australia, Denmark, Germany, Ireland, Spain and the United States of America in the effective integration of VRE sources. The research concludes that although there is no one-size-fits-all approach, each of these countries has crafted individual policies, market designs and system operations, which all revolve around five major points namely system operation improvement; developing enabling rules for system flexibility; public engagement; coordinated and integrated planning and access expansion to different resources.

In [36], Enslin investigates the impact of the grid integration of RE and proposes a combined effort solution on three main levels, gathering experiences from major utility companies and system operators in the United States of America. The research confirms that the remote locations of the renewable resources introduce unique challenges in the power system to which additional transmission capacity is required. Challenges introduced by the RE integration could be managed with traditional planning and operational measures as long as penetration levels remain between 10 – 15%. A dramatic change in system planning and operation is however required at penetration levels above 20%. Grid integration of RE at 'substantial' levels require the consideration of the steady-state and dynamic properties of the network with the available static and dynamic reactive power compensation. Studies are thus required to analyse the n-1 state, short-circuit, transient and voltage stability, power quality and electromagnetic transients of the network. Studies and experience however indicate that the availability of adequate conventional generating units to provide balancing power and precise load following in the power system is necessary for the successful integration of RE. Three major planning and operational solutions proposed for the integration of high penetration levels of RE include a) diverse generation mix in the power system, b) advanced transmission facilities such as flexible ac transmission system (FACTS), high-voltage direct-current (HVDC) transmission and fast responsive energy storage and c) demand response options like smart grid, demand-side management (DSM) and distributed energy storage. The research concludes that although experiences in other parts of the world are good examples to learn from, they may not necessarily be 100% appropriate for other countries due to the specific grid designs and load.

2.2 Methods of Improving System Stability

In the research of Essilfie et al [37], the use of Static VAR Compensators (SVC) to improve the stability of the Ghanaian power system is investigated. Small-signal stability and contingency (line and generator) analysis were carried out to compare the behaviour and response of the SVC and fixed compensator. While the line contingencies were performed on three major transmission lines in the north, middle and south of the network, the generator contingencies were carried out on generators from the three main generating stations. The continuation power flow (CPF) method was used to develop P-V curves to assess the static voltage stability of the network. The results indicate that a higher loadibility limit was

achieved with the SVC in all scenarios considered. The installation of the SVCs (at different points in the network) improved the stability of Ghana's power system and complemented one another during contingencies in the north and south. Contingencies in the mid part of the network were found to produce a counterreaction of the SVCs against one another. Some voltage 'critical' points in the network also did not react to the SVC which call for further analysis as the authors suspect the SVCs could not regulate the voltages at these points.

The effect of Static Synchronous Compensator (STATCOM) on the voltage stability of the Ghanaian power system is assessed in [29]. With prior information on the vulnerability of the northern part of the network to voltage instability, the proposed STATCOM was installed in the north and its effect on the overall system stability assessed. The effect of the STATCOM on the tie-line between Ghana and Burkina Faso, which is in the north is also investigated. The northern part of the network is identified to be voltage vulnerable due to its low load and very long transmission lines. The behaviours of the STATCOM and fixed compensator were compared during both line and generator contingencies. The effect of the tuning status of the STATCOM on its performance and the voltage stability is investigated using P-V curves. The results indicate that in addition to the STATCOM controlling the voltages of busbars within its proximity better than those far away, the voltage stability margin of the network was improved. A loadability limit of more than 20% was achieved with the STATCOM during both normal and contingency conditions. On the other hand, a loadability limit of only 6% was achieved with the fixed compensator for normal operating conditions while voltage collapse occurred during contingency. The proper tuning of the STATCOM also contributed to an optimum voltage control in the network. The authors conclude that the tie-line influences the loadability of the entire network as the receiving end of the bus has a relatively low voltage. Owing to the length and complexity of the tie-line, the voltage stabilizing effect of the STATCOM could not be confirmed, hence the need for further investigation on the tie-line.

The use of power system stabilizers (PSS) and AVR in improving the Chinese power system is presented in the research of Fang et al [38]. An experiment was performed by installing PSS on some generators and it was evident that the oscillatory stability was much improved. With the PSS in service, the theoretical maximum power transfer of the network was obtained. Without the PSS however, an AVR with a very high gain was required to keep the terminal voltage constant and increase the transient stability in order to achieve the theoretical maximum power transfer. As AVRs with very high gains tend to cause oscillations, the

combination with PSS proves to increase the maximum power transfer and reduce the oscillations. Simulation results further show that in addition to increasing the maximum power transfer, all swing modes were significantly damped with the PSS in service. The authors conclude that the installation of the PSS with the AVR not only improves system stability but also results in great economic benefits to the power system.

In [39], Qiao et al. investigate the effects of FACTS devices in a 12-bus benchmark power system with a high share of wind power generation and identifies the corresponding challenges in system operation. Challenges identified include voltage regulation problems, transient instability, power oscillation damping and power flow control. Two FACTS devices – the Static Synchronous Compensor (STATCOM) and Static Synchronous Series Compensator (SSSC) are proposed as solutions to the operational problems. Apart from providing dynamic voltage and active power control, these FACTS devices relieve transmission congestion and improve transient stability and power oscillation damping. The voltage support provision of the STATCOM improves the capability of the wind farm to ride through faults, which translates into uninterrupted system operation. The research concludes that FACTS devices are effective in providing dynamic voltage control for wind generating units, dynamic active power control for transmission lines while improving transient stability and relieving transmission congestion.

2.3 Impact of RE Integration on Grid Stability

The research of Eftekharnejad et al. [40] studies the impact of different penetration levels of PV on the steady-state voltage and transient stability of a large interconnected transmission system. A generic network model, which represents a portion of the Western U.S. interconnection is used for the analysis. While the lack of reactive power support is one of the main issues with high PV penetration, countries like Germany have allowed the use of distributed generation (DG) in voltage regulation as a means of managing the reactive power deficit. To mitigate the voltage problems caused by the high PV penetration, preventive measures like switching off capacitive shunts or adjusting the voltages of conventional generating units are enforced. Simulation results revealed that voltage and frequency oscillations in the network were well damped in the case of 20% PV penetration. The case with no PV however showed rotor instability and poorly damped voltage oscillations. The research draws the conclusion that

the grid integration of RE has both beneficial and detrimental impacts on the steady-state and transient performance of the network. Factors such as the penetration levels, type of disturbance, fault location and system topology are important factors that determine the level of impact on the network.

The impact of RE integration on voltage stability is investigated in the research of Toma and Gavrilas [41]. The Continuation Power Flow (CPF) method is employed to develop P-V curves to assess the static voltage of IEEE 14-bus test system. For the analysis, three different study cases are developed, which reflect different wind penetration levels. Contingencies were simulated to investigate the n-1 state of the network for the investigated study cases. Simulation results indicate that with increasing wind penetration, the stability limit of the network decreased as the system lost stability at lower loading values. The stability limit of the system under contingencies was as expected lower than in the case without contingencies. The research concludes that the grid integration of RE could have a negative impact on the voltage stability of the network depending on existing technical constraints.

The transient stability of a power system (simple test model) with large-scale wind power is analysed in the research of Pingping et al. [42].The stability analysis is carried out under two voltage control strategies – fixed power factor and fixed voltage. Single-phase-to-ground and three-phase faults are simulated in the network, which reveal that operating the wind generators in the fixed voltage control mode is beneficial in regulating the voltages at the stator terminals due to the available reactive capability. No reactive power support is provided in the fixed power factor mode, which leads to the DFIG absorbing reactive power from the system during fault and delaying the post-fault voltage recovery. The reactive capability of the DFIG in the fixed voltage mode showed improvement in the fault-ride-through and transient stability characteristics. The research concludes that the reactive power control of the DFIG can contribute to maintaining the voltage at the wind plant during a voltage sag depending on the control mode and as long as the DC voltage of the DFIG is within the given limits.

The research of EL-Shimy et al. [43] investigates the impacts of large scale wind power on the transient and dynamic voltage stability of the power system using the IEEE 9-bus system. The maximum penetration level required to ensure stability (voltage and transient) is determined by considering different penetration levels of wind power. The effect of a Static Var Compensator (SVC) on network stability is also analysed. The presence of the SVC in the network resulted in a

prolonged settling time of the power angles, which in effect is a reduction in the system damping. Both transient and voltage instability were observed when the penetration level was increased beyond 77%, due to the insufficient reactive power in the network. The research concludes that despite the increased settling time of the power angles, the network was found to be both voltage and transient stable.

The research of Bueno et al. [44] presents an assessment of the stability of transmission systems with large utility-scale PV units (USPVU) using a generic model. The transient and small-signal stability are analysed in a network with real loading conditions and high PV penetration levels. For the small-signal stability analysis, the eigenvalues of the network are calculated to identify the critical modes, which are used as the basis for the transient stability analysis. Analysis of the small-signal stability shows that the criteria for dispatching and committing conventional generating units by USPVUs play a significant role in the system behaviour. Thus, it is important to keep the 'critical' conventional units in service as they can be beneficial in reducing the negative impacts of the USPVUs. The transient stability analysis indicate that the voltage support provided by reactive current during voltage sags in USPVUs contribute to improving the voltage profile of the network. The fault-ride-through capabilities of the PV units also decrease the effects of the USPVUs on system stability. The research concludes that the unit commitment and dispatch strategies as well as the protection/control strategies are critical determinants for the (oscillatory) stability of the network.

In Shah et al. [45], the impact of large-scale PV integration on the static voltage stability of a sub-transmission network using the IEEE 14-bus test system is investigated. The research assesses the effects of large-scale PV penetration and the placement of the dynamic reactive compensation devices: Static Synchronous Compensation (STATCOM) and Static Voltage Compensator (SVC) on voltage stability. Three main methodologies: Q-V Modal Analysis, Continuation Power Flow (CPF) and the Trajectory Sensitivity Index (TSI) are used in the analysis. The TSI analysis is used to determine the suitable location of the dynamic reactive compensation devices while the Q-V analysis and CPF are used to analyse the effects of PV penetration on different system parameters. Simulation results indicate that the location and loading direction (conventional or realistic) of the PV units have an impact on the network's loading margin. Based on the simulation results, the authors conclude that the location, size and the PV integration approach (concentrated or dispersed) largely affect the static voltage stability of the network. The power factor control mode of operating the PV units

was found to worsen the voltage instability while the voltage control mode improved the stability in some cases. The STATCOM was found to improve the static voltage stability margin better and was more effective when used for short-term VAR support than when placed at the weakest bus and PV generator buses. The placement of SVC on the generator buses was found to be effective in improving the voltage stability margin than placement on the weakest bus or placement based on dynamic VAR support. Although the STATCOM proved to be more effective in improving the static voltage stability, both the STATCOM and SVC were found to be beneficial to the static voltage stability based on their locations and other network conditions.

2.4 Deductions from the Literature Reviewed

Although extensive research has been carried out on the grid integration of RE, methods of improving system stability and the impacts of RE on grid stability, certain gaps were identified, which will be addressed in this thesis.

Most research on the grid integration of RE extensively highlight the experiences and measures that have contributed to the success of the RE integration in the western / industrialised countries. In the case of Germany for instance, the economic incentives and legalities of network connections, which are identified to be the main success drivers are issues that are not yet fully addressed in Ghana. While several examples of 'best' practices are emphasised, all the practices fall within five main categories namely: system operation improvement, developing enabling rules for system flexibility, public engagement, coordinated and integrated planning and access expansion to different resources. These best practises are also applicable and required in Ghana, especially the need for transmission system expansion which is not only for the effective RE integration but also for the reliable day-to-day operation of Ghana's network. Although the researches make clear that adherence to the proposed guidelines make possible the integration of unlimited share of RE, Ghana's position as a developing country raises different sets of technical and economical questions on the RE development as seen in [46–49], which therefore require new methodologies and approaches specific to the needs of the Ghanaian network.

In all investigations presented so far, different penetration levels are simulated to analyse the effects on various network parameters. These studies conclude that high RE penetration levels have diverse effects on system stability depending on

the location, size and connection approach of the PV units (dispersed or concentrated). Methodologies for analysing the steady-state and dynamic properties of various networks with RE are also proposed. In analysing the impacts of the grid integration of RE on system stability for instance, various forms of power system stability are considered ranging from static and dynamic voltage stability to small-signal and transient stability. Most research consider the different forms of stability separately or as a combination using various techniques. Methods such as the use of P-V and Q-V curves, continuous power flow, VQ instability margin, etc are used in the static voltage stability analysis. Modal analysis and time domain simulations are also used for the small-signal and transient stability analysis. In developing a methodology that addresses the challenges of Ghana's network, this research proposes the use of load flow analysis to initially identify the existing bottlenecks in the grid. To supplement the methodologies for the stability analysis, different contingencies will be simulated to evaluate the (n-1) reliability of the network.

A few of the research that exist on networks of developing countries and as such on the Ghanaian network are presented, which propose the use of SVC and STATCOM for improving system stability in Ghana. The researches present the impacts of these FACTS devices on the stability of the Ghanaian NITS and identify the most critical bus in the network. The analysis carried out considered a network without RE and thus introduces the question on how the FACTS devices impact the stability of the NITS with RE, which is one of the main focuses of this thesis. The analysis in these research were carried out with prior knowledge of the voltage 'vulnerable' areas in the network, which were targeted for the installation of the FACTS device. This dissertation however aims to use voltage stability indices and the genetic algorithm method of optimization to determine the 'critical' buses and transmission lines and to also identify the reactive power deficient buses, which will serve as the optimum location for the FACTS devices.

The analysis presented in the reviewed literature were mainly carried out using generic network models and data. The studies in this thesis will be performed using a model of the Ghanaian power system with actual network data, which is developed in close consultation with system operators in Ghana. Additionally, while most researches perform the analysis of RE in the distribution network, existing constraints in the Ghanaian power system require that the RE be connected directly into the transmission network, thus requiring the modelling and simulation of the NITS, as will be addressed in this thesis.

The trend of research examined so far indicate that a lot of investigations have been carried out focussing on networks in industrialized countries with less focus on developing countries. As developing countries are currently the emerging economies driving global development, the power systems of such countries also require extensive consideration, including research on the grid integration of RE. In contrast to most literature, this thesis aims to consider the RE integration in the power system of a developing country. As most developing countries are currently in the initial stages of the RE integration, this research seeks to bridge the gap created by the trend of research on only developed countries. In so doing, this research will serve as an instrumental guideline to other countries with similar network features or in the same stage of the RE integration.

Findings of the literature review indicate that there is no one-size-fits-all approach for the grid integration of RE. It therefore remains the duty of the power system operators to develop their own operational policies and arrangements, which fit the needs of the respective countries. Even though experiences from different countries may be good examples to learn from, they may not necessarily be perfect-fit solutions for other countries due to the specific and individual grid designs, load densities as well as the technical and economical constraints.

3 Network Modelling

This chapter describes the development and modelling of the loads and generating units such as synchronous generators and their dynamic controls, the PV generators and the wind generating units as used in this research. Despite the use of actual network data, the lack of detailed data of some network components resulted in the use of a few generic models.

3.1 System Demand

System demand of the NITS was modelled by initially modifying the power factors of all loads to 0.90 (lagging), which is the required minimum specified by Ghana's transmission grid code [50]. The load power factors in the original transmission network data varied from 0.58 to 1 in different substations with 30% of the loads having power factors lower than the defined minimum. The low power factor is one of the reasons for the low voltages recorded at some points in the network [2]. To cater for the various power factor correction measures put in place in the distribution networks (DN), a unified power factor of 0.90 was used for all loads.

All other components of the DN were aggregated and modelled as equivalent loads in the substations. Each of these loads consist of medium and low voltage DN comprising the distribution voltage regulators, reactive compensation devices and different load components, such as lighting and electrical appliances for both residential and commercial purposes.

Loads in the NITS are made up of approximately 66.9% residential load, 2.4% commercial load, 22.1% industrial load and the remaining 8.6% for exports [51]. Due to the purely residential load in the NITS, motor loads which consume about 60 to 70% of the total demand of a power system [52], were neglected as they make up an infinitesimal percentage of the total load in the NITS. The loads were thus modelled as simple static loads, whose demand depend on the system frequency and voltage. Due to lack of adequate information on the exact load composition, the load models were represented by constant current models, whose demand vary proportionally with the voltage [52]. To consider the demand growth in the country, which varies annually between 9.8% and 11.5%, an average annual growth rate of 10% was applied to the system demand for the different scenarios. Figure 3-1 shows a sample load profile, which in contrast to the load profiles in

industrialised economies like Germany is largely characterised by the lifestyle of the Ghanaian populace (residential load) and not the industrial loads.

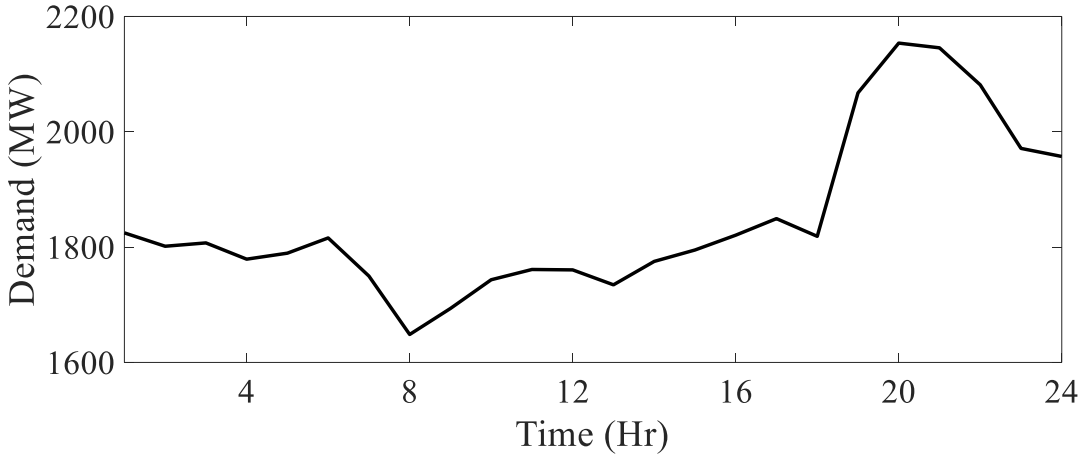

Figure 3-1: Typical Load Profile in the NITS

The profile has two peaks; a minor peak in the early morning around 05:00[9] and a major peak in the evening around 19:00[10]. Contrary to the case in industrialised countries, where most industries are active in the day and thus demand peaks during the day, the lowest system demand is recorded in the Ghanaian NITS during daytime.

3.2 Synchronous Generators

Salient pole and round rotor generators were respectively used for the hydro and thermal generating units. Parameters of the synchronous generators used are found in Appendix A.

3.2.1 Reactive Capability Curve

The reactive capability limits of synchronous generators are essential in both voltage and long-term stability studies [18]. The limits provided by the reactive capability curve define the SG's reactive power provision, which is the amount of reactive power the generator produces or absorbs. The capability curve also defines the range of operation of the generator's active and reactive power output. While a generator's active power output is limited by the prime mover's capability, the reactive power output is limited by the armature current, field

[9] That is the time when daily activities begin for most people

[10] The time when most people return from work and resume household activities

current and end-region heating [18]. A typical generator reactive capability curve is given in figure 3-2.

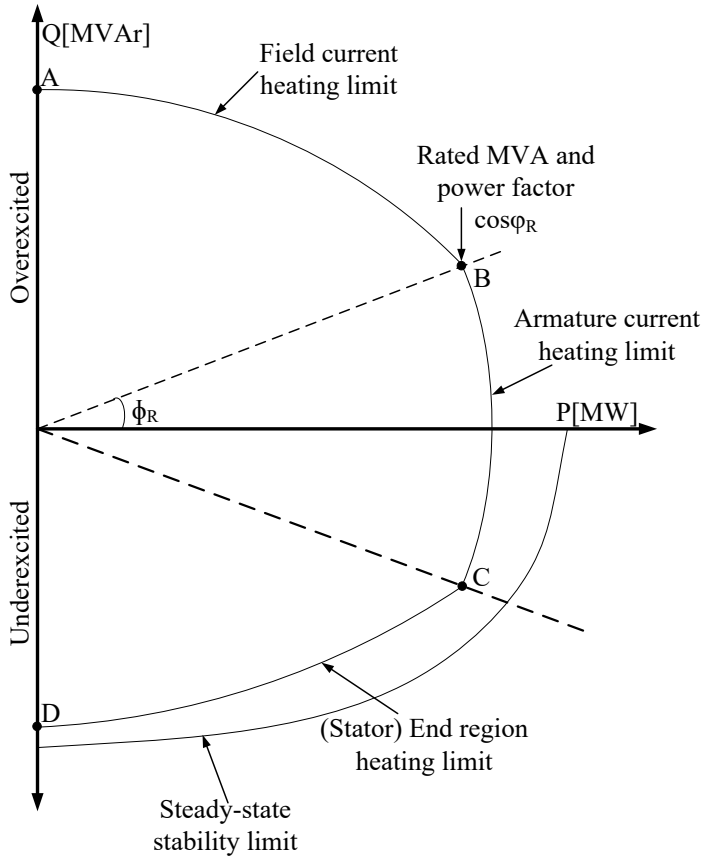

Figure 3-2: Synchronous Generator Reactive Capability Curve

The capability curve specifically defines the limits within which the field (rotor) current (curve A-B), armature (stator) current (curve B-C) and the stator end region (end-turn) (curve C-D) of the generator must be operated in order not to cause overheating of the respective windings. Based on the depiction of the capability curve in the P-Q plane, the armature current limit appears as a circle with the centre at the origin and the radius equal to the generator's rated MVA and power factor (point B in Figure 3-2). For a balanced design, point B represents the intersection of the field and armature thermal limits. Additional limits imposed by the stability limits may also be shown in the reactive capability curve [18]. The steady-state stability limit for instance is depicted with the curve beneath the end-region heating limit [53] (see Figure 3-2). The maximum power angle for a stable generator operation as well as the maximum turbine power, which determines the generator's real power are also defined by the capability curve [52].

Synchronous generators in the NITS were equipped with their respective manufacturer-specific capability curves as provided by the transmission system operator (TSO) and based on a few generic data for the newly added generators.

3.2.2 Dynamic Controllers of Synchronous Generators

The dynamic controller models of the synchronous generators; exciter, turbine governor and PSS in the network are represented by standard controller models. These models were updated with real values to accurately represent the current practice in Ghana.

Excitation System Models

The principal function of the SG excitation system is to provide direct current to the generator field windings. The exciter uses the field current to control the field voltage while performing other control and protective functions necessary for the efficient performance of the power system. The block diagram of the synchronous generator excitation with its subsystems is presented in Figure 3-3.

The *excitation control elements* carry out stabilizing, controlling and excitation regulation functions [54]. Components of this block include the AC and/or DC voltage regulator, excitation system stabilizer and transient gain reduction. The AC voltage regulator is responsible for maintaining the generator stator voltage while the DC regulator maintains a constant field voltage when the ac regulator is out of service. The automatic process of regulating system voltage results in the name automatic voltage regulation (regulators) – AVR, which conditions the required signal to the appropriate level before being fed into the exciter [18]. The type of exciter and corresponding AVR are mostly defined by the generator manufacturers. Based on generator data from Ghana's network database, three AVR types – IEEEAC8B, IEEEST1A and IEEEST4B were implemented in the generators in the model (details can be found in [54]).

The *exciter* serves as the power source of the excitation system through its provision of DC power (excitation current) to the generator field windings [18]. The exciter is often a separate DC or AC generator with its field windings in the stator and the armature windings in the rotor [55]. The exciter is regulated by the AVR, which is part of the excitation control elements. The generator field voltage E_{FD} is also produced by the exciter.

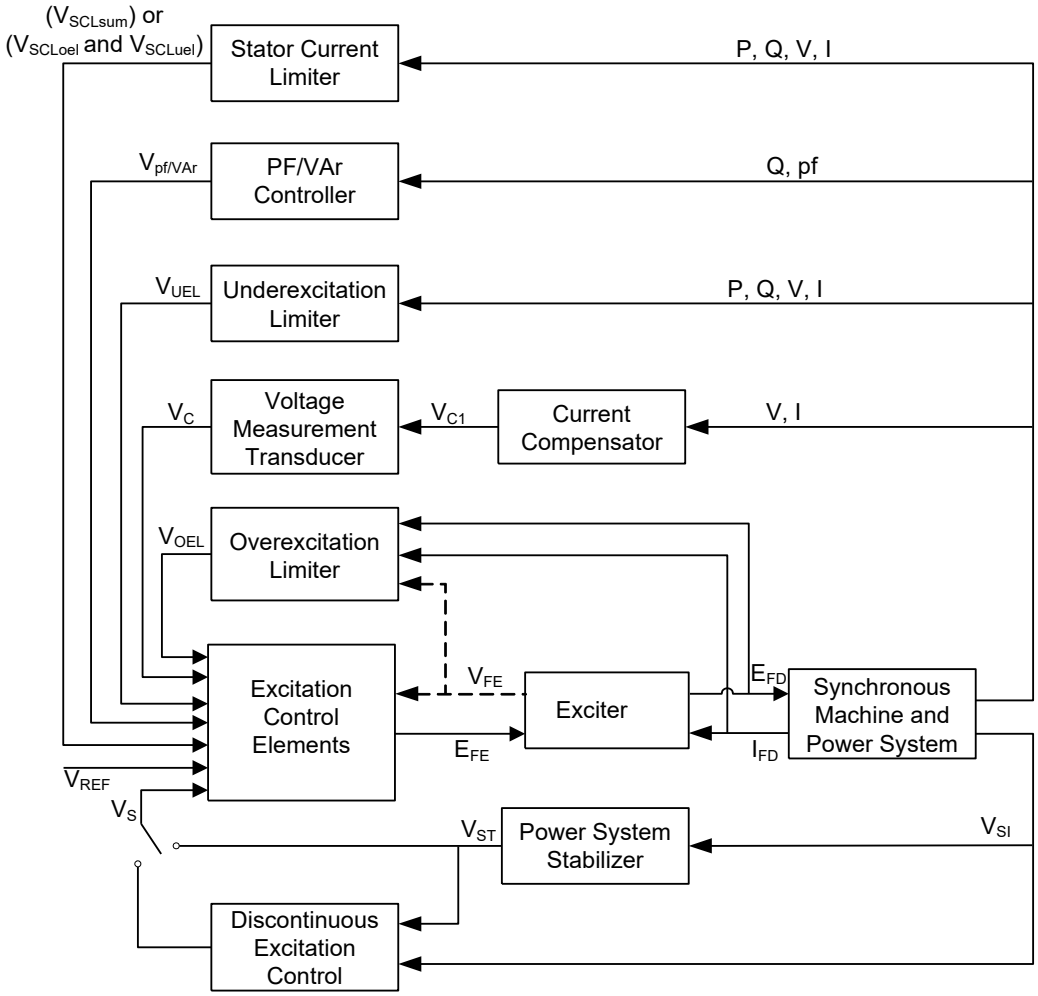

Figure 3-3: Block Diagram of a Synchronous Machine Excitation Control System [18, 54]

Thermal generators (gas operated) in the NITS were equipped with the *IEEEAC8B* model, which is a model suitable for internal combustion engines [56]. The model consists of a proportional-integral-derivative (PID) controller with separate constants for the proportional, integral and derivative gains. The IEEEAC8B model is also used to represent static voltage regulators applied to brushless excitation systems [54, 57].

Generators of the crude oil operated power plants were equipped with the *IEEEST1A* model, which is the most widely implemented excitation system type [58]. The model represents potential-source controlled rectifier excitation systems used for systems with excitation whose power is supplied through a transformer from the generator terminals and is regulated by a controlled rectifier [57].

The hydro generators were equipped with the *IEEEST4B* static exciter model – potential or compound source-controlled rectifier-exciter, based on industrial experience, which confirms the use of static excitation for modern hydro units [56]. This model has both a potential and compound source rectifier excitation

system and is equipped with a PI (proportional-integral) regulator block [56, 57]. The voltage regulator of this model is digitally implemented [57].

Turbine Governor Models

The block diagram and basic structure of the frequency control – turbine governor in a power system is presented in the figure below.

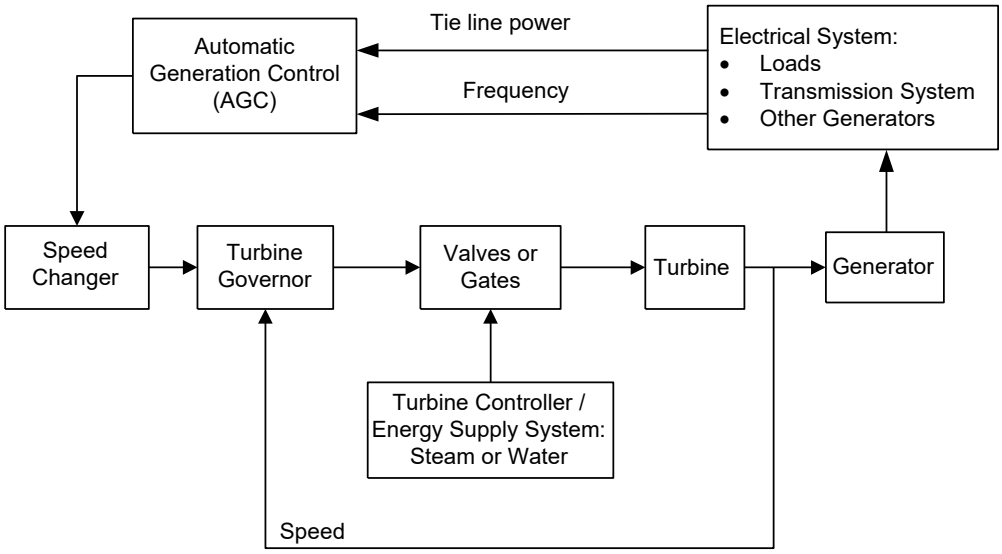

Figure 3-4: Block Diagram for Frequency Control in Power Systems [18, 59, 60]

The main function of the turbine governor is to control the opening and closing of the gates or valves (for either thermal or hydro turbine) to allow more energy supply to regulate system frequency. The choice of governor is thus dictated by the type of SG being used, which is also dependent on the type of energy supply, i.e., round rotor for thermal generators or salient pole rotor for hydro generators. Details of the individualised blocks can be found in literature [18, 59, 60]. The dynamics of the water flow in the penstock for hydro generation such as the water inertia establishes the nature of the transient characteristics and influences the requirements of the speed governor [18, 60]. It is therefore important to select a governor model, which considers the penstock dynamics, especially considering the stability studies to be carried out in this research. The hydro generators in the model were equipped with the hydro turbine governor (HYGOV) model. This model combines both mechanical and hydraulic controls and is suitable for system planning studies with generators, which have mechanical and/or hydraulic controls [56, 61]. The HYGOV model is a simplified representation of a hydroelectric plant governor, which captures the detailed dynamics of the penstock [56]. Research also indicates that the HYGOV model is among the most commonly used hydro governors in practice.

The thermal generators in the NITS were equipped with the gas turbine (GAST) model, which is a simplified representation of gas turbines in system studies when detailed information are not available [61]. The GAST model is used for operation near the rated speed [56] and consists of a simple droop[11] control, constant load limit and three different time constants to represent the individual responses in the turbine control [61].

3.2.3 Wind Turbines

As wind power generation in Ghana is relatively new, there was inadequate information[12] on the specifications of the wind turbines. The IEC 61400-27 standard on 'Electrical Simulation Models of Wind Turbine Models' was thus used as a guide to select the appropriate model for use in this research.

A typical functional block diagram of the modular structure of a wind turbine with the individual components is shown in figure 3-5. The model comprises six basic blocks: the aerodynamic, mechanical, generator system, electrical equipment and grid protection blocks, which are responsible for different control functions.

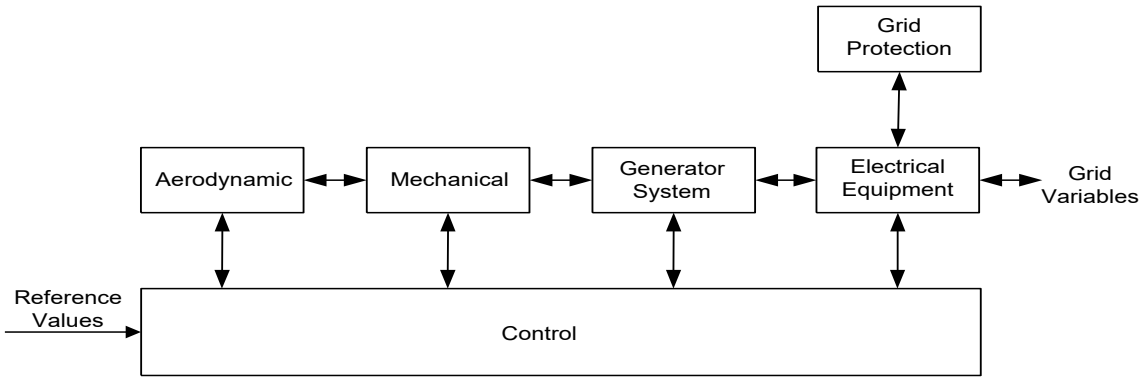

Figure 3-5: General Structure (Block Diagram) of a Wind Turbine Model [62]

The *aerodynamic* block is responsible for computing the mechanical power of the wind turbine based on the wind energy. Inputs to this block include the pitch angle of the rotor blade, rotor speed and wind speed [63]. Three different subsystems are located in the aerodynamic block, which are responsible for the calculation of the rotor power coefficient, aerodynamic torque and tip-speed ratio parameters used to compute the turbine's mechanical power [64]. The turbine rotor (blades of the wind turbine) form part of the aerodynamic block and transforms the kinetic energy of air into mechanical power, P_{MECH} [65]. The aerodynamic block is thus

[11] The droop is responsible for the equal distribution of loads among the generating units.

[12] Only the proposed plant sizes are currently available to the public. All other information is confidential and remain unpublished until the projects are completed.

responsible for converting the wind power (kinetic energy) to mechanical power [66]. The mechanical power output of the turbine depends on rotational speed ω_{turb}, wind speed V_{wind} and blade angle β and is expressed as a function of these quantities.

$$P_{\text{MECH}} = f_{\text{Pmech}}(\omega_{\text{turb}}, V_{\text{wind}}, \beta) \tag{3.1}$$

The *mechanical* block is also known as the 'drive-train' due to its representation of the wind turbine's inertial components [67]. The prime mover of the wind turbine generator (WTG), which includes the rotating masses, gear system and connecting shafts (rotor and generator shafts) is also located in the mechanical block [64, 65, 68]. The mechanical behaviour of the turbine is represented by torque equations and is modelled using single-mass or multi-mass (often two-mass) drive-train models. The mechanical model additionally calculates the instantaneous shaft speed of the WTG [64].

The *generator system* block acts as a current regulator by injecting inverter currents into the other blocks in response to a given current command. Inputs to this block, which represent the simplified fast controls are commands from the control block [67, 69]. The block additionally contains a reference rotation between the generator pq-coordinates and the grid coordinates [70]. The type of generator model used in the wind turbine is also located in this block.

The *electrical equipment* block contains the electrical systems – transformers, cables, switchgear, and the respective power electronic converters [62, 64].

The *grid protection* block as its name suggests, provides the main protection function for the wind turbine model. The components of this block include over- and under-voltage and –frequency protection elements, which control various circuit breakers in the electrical equipment [62, 70]. Additional crowbar circuits are available on some wind turbine models to protect the rotor circuit against very high rotor currents [64]. The protection function of the wind turbine model is based on the fault-ride-through capabilities of the wind turbine generator [70].

The *grid variables* comprise the grid parameters such as active, reactive power and power factor, etc. that are fed into the wind turbine terminals from the grid.

The *control block* is responsible for controlling the pitch angle, active and reactive power in the WTG converter [64, 67, 69]. It is connected to all blocks of the wind turbine model except the grid protection block. Reactive power control is achieved through the available reactive power control options such as voltage regulation, referenced reactive power setpoint and power factor control. The

model is additionally equipped with a current limiter, which prioritizes the active and reactive power selection [62, 67]. The current limiter has voltage-dependent limits of the reactive power, which are used to limit the turbine voltage from exceeding the maximum in an event of an increased reactive current injection [70]. Fixed-speed wind turbine models for instance have extra Proportional-Integral (PI) controllers in the control block that are used to minimize the errors between the reference and the measured values [64].

The horizontal positioned blocks; aerodynamic, mechanical, generator system and electrical equipment indicate the flow of physical power in the wind turbine [62]. Although not all blocks are available in all types of wind turbine models, the generator system, electrical equipment and grid protection block are found in all wind turbine models irrespective of the type.

Four main types of wind turbines are proposed by the IEC standard 61400-27-1 – Electrical Simulation Models of Wind Turbine Models [71] and the Western Electricity Coordinating Council (WECC) [72]. The WTG types include *Type 1 – WTG with conventional induction generator; Type 2 – WTG with variable rotor-resistance induction generator; Type 3 – WTG with doubly-fed (asynchronous) induction generator, DFIG and Type 4 – WTG connected through full converter unit*. Types 3 and 4 possess more control features than types 1 and 2 and also have similar control features though very different in their individual hardware [62]. These control features enable the types 3 and 4 to participate in system control. The four WTG types are additionally sub-divided into seven models, which reflect their respective differences based on additional unique features. The seven models include: Type 1A – without power control; Type 1B – with power control; Type 2; Type 3A – without crowbar[13] protection; Type 3B – with crowbar protection; Type 4A – without mechanical and aerodynamic models and Type 4B – with mechanical and (constant) aerodynamic model [56, 62, 64, 68, 72, 73].

Type 1 wind turbines generally operate at fixed wind speeds with a very narrow speed range above the synchronous speed. The conventional induction machine used in this type consumes reactive power such that additional reactive compensation devices such as shunt capacitors are needed to supply the required reactive power [68]. Furthermore, due to their direct connection to the grid, wind speed variations are directly translated into voltage and power fluctuations at the point of common coupling.

[13] The crowbar is a circuit used to prevent overvoltages in the WTG through the use of a short circuit or a low resistance (braking resistor) across the voltage output.

The type 3 model, uses a DFIG, whose generator is connected to the grid through a back-to-back voltage source converter [62, 64, 68]. The use of the converter makes possible the generation and consumption as well as the independent control of active and reactive power [68], which is beneficial in the Ghanaian NITS. This consequently eliminates the need for additional compensation devices. The variable speed wind characteristics of the type 3 WT also allows operation within a wide range of rotor speeds.

A two-mass model drive train is generally used in the DFIG WTG due its ability to better mimic the dynamic characteristics of the WTG [74]. The type 3 WTG model has an additional control system, which regulates the active and reactive power to ensure the maximum possible wind output and control the generator's reactive power output [64]. Specifically, the type 3B with the crowbar protection for preventing overvoltages was selected for use in this thesis, due to the existing voltage issues in the NITS. Details of the type 3B WTG model can be found in the following references [56, 62, 64, 68, 70].

Detailed multi-mass models, which are approximated by at least two-mass models are required for analysing the system's response to large disturbances in stability analysis [66]. The two-mass model is used to represent the turbine and generator inertia respectively. The two-mass model implemented in the DFIG WTG in this research is described by the following equations [74, 75]:

$$2H_T \frac{d\omega_T}{dt} = T_{WM} - T_{Sh} \tag{3.2}$$

$$2H_G \frac{ds_r}{dt} = T_{EM} - T_{Sh} \tag{3.3}$$

$$T_{Sh} = K_{Sh}\theta_{ShTw} + D_{Sh} \frac{d\theta_{ShTw}}{dt} \tag{3.4}$$

where H_T is the turbine inertia constant, which comprises the inertia of the blades, hub and low-speed shaft; ω_T is the turbine angle speed; T_{WM} is the wind torque, which serves as the input mechanical torque to the wind turbine; T_{Sh} is the shaft torque; H_G is the generator inertia constant, which stands for the high-speed shaft; s_r is the rotor slip; T_{EM} is the electromagnetic (electrical) torque; K_{Sh} is the shaft stiffness coefficient (torsion stiffness); θ_{ShTw} is the shaft twist (torsion) angle; D_{Sh} is the damping coefficient (torsion damping) .

Neglecting the electromagnetic transients of the stator, a simplified transient model of the DFIG is described by the following equations based on [74, 75] :

$$\frac{dE'_d}{dt} = s_r\omega_s E'_q - \omega_s \frac{L_m}{L_{rr}} v_{qr} - \frac{1}{T'_0}\left[E'_d + (X_s - X'_s) i_{qs}\right] \quad (3.5)$$

$$\frac{dE'_q}{dt} = -s_r\omega_s E'_d - \omega_s \frac{L_m}{L_{rr}} v_{dr} - \frac{1}{T'_0}\left[E'_q - (X_s - X'_s) i_{ds}\right] \quad (3.6)$$

where E'_d and E'_q are the direct (d) and quadrature (q) axis transient voltages; s_r is the rotor slip; ω_s is the synchronous angle speed; L_m is the mutual inductance; L_{rr} is the rotor self-inductance; v_{dr} and v_{qr} are the d and q axis rotor voltages; T'_0 is the rotor circuit time constant; X_s is the stator reactance while X'_s is the stator transient reactance. Currents i_{ds} and i_{qs} are the d and q axis stator currents.

Wind Park Aggregation

The wind park was created by aggregating several individual wind turbine units to make up the required rated power. Wind turbine models of capacity 2 MW[14] were used for the wind parks in this thesis. The model simplification and aggregation was carried out to avoid the larger computation requirements and longer simulation times involved in the detailed modelling of the individual units, especially for dynamic studies [66, 76, 77]. For the purpose of the dynamic simulations, an aggregated wind park with approximately 41 - 123 DFIG units, each dispatched at 1.82 MW was used in this research.

3.2.4 Photovoltaic Systems

Power generation from PV units in Ghana is expected to start at 150 MW and eventually increase to over 500 MW, which will make up more than 15% of the total installed generation by the end of the study period. Seven out of the nine proposed PV parks with more than 90% of the total PV generation are located in the north of the NITS, where higher voltages are often recorded. The location of these PV units thus proves to be strategic in contributing to the efficient control of reactive power and system voltage through their reactive power provision.

PV generators are connected to the power system through DC-to-AC inverters and hence do not have inertia as compared to synchronous generators. Despite the inverters' capability to provide reactive power in addition to the active power, the reactive capability of the inverter is restricted by its ratings and the PV units. A simplified functional block diagram of a PV system is presented in Figure 3-6.

[14] This is based on information from the website of the project developer, which states that the sizes of the wind turbines being used for the project range between 2 – 4 MW.

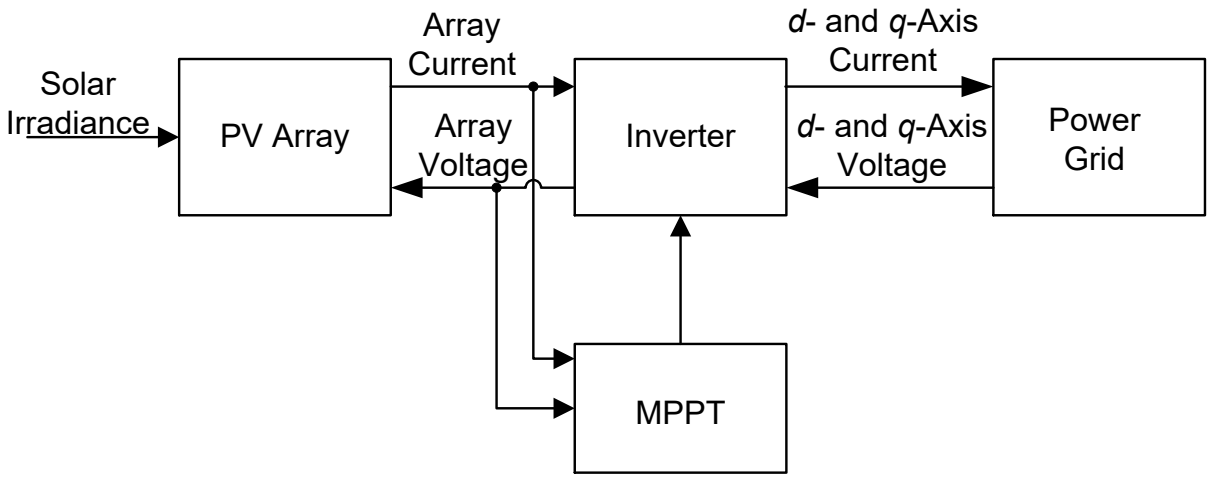

Figure 3-6: Block Diagram of a PV System [56, 78, 79]

The **PV array** is made up of several photovoltaic cells connected in series and parallel to obtain the required output power rating. The array converts solar irradiation into electrical energy [80], which is then supplied into the inverter as the array current and voltage (both DC quantities). The array current and voltage depend on the solar irradiance and cell temperature [56, 79, 80]. The **inverter** converts the array current into AC and injects it into the grid in the appropriate forms. The **MPPT** (Maximum Power Point Tracking) block is responsible for optimizing the efficiency of the photovoltaic energy conversion.

Due to the lack of detailed information on the model of the PV systems in Ghana, a generic PV system model was used. The generic model is represented by a static generator that mimics the grid side converter and photovoltaic cell and is suitable for both static and dynamic stability analysis. As with the wind plants, the PV plants were represented by aggregated PV model using the PV modules of 0.5 MVA at 0.4 kV.

3.3 Single Line Diagram

The resulting simplified single line diagram (SLD) of the NITS with all the modelled elements is presented in Figure 3-8. The external grids represent the transmission systems of the neighbouring countries. The loads in the network as previously mentioned represent the aggregation of individual loads and other elements in the distribution system. The SLD also depicts the path of power flows between the generating units and the various loads.

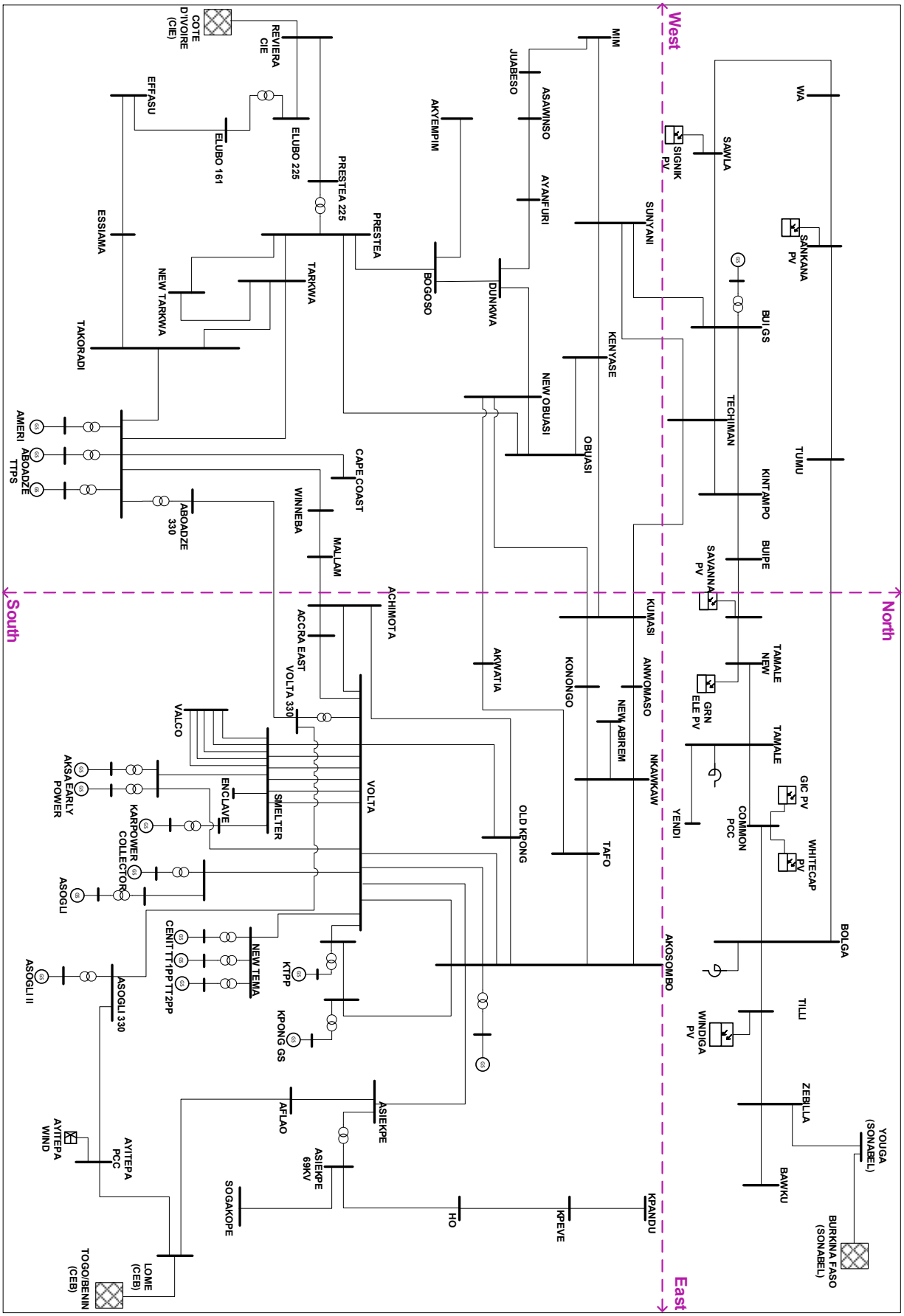

Figure 3-7: Single Line Diagram of the Ghanaian NITS

3.4 Review of the RE Grid Code

Renewable Energy Sub-Codes (subsequently referred to as RE grid code) for the transmission and distribution systems have been instituted to serve as a guide for the connection and dispatch of variable RE (VRE) in Ghana. Ghana's RE grid code, which is an addendum to the National Electricity Grid Code specifies the technical requirements for the connection of VRE. For this research, a brief review of the RE grid code for the transmission network is provided below.

3.4.1 Range of Frequency

With a 50 Hz operational frequency in the NITS, a frequency range of $48.75 \leq f \leq 51.25$ Hz is specified for the continuous operation, within which active and reactive power is to be delivered without restrictions. Frequencies outside the continuous operation range but within the ranges of $47.5 \leq f < 48.75$ Hz and $51.25 < f \leq 51.5$ Hz require that the RE units remain connected to the network for 90 minutes [81].

3.4.2 Voltage Range

The range of normal operation +/-5 p.u. is specified as the unrestricted voltage range of operation for the provision of active and reactive power. No unit disconnections are permitted in this range and as long as the voltage is within the continuous voltage range of +/-10 p.u. or within the IEC voltage limits for continuous operation – depending on which range is narrower [81]. Operation in the continuous voltage range however requires that the RE units provide the appropriate reactive power support to the grid.

3.4.3 Reactive Power Capability

RE units in the NITS are required to operate within power factors of 0.95 under-excited and 0.925 over-excited. The continuous variation of the power factor is allowed within these limits as defined by the reactive capability curve (see figure 3-8) for operations within the unrestricted voltage range. Operation outside the unrestricted voltage range but within the continuous voltage range is permitted as long as the reactive capability limits of the RE units are adjusted to their voltage dependent limits [81]. RE units which operate with active power below 5% are

not required to provide reactive power. This reactive power capability curve as specified in the RE grid code was implemented in the RE units in this thesis.

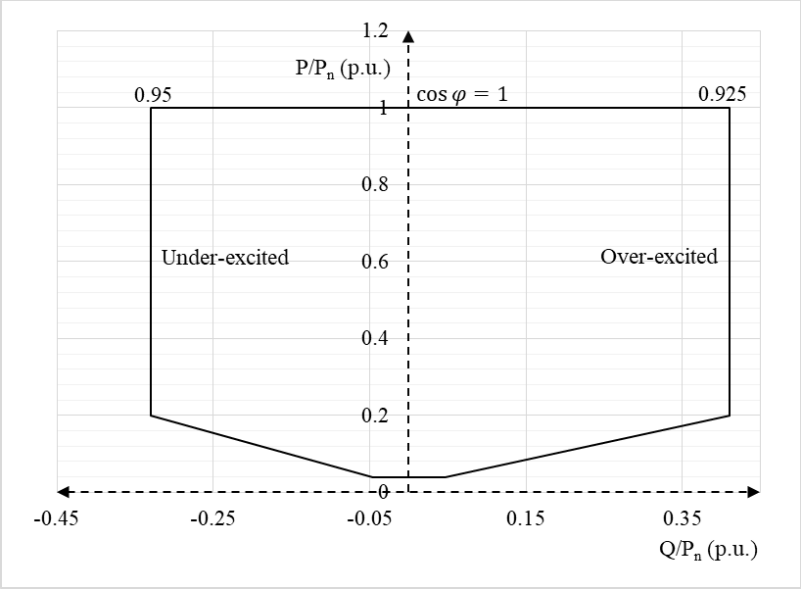

Figure 3-8: Reactive Power Requirements for RE Units to be connected in the NITS [81]

3.4.4 Voltage/Reactive Power Control

RE units are required to control reactive power or voltage at the points of common coupling (PCC) using one of the following control schemes: *voltage, reactive power and power factor control*. The choice of control schemes and limits for all grid connected generators remain the tasks of the transmission utility operator [33, 81].

The voltage control scheme locally controls system voltage by regulating the reactive power output of the generator to achieve the given terminal voltage [56]. A thorough analysis of the three control schemes reveals that the operation of RE units in the voltage control mode is the best way to effectively utilize both the static and dynamic reactive power capability of the RE units [42, 45, 68, 82, 83]. The other two control schemes though still in use, are generally recommended for very strong transmission networks as they may lead to the under-utilization of the full reactive capability of the units [76]. All generators in this thesis were thus operated in the 'voltage control' control mode.

3.4.5 Low- and High Voltage Ride Through Capability of the RE Units

RE units are required to remain connected in the network for a specific period during abnormal network conditions like faults before being disconnected. This

requirement is necessary to ensure that generation is not lost for normally cleared faults as the early disconnection of RE units may have negative effects on the entire network. The specific connection times and required voltage levels are defined by the low voltage ride through (LVRT) and high voltage ride through (HVRT) curves in the figure below. Grid connected RE shall have the operating region as defined by the figure during faults. The figure describes the allowed voltage at the PCC, V_{PCC} and the corresponding dis/connection times.

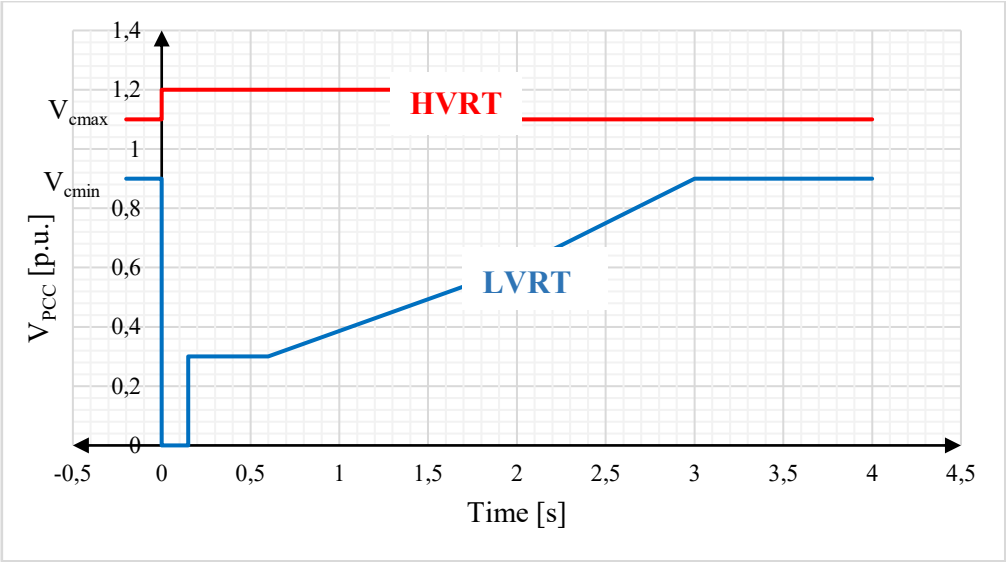

Figure 3-9: LVRT and HVRT Capability for RE Units in the NITS [81]

The first part of the LVRT is the period between the occurrence of the fault and its clearance, which generally lasts between 150 ms to 500 ms. In the second part of the curve, disconnection of the RE units is not allowed. This means the RE unit shall remain connected to the grid as long as the operation is within the LVRT (lower line) and HVRT (upper line) and the voltage is in the continuous voltage range (between V_{cmax}, 1.1 p.u. and V_{cmin}, 0.9 p.u). Notwithstanding, an automatic disconnection of the RE units is required for voltages higher than 1.2 p.u.

RE units are further required to provide reactive current support (produce or absorb the additional reactive current) during fault conditions. The reactive current, which is to be produced at the generator terminals should be equivalent to the change in the RE unit's terminal voltage.

3.5 Development of Study Scenarios

The effective analysis of the network requires the consideration of power system conditions that take into account changes in load (local demand, import and

export) and generation patterns (both existing and planned) in the network. Scenarios for three different years with varying penetration levels were thus developed for the analysis to be performed in this thesis. The most common and simplest definition of the penetration level in literature - the ratio of the aggregate capacity of RE units to the installed generation capacity of the network (see equation) [84] was used in this research.

$$Penetration\ Level = \frac{Capacity\ of\ RE\ Units\ (Aggregate)}{Installed\ Generation\ Capacity} \tag{3.7}$$

The years 2017, 2020 and 2023 were defined respectively as the base case, target and post-target scenarios, also referred to as scenarios 1, 2 and 3. The network expansion plans outlined in the generation and transmission master plans [15], [51] and the electricity supply plans [1–3, 85] were used to develop the scenarios.

3.5.1 Scenario 1 (2017 – Base Case)

Scenario 1 (S1) is the **base case scenario,** which serves as the reference scenario for the network analysis. The scenario represents the actual network conditions (generation, demand and existing transmission infrastructure) as at the end of the year 2017 with a proposed RE penetration level of 5%.

3.5.2 Scenario 2 (2020 – Target Scenario)

Scenario 2 (S2), the **target scenario** represents the network conditions for the year 2020 and is the main scenario for the analysis in this research. In this scenario, the percentage share of RE is increased to 10% to meet the given national target. A 10% annual load growth [86] is further considered for the local demand, which results in an increase in the demand in S1 by a factor of 1.33%. Exports to Burkina Faso and Togo/Benin are also increased to 150 MW and 200 MW respectively [85] as new 330 kV transmission lines are commissioned in that year. Approximately 900 km of new 330 kV transmission lines are hence introduced in S2. The number of potlines in operation at the VALCO Aluminum smelter is also increased from one to five [85] in this scenario, which translates into a 230 MW additional demand increase.

3.5.3 Scenario 3 (2023 – Post-target Scenario)

Scenario 3 (S3) mimics the network conditions beyond the target year by considering an RE penetration level of approximately 15%. Local demand in this scenario is increased by a factor of 1.771% while the number of potlines of

operations at VALCO is increased to the maximum of six potlines with a demand of 377 MW. Power exports in this scenario is increased to a total of 500 MW consisting of 150 MW to Mali[15] [85] through Burkina Faso and 350 MW to Burkina Faso and Togo/Benin.

The 15% penetration limit set for the post-target year is based on results from preliminary steady-state voltage analysis carried out in [87], which indicates 15% as the maximum RE penetration level the current network can accommodate to maintain system stability. A 15% RE penetration thus requires the shutdown of equivalent amount of conventional generation in the south, which adversely affects system voltage. Maintaining system stability however requires the compliance with the 15% limit until new transmission infrastructure are put in place and provisions are made for additional reactive power supply in the south.

The table below summarises the network infrastructure, generation and demand overview for the scenarios.

Table 3-1: Overview of Network Infrastructure, Generation and Demand for the three scenarios

	S1 (2017)	*S2 (2020)*	*S3 (2023)*
Transmission Lines			
Number of Line	143	158	160
Operating Voltage (kV)	Length (km)		
330	395	1120	1364
225	205	440	440
161	5060	5090	5090
69	133	133	133
34.5	107	125	125
Transformers	**Capacity (MVA)**		
2-Winding Transformers	11,000	15,000	18,000
	(138)[16]	(161)	(173)
3-Winding Transformers	1,070	1,090	1,090
	(30)	(30)	(30)
Power	**Capacity (MW)**		
Installed Generation	4342	5012	5012
RE Generation	240	530	785
Total Installed Generation	**4580**	**5540**	**5800**
Load Growth	1%	1.33%	1.77%
Exports	5 MW	350 MW	500 MW

[15] From 2021 onwards

[16] Represents the number of installed transformers

3.6 Generation Scheduling

Generation scheduling in Ghana is carried out based on the 'merit-order'[17] of the generating units [51]. Hydro generation is considered first in the scheduling due to the affordable costs of production and operation. Combined-cycle gas plants are considered next, followed by the simple-cycle gas plants. Nonetheless, with the integration of RE in Ghana's power system and the associated regulations such as the '*renewable energy purchase obligation'* and '*connection to the transmission and distribution systems'* of the 2011 RE Act 832 [10], RE units are offered connection priorities in the network. The original dispatch order is thus altered to offer priority to RE units especially during the off-peak period when, RE generation is highest. A summary of the generation schedules for the scenarios is presented in Table 3-2.

Regardless of the generation dispatch, a minimum of 300 MW generation from the west in addition to three fully loaded units at the main hydro generating station (Akosombo), which amounts to approximately 500 MW is always required to maintain the system stability during normal operating conditions [2].

17 'Merit-order' dispatch refers to an order of generation dispatch in which generating units are operated in an ascending order of operational costs in correlation to the amount of electricity they each generate

Table 3-2: Generation Scheduling for the Three Scenarios

Generating Unit	***Total Output (MW)***		
	S1 (2017)	S2 (2020)	S3 (2023)
Conventional Generation			
Akosombo	520	520	520
Kpong	0	120	120
Aboadze	472.5	472.5	315
CENIT	0	100	100
TT1PP	0	100	100
Asogli I	0	0	0
Asogli II	157.5	0	330
Collector	0	309	220
Ameri	300	300	300
KTPP	0	200	0
Karpower	225	225	225
AKSA	0	0	370
TEI	0	0	100
Early Power	0	0	200
Total Conventional Generation	**1675**	**2346.5**	**2900**
PV			
Ayitepa	-	20	20
GIC	20	50	50
Grn Ele	20	40	40
Sankana	20	50	100
Savanah	30	50	100
Signik	20	50	50
TFI Solar	-	-	30
White Cap	20	50	100
Windiga	20	20	20
Total Solar Generation	**150**	**330**	**510**
Wind			
Ayitepa Wind	90	150	225
Ada Wind	-	50	50
Total Wind Generation	**90**	**200**	**275**
Total Generation	**1915**	**2876.5**	**3685**

4 Steady-State Analysis

This chapter presents details of the steady-state analysis performed on the NITS for the three scenarios. These studies are carried out to investigate the state of the network and its readiness to accommodate RE.

4.1 Study Assumptions

Due to data confidentiality in Ghana, not all information on the network were made available for the research. Some assumptions and simplifications were therefore made to enable the modelling, simulations and subsequent analysis to be performed in this thesis.

4.1.1 Study Time Period and Demand Adjustment

Based on the focus of this research on the analysis of the impact of RE generation, the study time was identified to be the period of maximum RE generation, which occurs during the off-peak as explained below.

The figure below presents the daily system demand curve for randomly selected days in the NITS. An observation of the load curves indicates a slight variation of the demand pattern in the different seasons: rainy (April, May and June) and dry seasons (January and February).

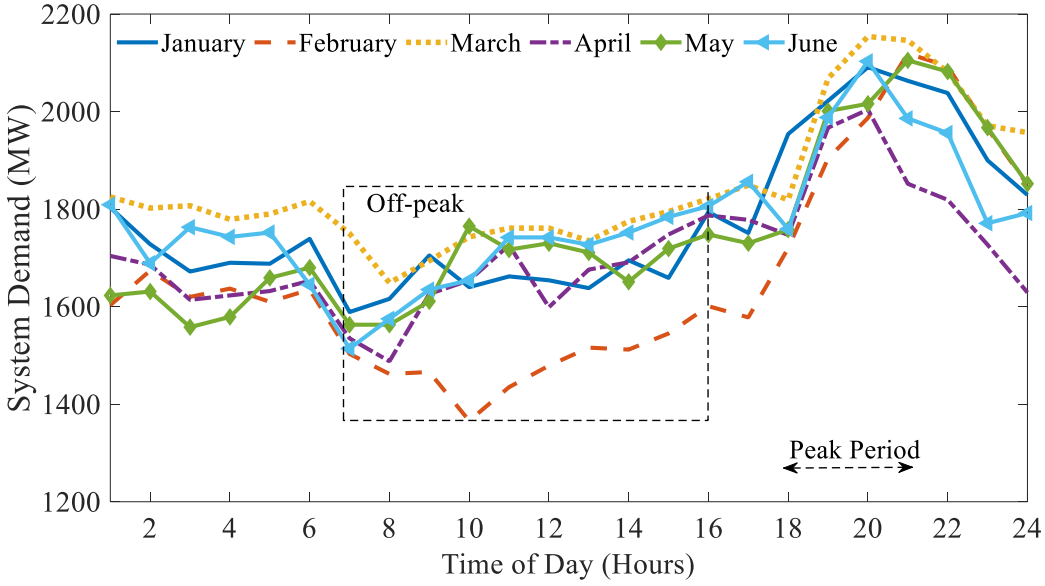

Figure 4-1: Hourly System Demand in the NITS

As seen from the figure, the demand curve consists of two system peaks; a minor peak in the early morning hours between 05:00 and 06:00 and a major peak (marked with the arrow) in the evening between 18:00 and 21:00. The main system peak however occurs mostly at 19:00.

The time frame outside the peak period is the off-peak period, which in the NITS occurs between 7:00 and 16:00 due to the low demands recorded during that time.

On the other hand, a consideration of the daily irradiation distribution in Ghana (see Figure 4-2) indicates that the solar irradiation peaks between 10:00 and 16:00 with the maximum irradiation occurring between 11:00 and 14:00, which is also the off-peak period in the NITS.

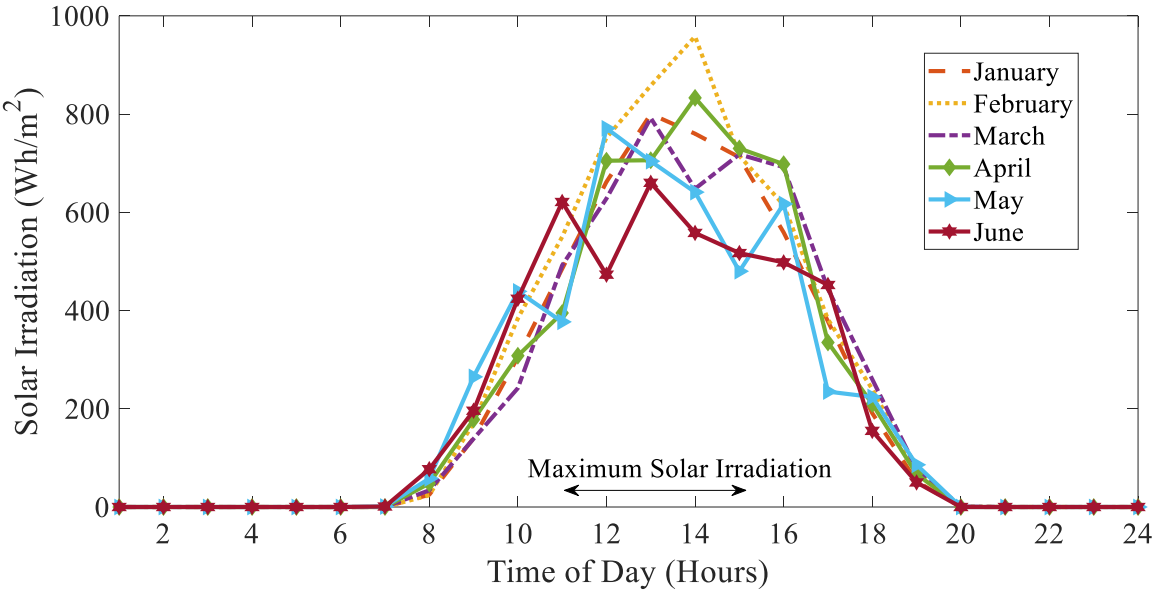

Figure 4-2: Sample Daily Solar Irradiation of Selected Days

The superposition of the daily demand curve with the solar irradiation curve (see Figure 4-3) indicates that the maximum solar irradiation in Ghana occurs during the off-peak period and thus justifies the use of the 'off-peak' period as the time for the analysis in this thesis.

About eight hours of sunshine hours per day and an average solar irradiation of 4-6 kWh/m^2-day (maximum irradiation of 5.6 kWh/m^2-day) is recorded in the north of the country [88].

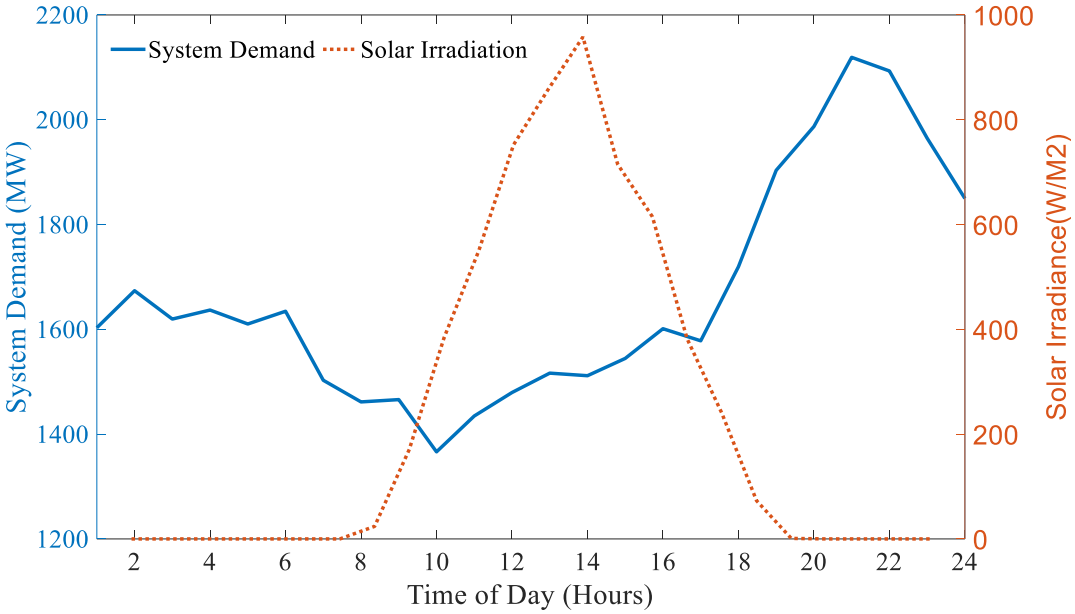

Figure 4-3: Hourly Solar Irradiation and System Demand

To calculate the off-peak demand, a parameter known as the load factor was defined and calculated for the NITS. The load factor (LF) is defined as the ratio of the average off-peak demand to the peak demand in a specified period of time. Load factors provide information on the variability of demand in a power system. Low load factors (typically less than 75%) are indicative of a highly variable system demand while load factors greater than 75% depict a constant system, which is ideal for every power system [89].

$$\text{Load Factor (LF)} = \frac{\text{Average Load}}{\text{Peak Load}} \tag{4.1}$$

Calculation of the load factor for the NITS resulted in values within the range of 80% and 89%, which also coincide with the 84% average load factor defined by the VRA [21]. A load factor of 85% was thus used to model the system demand to the off-peak characteristics.

Owing to the high load factor of the NITS, the variability of the loads was not considered in the analysis. All loads were assumed to be static with no motor loads. The voltage dependency of the loads was not considered in the load flow and other subsequent analysis.

4.1.2 Uniform Load Power Factor

Low load power factors in parts of the NITS lead to voltage problems to which various measures have been put in place to deal with. These measures include

reactive compensation and power factor correction measures such as penalty charges to customers with poor power factors (less than 0.90 lagging) [50]. In taking into accounts the improvement measures, which are mostly employed in the distribution networks and not represented in the NITS, loads in the model were assigned a power factor of 0.90[18]. The 0.90 (lagging) power factor used also complies with the minimum average power factor specified in the national grid code (0.90 lagging ≤ PF ≤ 1) [2, 50] to be used by all connections in the transmission network.

4.1.3 Load Growth in the NITS

Economic development in Ghana has resulted in a constant increase in system demand, which translates into an average annual demand growth rate of between 7 and 13% [21, 85]. The Compound Annual Growth Rate (CAGR) was thus fixed at **10%** [86, 90] to be used in the simulations. Demand in the NITS was therefore increased by 10% in each year till the end of the study year.

Summary

- Based on the focus of the research on the impact of RE in the NITS, the study time for the analysis was determined to be the off-peak period, which is also the period of maximum RE generation.
- The load factor, which gives information on the demand variability in the network was calculated to be 85% in the NITS.
- The off-peak demand was subsequently determined using the load factor.
- The load models were assumed to have a uniform power factor of 0.90 to take into consideration the diverse power factor correction measures utilised in the power system.
- Load growth in the NITS was set at an annual rate of 10% for the simulations.

18 Based on a discussion with the Ghana Grid Company (GridCo)

4.2 Load Flow

Load flow analysis is performed in the power system to determine the power flow and voltages at various busbars in the network for any given condition. Load flow analysis forms the basis of static security analysis [91] and also constitutes an important study for network planning, operation and expansion. The analysis of load flow therefore serves as the starting point for further grid studies and analysis [56] as presented here. A summary of the basic theory of load flow analysis is given in the next sub-chapter, followed by the identification of the bottlenecks in the NITS and the corresponding measures to manage the bottlenecks.

4.2.1 Introduction to Basic Theory

Load flow analysis is a steady-state network analysis used in power system studies to determine the state of a power system in a given steady-state condition. Load flow analysis involves the computation of the voltage (magnitude and angle) at each bus as well as the power flow (active and reactive) in each line in the network [18, 52]. The magnitude and angle of the bus voltage are known as the system state (independent) variables as their values describe the state of the system. These state variables are further used to calculate other system quantities such as voltage drop, power flow and power losses, etc. [52, 92].

Load flow is computed using a set of non-linear algebraic equations that are built using the generation and load data of a power system. The nodal equation of the network used to compute the load flow [92] comprises the π-equivalent models of the transformers and transmission lines together with the numerical values of the series impedance, Z or line admittance, Y [52] and is written as follows:

$$\underline{I} = \underline{Y} \cdot \underline{V} \; or \; \begin{bmatrix} \underline{I}_1 \\ \underline{I}_2 \\ \cdots \\ \underline{I}_N \end{bmatrix} = \begin{bmatrix} \underline{Y}_{11} & \underline{Y}_{12} & \cdots & \underline{Y}_{1N} \\ \underline{Y}_{21} & \underline{Y}_{22} & \cdots & \underline{Y}_{2N} \\ \cdots & \cdots & \cdots & \cdots \\ \underline{Y}_{N1} & \underline{Y}_{N2} & \ldots & \underline{Y}_{NN} \end{bmatrix} \cdot \begin{bmatrix} \underline{V}_1 \\ \underline{V}_2 \\ \cdots \\ \underline{V}_N \end{bmatrix} \tag{4.2}$$

where the subscript *N* represents the total number of nodes in the network; $\underline{Y}_{ii}$ is the *self-admittance* of node i (equal to $\underline{Y}_{ii} = \sum_{i=1}^{N} \underline{Y}_{jj}$, the sum of all the admittances terminating at node i); $\underline{Y}_{ij}$ is the *mutual admittance* between nodes i and j (equal to the negative sum of all admittance between nodes i and j).

The nodal admittance matrix $\underline{Y}$ made of $\underline{Y}_{ij}$ is described by the following equation:

$$\underline{Y_{ij}} = \left|\underline{Y_{ij}}\right|\angle\theta_{ij} = \left|\underline{Y_{ij}}\right|\cos\theta_{ij} + j\left|\underline{Y_{ij}}\right|\sin\theta_{ij} = G_{ij} + B_{ij} \quad (4.3)$$

where G_{ij} and B_{ij} are the conductance and susceptance of the element $\underline{Y_{ij}}$.

The voltage at a given bus *i* of the system is also given as

$$\underline{V_i} = |V_i|\angle\delta_i = |V_i|(\cos\delta_i + \mathrm{j}\sin\delta_i) \quad (4.4)$$

The current injection at node *i* in the network can also be calculated as follows using the admittance at node ij, Y_{ij}

$$\underline{I_i} = \underline{Y_{ii}}\underline{V_i} + \sum_{j=1;j\neq 1}^{N} \underline{Y_{ij}}\underline{V_j} \quad (4.5)$$

The complex conjugate of the total power injected (real $\underline{P_i}$ and reactive power $\underline{Q_i}$ entering the network) at the node *i* is expressed as

$$P_i - jQ_i = V_i^* \sum_{j=1}^{N} \underline{Y_{ij}}\underline{V_j} \quad (4.6)$$

Substituting equations (4.3) and (4.4) into equation (4.6) and expanding into real and imaginary parts results in the following

$$P_i = |V_i|^2 Y_{ii}\cos\theta_{ii} + \sum_{j=1,j\neq 1}^{N} \left|\underline{Y_{ij}}\underline{V_i}\underline{V_j}\right|\cos\left(\theta_{ij} + \delta_j - \delta_i\right) \quad (4.7)$$

$$Q_i = -|V_i|^2 Y_{ii}\sin\theta_{ii} + \sum_{j=1,j\neq 1}^{N} \left|\underline{Y_{ij}}\underline{V_i}\underline{V_j}\right|\sin\left(\theta_{ij} + \delta_j - \delta_i\right) \quad (4.8)$$

The load flow is computed based on equations (4.7) and (4.8) to solve for the values of the unknown bus voltages and other quantities P_i, Q_i, $|V_i|$, δ_i.

Iterative Methods for Solving Load Flow

The non-linearity of load flow problems requires iterative techniques to solving them. Existing iterative methods include the Gauss-Seidel and Newton-Raphson methods, which are developed using the admittance equations (4.5 above) [92].

The Gauss-Seidel method involves the process of solving linear algebraic equations (in rectangular form) and is based on the expression of the bus voltage as a function of real and reactive power [92, 93]. The Gauss-Seidel method is simple, reliable and tolerant of poor voltage conditions [18]. It however has the disadvantage of a slow convergence due to the excessive number of iterations required [93] and the weak diagonal dominance of the admittance matrix [18]. Nonetheless, acceleration factors are used to improve the rate of convergence [18, 93, 94]. As the computation time increases proportionally with the size of the system, the method is considered highly time intensive, as much time is required for all parameters to be solved [95].

The Newton-Raphson method involves solving equations of the voltage and line admittance expressed in polar forms [92–94]. The Taylor's series expansion forms the basis of this method of solving load flow problems [18, 93]. Contrary to the Gauss-Seidel method, this method has a good convergence rate [18] but is not suitable for load flow problems which have initial voltages that differ from their actual values (flat start). Despite, the method is also ideal for large power systems that require accurate solutions [18].

4.2.2 Load Flow in the NITS

The Newton-Raphson method was used to compute the load flow in the NITS. The resulting voltages of the busbars during the load flow is presented in Figure 4-4, which also shows the 5% voltage margin (0.95 – 1.05 p.u.) during normal operation.

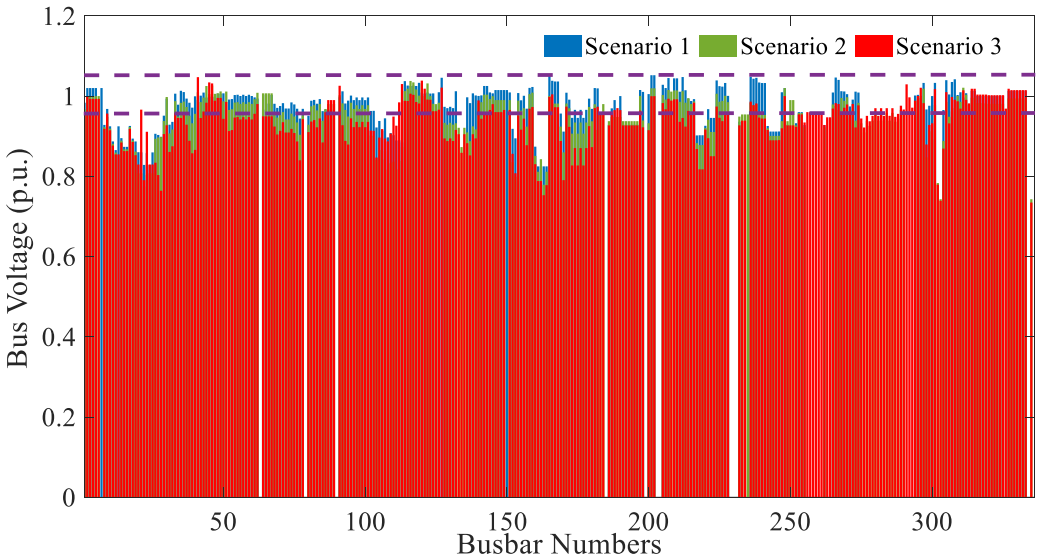

Figure 4-4: Voltage Profile of the Busbars in the NITS

The figure shows that the 5% voltage margin for normal operation was violated on several busbars. The voltages on these busbars were lower than the 0.95 p.u. limit (as seen from the figure) - currently a major challenge in the NITS. Voltages on busbars in the heavily loaded areas of the network were recorded to be as low as 0.83 p.u. and 0.74 p.u. in scenarios 1 and 2 respectively. This confirms the prevailing voltage issues in the NITS, which is expected to worsen with the increase in RE generation (due to the reduction in conventional generation leading to a reduction in the available reactive power), when no measures are taken. Existing bottlenecks in the NITS will thus be identified as follows.

4.2.3 Identification of Existing Bottlenecks

The monitoring and identification of violations (of defined limits) form the main aspect of system security assessment [91], especially as the overloads recorded: the voltage and transient stability margins, etc. form the basis for classifying a power system [96]. The limits specified in the national grid code for normal system operation are 0.95 p.u. – 1.05 p.u. for system voltage and ≤ 85% for equipment loading[19] [50]. The bus voltage and equipment (transformers and transmission lines) loading during load flow were thus monitored to identify the bottlenecks based on the limit violations.

Equipment Overload

The transformer and transmission line loadings recorded in the three scenarios are presented respectively in Figures 4-6 and 4-7. The percentage loading is shown on the y-axis and the equipment (indicated with numbers) on the x-axis. The 85% loading threshold for normal operation is also shown in the figure.

[19] Refers to both short-term and long-term loadings

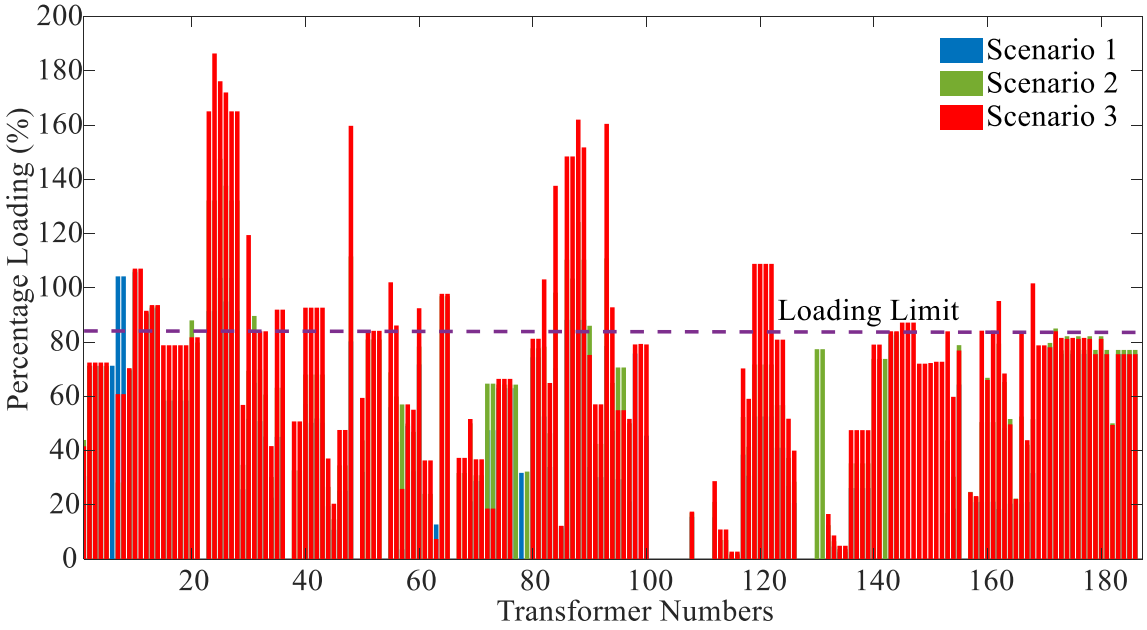

Figure 4-5: Transformer Loading in the NITS for Scenarios 1 - 3

An observation of the figure indicates an increased number of transformer overloads with increasing demand and generation from scenarios 1 to 3 (S1 to S3). As introduced in Chapter 3.7, the future scenarios (S2 and S3) are developed based on increasing demand and generation as well as network infrastructure. As expected, the demand and capacity additions in these scenarios resulted in an increased number of transformer overloads. For scenario 1, only a few transformers were loaded above the 85% allowed loading limit. The increased number of overloads in scenarios 2 and 3 is a clear indication of the need for the transmission network expansion and reinforcement.

The loading of the transmission lines in the NITS is also presented below. While no line overload was recorded for scenario 1, a few overloads were recorded in scenarios 2 and 3, particularly in the load-dense areas of the NITS. The increased transmission line usage for the evacuation of larger amounts of power in S3 resulted in very high transmission line overloads such as 187%.

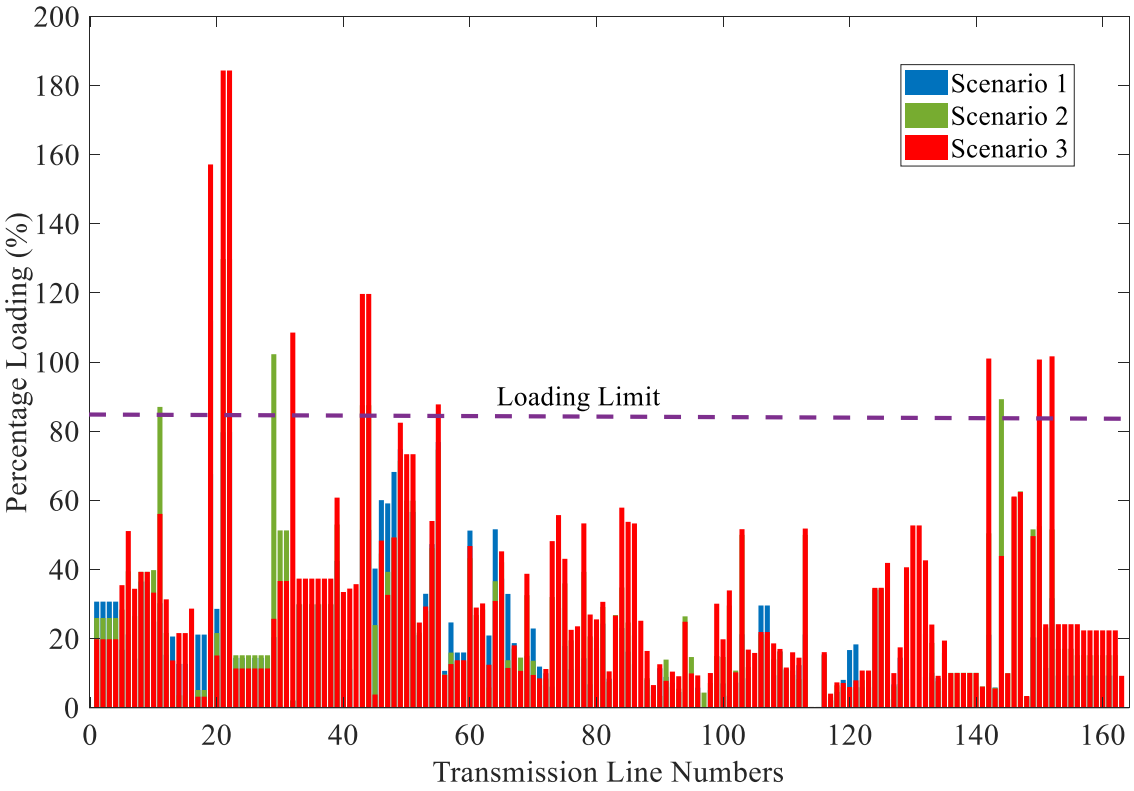

Figure 4-6: Transmission Line Loading in the NITS for Scenarios 1 - 3

Below is a single line diagram (SLD) of the NITs, which shows the locations of the transmission line and transformer overloads in the network.

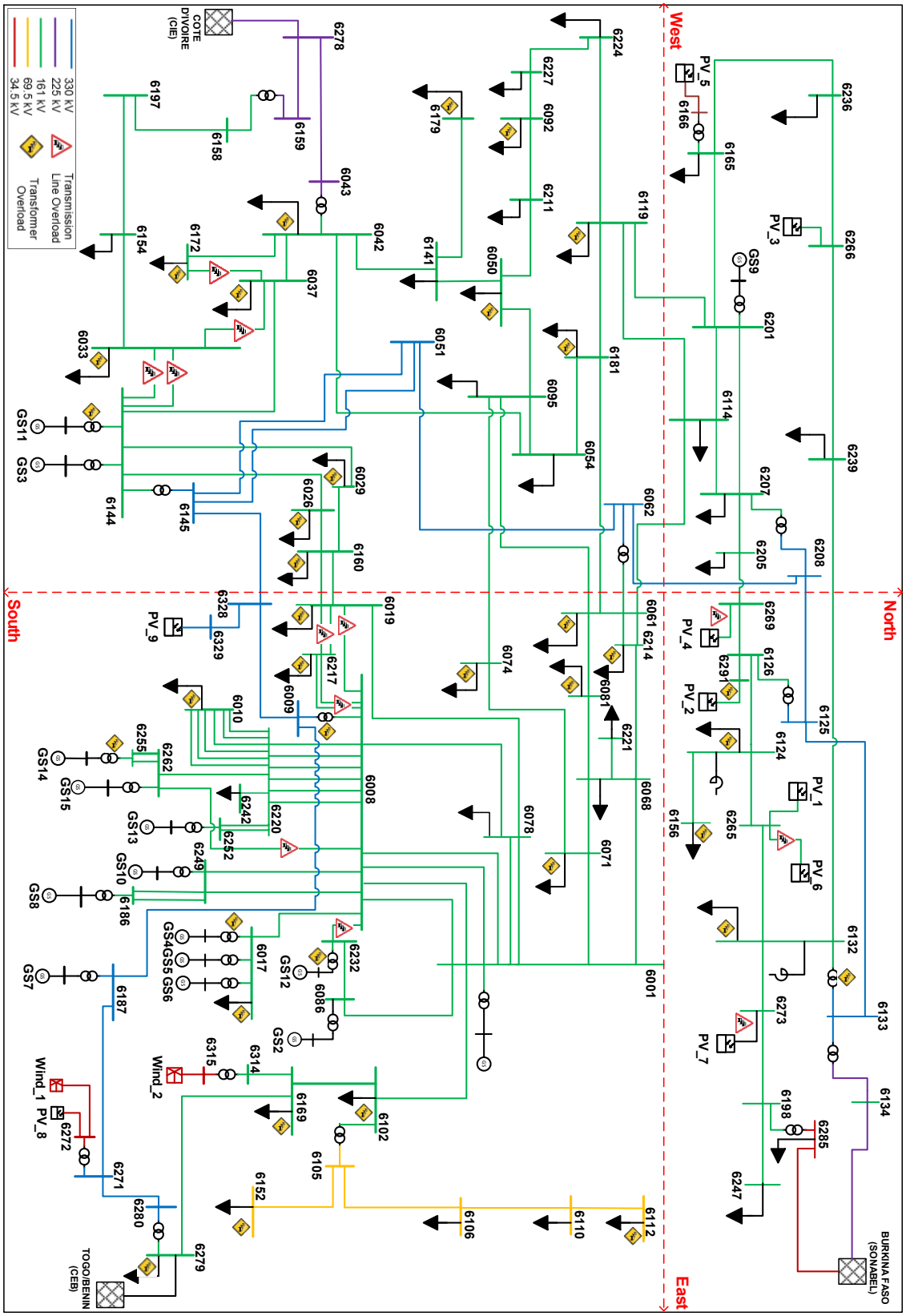

Figure 4-7: Single Line Diagram of the NITS with the overloaded equipment

Sustained overloading on power system equipment leads to voltage reduction with subsequent increase in the transformer current flow and thermal capability of transmission lines [97]. Transmission line overload for instance has the potential

of leading to system instability as has been recorded in the past (was the cause of the 2003 blackout in Italy [30]). The dynamics of the line loading as well as the loading of the transformers and cables depend not only on the load but also on the location and size of the generator, especially as the generators largely contribute to the increased loading [33]. Thus, the transmission line and transformer overloads recorded in the NITS highlights the importance of planning and coordinating the generation increase and (proposed) network expansion measures to cater for the load growth in the different scenarios.

Voltage Violations

Several busbars in the NITS experience low voltages even during normal operation, which is attributed to the transfer of large amounts of power and the resulting reduction in reactive power. The inadequate reactive compensation in some parts of the network also results in poor supply voltage [2], which when not properly dealt with culminates in voltage collapse [30]. High voltages are also recorded at the end of most long transmission lines that run from the south to the north of the NITS. In addition to the voltage control functions of the synchronous generators, diverse compensation devices have been installed to make up for the reactive power imbalance and hence regulate system voltage. The bus voltages recorded for the three scenarios are presented in Figure 4-8 below. The figure shows the violation of the 5% (0.95 p.u. – 1.05p.u.) voltage stability margin (indicated with the lines) on some busbars even for normal operation.

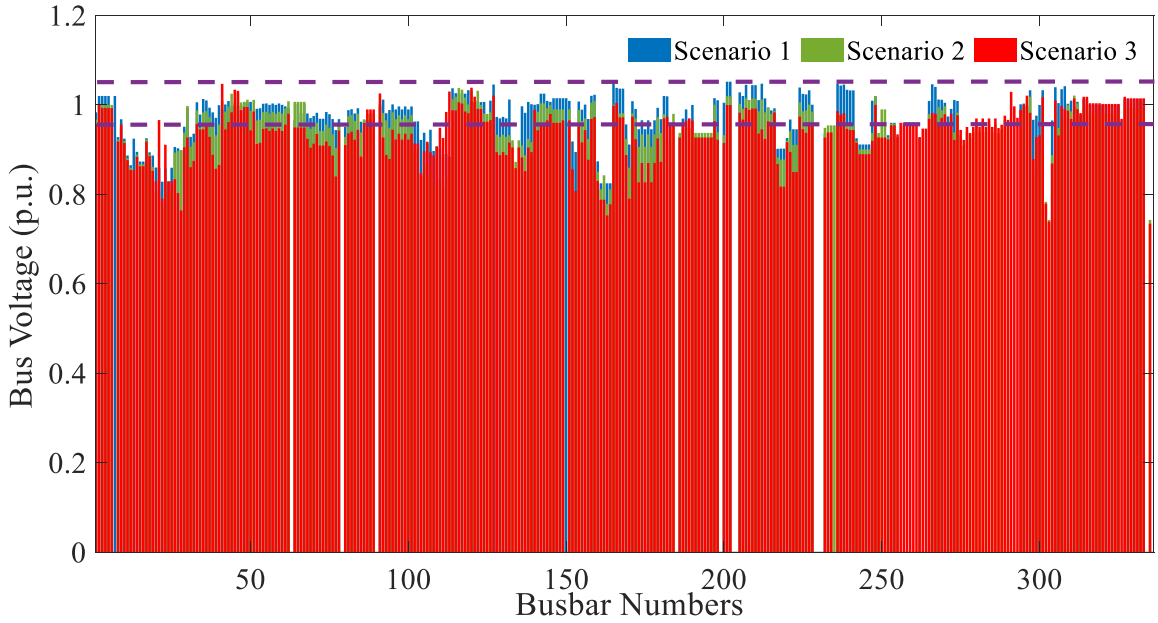

Figure 4-8: Bus Voltages in the NITS for Scenarios 1 - 3

While no violation of the upper voltage limit (1.05 p.u.) was recorded, several busbars had voltages that violated the 0.95 p.u. lower voltage limit. Transmission networks generally have a high X/R ratio, which implies that slight changes in the reactive power lead to significantly high changes in the voltage. Voltage variations in transmission networks are therefore solely determined by the reactive power flow due to their high sensitivity to voltage changes [33]. The increased reactive power demand in the network in scenario 3 thus resulted in very poor bus voltages.

4.2.4 Correction Measures for the Bottlenecks

The identified equipment overloads were resolved with a capacity upgrade, which considers an 80% maximum loading.[20] The new ratings of the transmission lines and transformers were calculated using their respective currents and voltages.

Transmission Line Uprating

Resolving transmission line overloads usually involves the construction of new lines or increasing the current carrying capacity of existing lines, by either increasing the transmission voltage or rated current (thermal rating) of the line. The limited availability of Right-Of-Way (ROW) for new transmission lines in most networks however lead to restrictions and delays in transmission network expansion, which mostly results in several conditions of overloading as power is continuously evacuated in the operation of the power system [98]. Due to the high population density and land scarcity in parts of the NITS coupled with severe transmission line overloads and the prolonged project execution times, the methods of increasing the line capacity using the 'line uprating' method is preferred over the construction of new transmission lines.

Traditional methods of uprating transmission lines, i.e., increasing the current carrying capacity include increasing the line voltage, number of conductors or the thermal ratings of the lines, which in most cases require the strengthening of the transmission line towers too [99, 100]. Uprating the transmission line by increasing the line voltage is the most expensive option as additional electrical isolation and infrastructures such as insulators, substation equipment, etc. must be changed to the new voltage level. Substation equipment (and their insulation) also need to be upgraded to the new voltage, which translates into additional costs [99–101]. Increasing the line voltage to uprate transmission lines additionally requires

[20] Although 85% is prescribed by the grid code as the load limit, a safety limit of 80% is used to ensure that the loading limit is not violated at any point.

an increase in the conductor cross-section, which results in double cost as against increasing only the conductor cross-section. This method is also associated with an increase in the corona effect due to the increase in the electrical field, which is minimized by bundling the conductors. Thorough economic and technical assessments are thus required for this method.

The method of increasing the operating temperature of the line conductor is one of the simplest methods currently utilised in the industry [99, 100, 102]. With operating temperature of 80℃, the lines in the NITS cannot be increased any further due to the increased likelihood of the occurrence of annealing at temperatures above 90℃. Although increasing the conductor temperature to 90℃ results in a significant increase in the rating at minimum cost and implementation time [102], the significant sunshine in Ghana limits a further increase of the conductor operating temperature to 90℃. Increasing the operating temperature as a means of uprating additionally requires the analysis of the impacts of annealing, the effectiveness of the compression joints and high temperature creep [102].

An alternative method to uprating transmission lines is to increase the thermal properties of the lines in a process known as thermal uprating, which indirectly increases the lines' rated currents [100, 102]. The choice of the appropriate conductor or upgrading method is not always a simple task and may vary depending on existing technical and economic constraints. Considering the information on the NITS available for this thesis, the thermal uprating method is used to uprate the overloaded transmission lines as explained below.

Thermal Uprating of Transmission Lines

The rated currents of the overloaded lines are increased to values, which maintain a loading level of less than 85%. The new current ratings of the lines are calculated using the equations below.

$$I_{rated} = \frac{A}{\sqrt{3} \cdot U_n} \tag{4.9}$$

where I_{rated} is the rated current in kA, A is the line ampacity, also known as the MVA rating or thermal limit and U_n is the rated voltage in kV. The line ampacity is further calculated as follows:

$$A = \frac{\sqrt{3} \cdot U_n \cdot I_{rated}}{1000} \tag{4.10}$$

The ampacity of the line is limited by the physical make-up and the maximum allowable sag of the cable, which are also dependent on weather conditions such as solar irradiation, wind speed and ambient temperature, etc. [103, 104].

Based on the 85% maximum loading specified by the grid code for normal operation, an 80%[21] safety limit is used to calculate the new rated currents and ampacities as follows:

$$I_{rated,new} = \frac{A_{new}}{\sqrt{3} \cdot U_n} \tag{4.11}$$

$$A_{new} = \frac{I_{(hv)}}{0.8} \cdot \sqrt{3} \cdot U_n \tag{4.12}$$

$I_{rated,\ new}$ is the new rated current in kA and A_{new} is the newly calculated ampacity.

The figure below presents results of load flow analysis for all three scenarios using the updated ratings. By implementing the thermal uprating method described above, line overloads were cleared, as the loadings on all transmission lines were within the 85% limit.

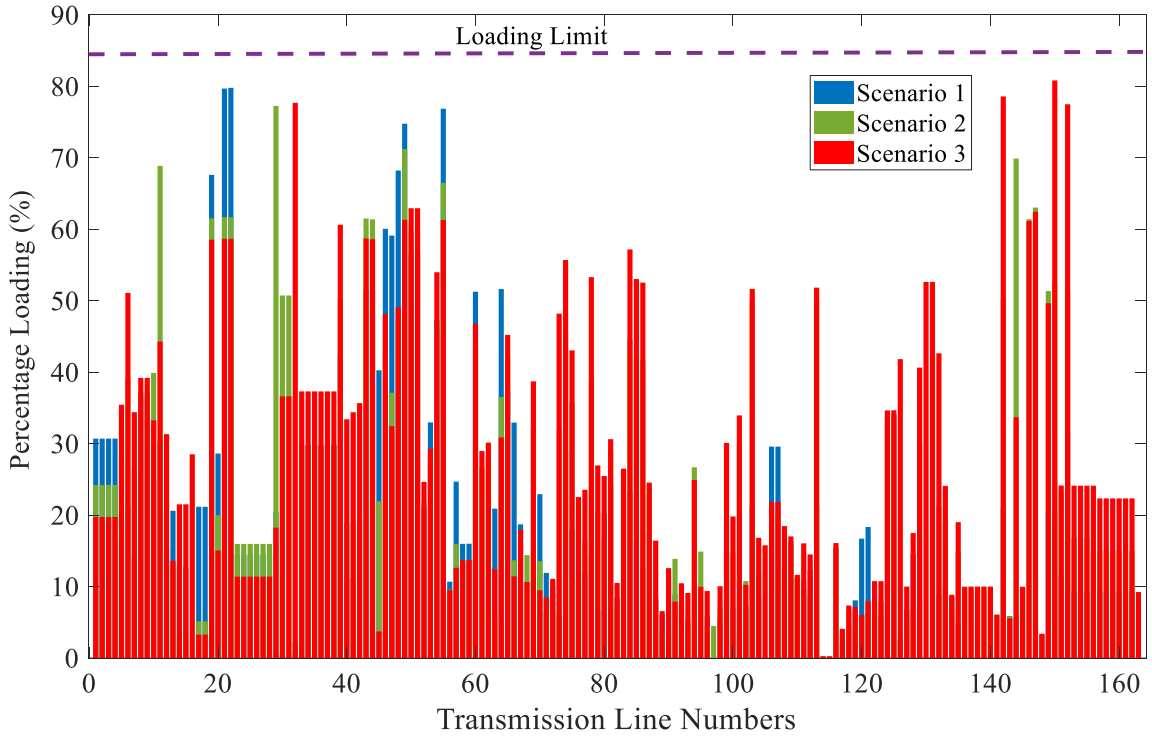

Figure 4-9: Transmission Line Loading in the NITS with Updated Transmission Line Ratings

[21] An 80% safety limit is used in this research as a means of safeguarding the lines against possible load increase in the near future.

Transformer Upgrading

A process similar to the transmission line upgrade was used to resolve the transformer overloads in the NITS. The new transformer ratings were calculated using equations 4.13 and 4.14 below, with all parameters referred to the high voltage side of the transformer.

$$loading_{hv} = \frac{|I_{(hv)}|}{I_{rated\ (hv)}} \cdot 100 \tag{4.13}$$

$$I_{rated(hv)} = \frac{S_{rated(hv)}}{\sqrt{3} \cdot U_{n(hv)}} \tag{4.14}$$

$I_{(hv)}$ is the transformer current; $I_{rated(hv)}$ the rated current of the transformer; $S_{rated(hv)}$ the transformer rated ampacity and $U_{n(hv)}$ the rated voltage of the transformer all referred to the high voltage side of the transformer.

To further ensure the transformers are not loaded above the 85% limit, the transformer loading at any given time was set to be less than 85%. New MVA ratings[22] for the transformers were similarly calculated using a percentage loading of 80%:

$$S_{rated,new} = \sqrt{3} \cdot U_{n(hv)} \cdot I_{rated\_new} \tag{4.15}$$

$$I_{rated,new} = \frac{I_{(hv)}}{0.8} \tag{4.16}$$

Figure 4-10 below shows the results of load flow analysis with the updated transformer sizes, which indicate no transformer overload for all three scenarios.

[22] The S-rated values were selected based on the list of available transformer sizes in the NITS.

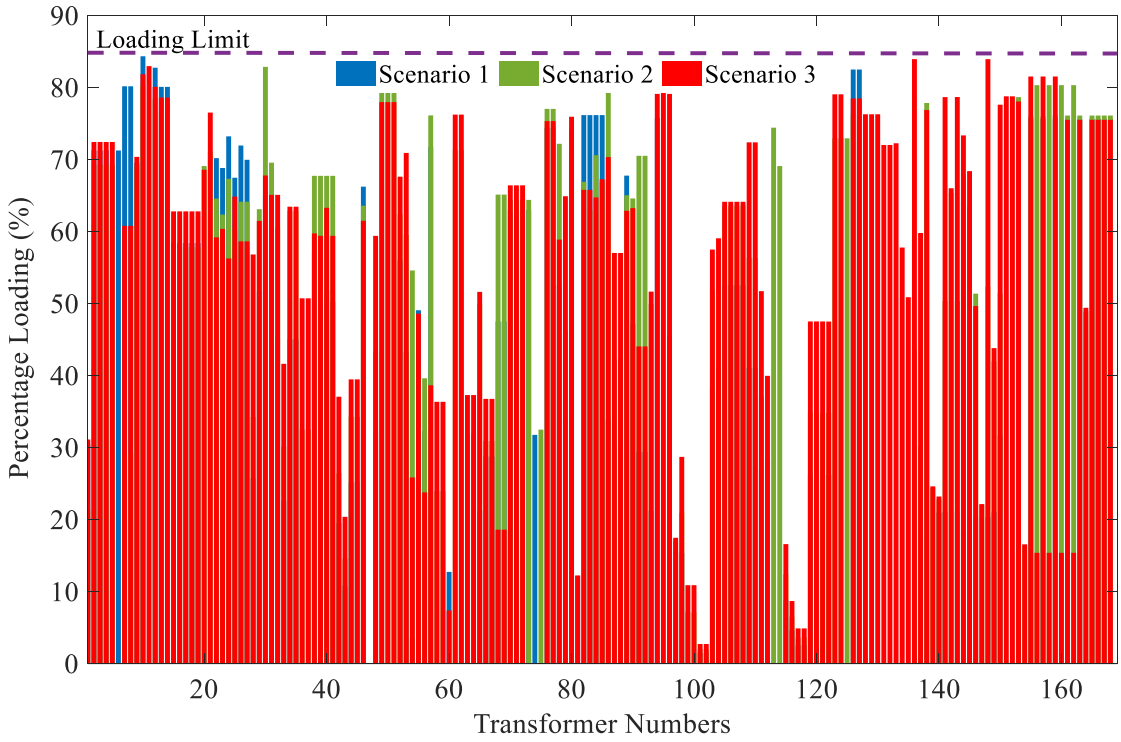

Figure 4-10: Transformer Loading in the NITS with Updated Transformer Ratings

4.3 Optimum RE Penetration in the NITS

This section describes the process of identifying the maximum RE penetration that the NITS can accommodate considering violations of defined limits. The genetic algorithm (GA) method of solving constrained and unconstrained optimization problems is used. Originally proposed locations of the RE units in the NITS are thus maintained with the aim of determining the maximum sizing of the RE units. The objective is to minimise grid losses and ensure that busbar voltages and equipment loadings are within defined limits at all times. The decision/control variables of the optimization will be the outputs of the RE units, which are their respective maximum power output as specified in the network model.

The objective function for minimizing grid losses is expressed in (4.17) as

$$S = I^2 \cdot Z \tag{4.17}$$

The constraints based on the bus voltage and thermal ratings of the transmission lines are given as

$$V_i^{min} \leq V_i \leq V_i^{max} \tag{4.18}$$

$$S_i = S_{rating} \tag{4.19}$$

The GA starts by randomly selecting the initial values of the control variables (outputs of RE units) which are within the maximum and minimum values as shown in table 4-1. The table presents the minimum and maximum outputs of the RE units as specified by the Energy Commission of Ghana.

Table 4-1: Maximum and Minimum Values of the Decision Variables

PV Units	Active Power Output, P (MW)	
	Minimum	Maximum
Ayitepa Wind	0	225
GIC PLANT	0	50
Green Electric	0	40
Sankana	0	100
Savannah	0	100
Signik	0	50
Whitcap	0	100
Windiga	0	20

The flow chart for the optimization process is presented in Figure 4.11 below:

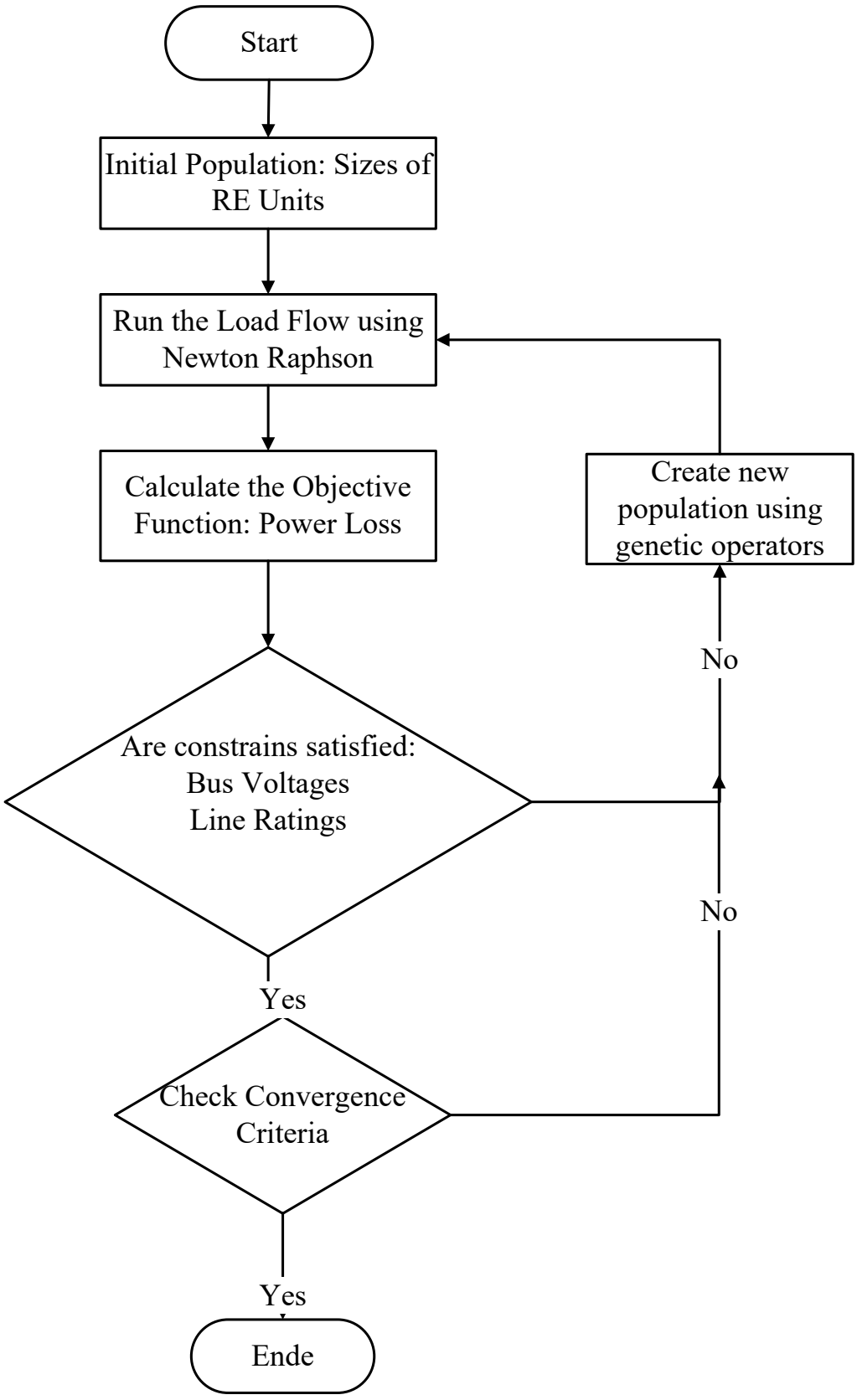

Figure 4-11: Flowchart for the Optimization Algorithm to Determine the Optimum Sizes of RE Units

The results of the optimization are presented in Table 4-2 below for the three scenarios under consideration in this research.

Table 4-2: Optimal Sizing of RE Units in the NITS

RE Unit	*Scenario 1*	*Scenario 2*	*Scenario 3*
Ayitepa Wind	**27.68**	**54.84**	**93.05**
GIC	**9.15**	**32.40**	50
Green Electric	**35.10**	40	40
Sankana	20.16	**45.11**	100
Savannah	**24.81**	**68.65**	100
Signik	**28.86**	**37.52**	50
Whitecap	**13.82**	**47.94**	100
Windiga	20	20	20

The table shows the optimal sizes for the RE units in the NITS that will not violate the 5% voltage margin and 85% loading limit for normal operation. Comparing the optimization results with the proposed sizes of the RE units (see Table 4-3) indicates that most of the RE units are either 'oversized' or undersized (highlighted in bold in the two tables). This implies that the inappropriately sized RE units may be contributing to violations of the voltage and loading limits as these were used as the constraints in solving the optimization.

Table 4-3: Proposed Sizes of RE Units in the NITS

RE Units	*Scenario 1*	*Scenario 2*	*Scenario 3*
Ayitepa Wind	90	150	225
GIC	20	50	50
Green Electric	20	40	40
Sankana	20	50	100
Savanah	30	50	100
Signik	20	50	50
WhiteCap	20	50	100
Windiga	20	20	20

Table 4-2 further shows that, the sizes of the 'Green Electric' and 'Signik' RE units could be increased in scenario 1 without any violation to given constraints. With an expansion of the network infrastructure in scenarios 2 and 3, the capacity of the RE units also increase further up to their maximum outputs in scenario 3. The results however indicate that the 'Ayitepa Wind' unit, which is the most oversized unit (optimum capacity of 93.05 MW as against the proposed capacity

of 225 MW) remains oversized in scenario 3, where all RE units are at their optimum capacities.

Summary of Results

- Load flow analyses were used to identify the bottlenecks in the NITS, which were mainly equipment overloads and voltage violations.
- Transformer overloads as high as 187% were recorded in parts of the network, especially for scenario 3 without any prior reinforcement measures. Loadings on the transmission lines were all within the defined limits.
- Regarding the voltage violation, no violation of the upper voltage limit was recorded, while several violations of the lower limit were recorded - in some cases 0.50 p.u..
- The method of thermal uprating was used to eliminate the transmission line overloads while the transformer overloads were remedied with capacity upgrades. Implementing such overloads resulted in loadings, which were within the 85% limit.
- The method of solving optimization using genetic algorithm is used to identify the maximum sizes of the RE units under the constraints of voltage and loading limits. The results of the optimization indicate that most RE units have been oversized in scenarios 1 and 2 while being at their optimum capacities in scenario 3. Resizing these RE units could lead to a significant improvement in voltage violations and overloading.

4.4 Identification of Critical Transmission Lines

Despite efforts from the Ghanaian TSO to manage existing voltage and reactive power problems in the NITS, the location of some transmission lines and their respective loadings increase the risks of voltage instability. These transmission lines are termed ‘critical’ or ‘weak’ and are located electrically and physically farthest away from the generating units in 'radial' transmission networks [105]. The critical transmission lines are located in areas of the power system with reactive power deficiencies [106]. Such lines are characterized by lower reactive

power margin, higher voltage change (in percentage), larger reactive power deficiency, higher voltage collapse point on the V-Q curve as well as larger $\partial Q / \partial V$ component (higher sensitivity to reactive power). The above-mentioned characteristics, which are even more pronounced during contingencies are used to identify the critical lines during normal operating conditions. Different indices exist in literature and practice, which are used to identify the critical transmission lines based on diverse data availability and efficiency. Voltage stability indices such as the Fast Voltage Stability Index (FVSI), Line Stability Factor (L_{QP}) and New Voltage Stability Index (NVSI) [106–109] were examined and used in this research.

4.4.1 Voltage Stability Indices

Voltage stability indices (VSI) are the most common indices used to identify critical transmission lines or weak buses in power networks. VSIs are classified into the Jacobian-based and system-variable-based indices according to the input variables for solving the equations.

The Jacobian-based VSI are used in the planning and design of power systems to identify the voltage stability margin (network's proximity to voltage collapse). They are used offline and have a high computation demand. The system-variable-based VSI, with their low computation demands are used to identify the weak areas (transmission lines and busbars) in the network during the planning, design and operation of the power system. These VSI have the added benefit of being used both online and offline. The system-variable-based methods will be subsequently used in this thesis.

The system-variable-based methods, as the name indicates, use system variables such as admittance matrices, bus voltage, power flow, etc. They are further classified into the bus and line indices, calculated respectively for busbars and transmission lines. The indices are used to indicate the voltage stability of the network and are formulated based on line and bus parameters [110]. They also provide information on how far a system is from the point of collapse. Line index methods such as the Fast Voltage Stability Index (FVSI), Line Stability Factor (L_{QP}), and New Voltage Stability Index (NVSI) will be considered in this thesis.

The stability criteria for all three indices under consideration (FVSI, L_{QP} and NVSI) is an index value less than one (< 1). As long as the index remains less than one, the system is stable. The power system loses stability with eventual

voltage collapse when the index value exceeds one. An index value greater than 1 is therefore considered unstable, i.e., the closer the index value is to 1, the higher the risk of instability.

Fast Voltage Stability Index (FVSI)

The FVSI is derived from the voltage quadratic equation at the receiving bus of a two-bus system. It is calculated based on the reactive power flow in the lines according to the equation below.

A FVSI value close to one is indicative of the closeness of the particular line to instability $0 \leq FVSI < 1$. This also gives an indication of how stressed a line is in the transmission system [111].

$$FVSI = \frac{4Z^2 Q_r}{{V_s}^2 X} \tag{4.17}$$

Z is the line impedance, Q_r is the receiving end reactive power, V_s is the sending end voltage and X is the line reactance.

Line Stability Factor (L_{QP})

The line stability factor, L_{QP} considers both active and reactive power and is more sensitive to reactive power changes as seen in the equation below:

$$L_{QP} = 4\left(\frac{X}{{V_s}^2}\right)\left(\frac{X}{{V_s}^2}{P_s}^2 + Q_r\right) \tag{4.18}$$

The stability criteria is $0 \leq L_{QP} < 1$

X is the line reactance, Q_r is the receiving end reactive power and V_s and P_s representing respectively the sending end voltage and active power. The L_{QP} is ideal for comparison due to its sensitivity to changes in reactive power [112].

New Voltage Stability Index (NVSI)

The NVSI is suitable for on-line monitoring of the power system under different loading conditions. This index considers to a larger extent the reactive and active powers and does not consider the resistance of the transmission lines [113]. The stability criteria is $0 \leq NVSI < 1$ for all transmission lines.

$$NVSI = \frac{2X\sqrt{{P_r}^2 + {Q_r}^2}}{2Q_rX - {V_s}^2} \tag{4.19}$$

X is the line reactance, P_r and Q_r the receiving end active and reactive power and V_s, the sending end voltage.

Methodology

The process of obtaining the voltage stability indices for the transmission lines is summarised in the flow chart below. System parameters such as voltage, transmission line impedance, and reactance, the sending and receiving end active and reactive power are used to identify the indices.

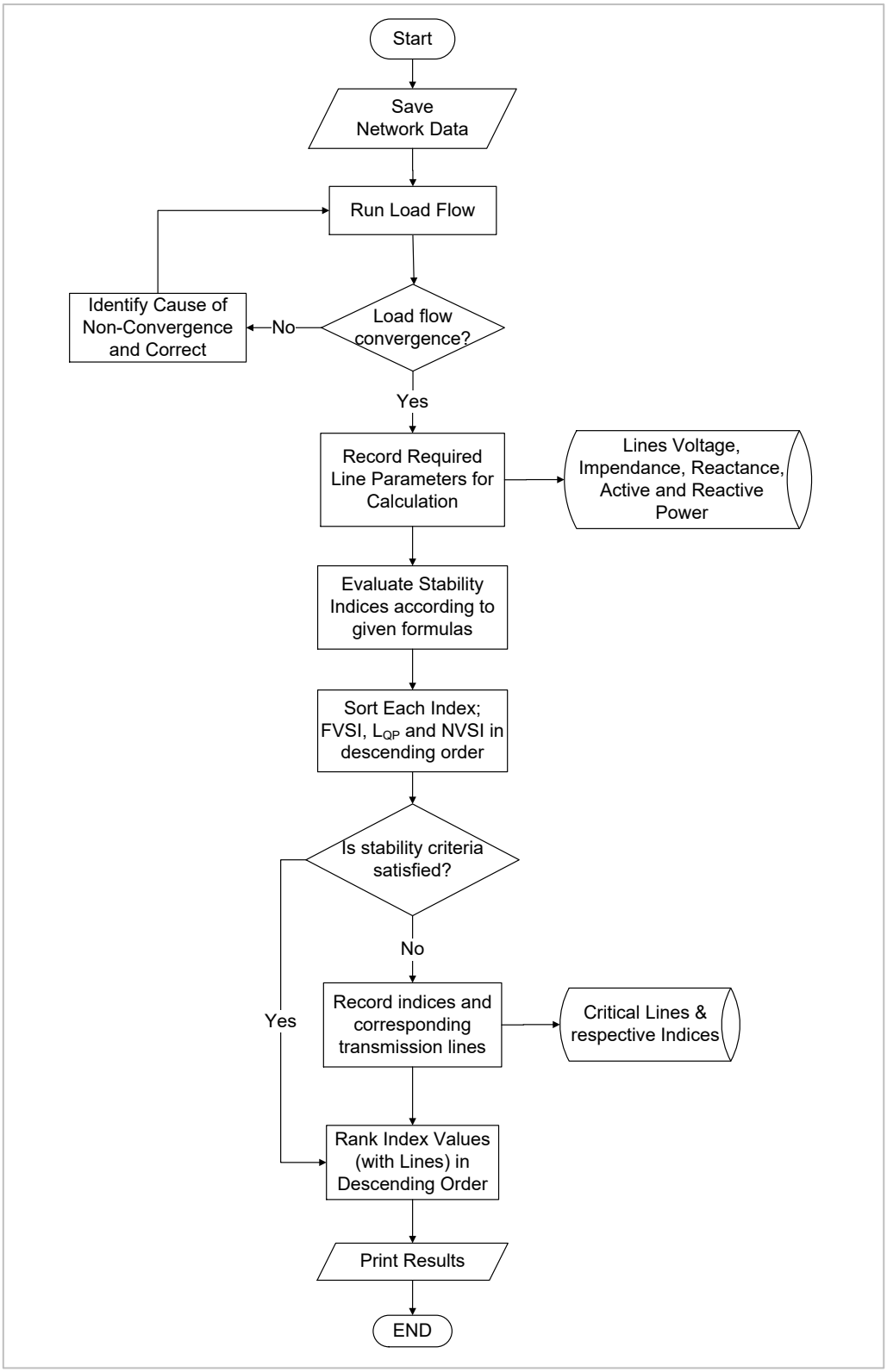

Figure 4-12: Flow Chart for Calculating the Voltage Stability Indices

Results

The transmission lines identified as critical using the stability indices are presented below. With a stability criterion of $0 \leq Index < 1$, values equal to or greater than one on any transmission line denotes increased risks of instability.

The transmission lines with the highest index values (index values closer to unity) are thus defined as critical since the least increase in demand may lead to instability. In other words, these critical lines can only withstand just small amount of load increase before causing voltage collapse.

The figure below shows the results of the FVSI calculated for all transmission lines in the NITS (for all three scenarios). The results indicate only one transmission line (line 147) with an index value greater than 1 (1.003), which is identified in scenario 3. This transmission line, which is the tie-line between Ghana and Burkina Faso also had the highest value in scenario 2, though not greater than 1. The tie-line was commissioned in scenario 2 and was thus absent in scenario 1. The long length of the tie-line (235 km) and the large amount of power exported to Burkina Faso through the line results in very high reactive power losses, which is reflected in the higher stability indices.

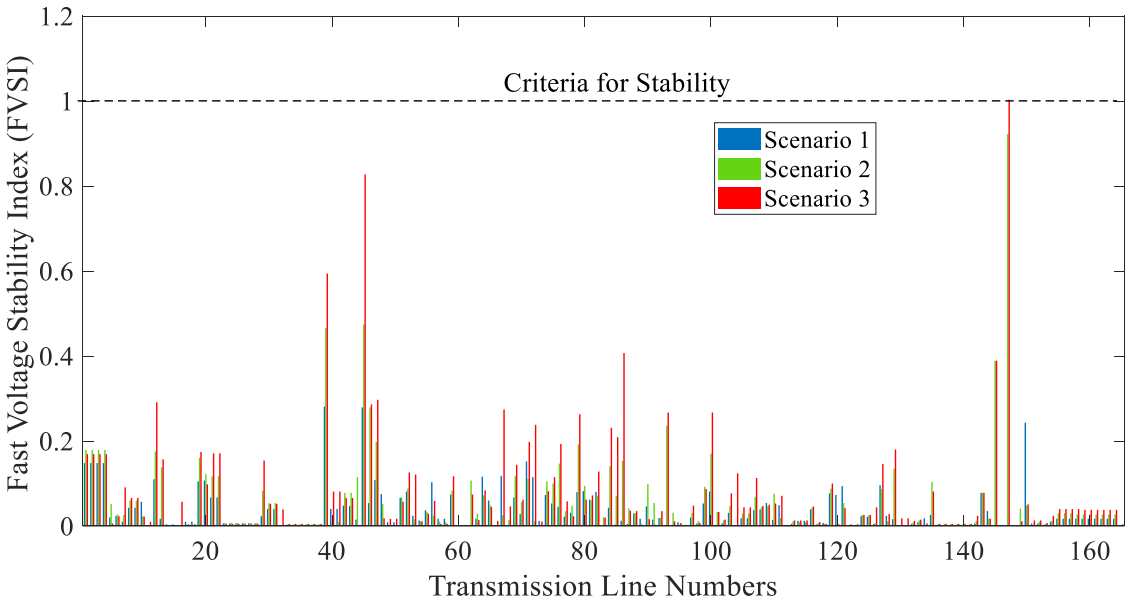

Figure 4-13: Fast Voltage Stability Index (FVSI) for the Transmission Lines in the NITS

It is observed from the figure that the FVSI values increased from scenarios 1 to 3 as a result of changes in the network such as increase in both active and reactive power load. The results indicate scenarios 1 and 2 to be stable as no transmission line was identified critical. The highest index values in scenarios 1 and 2 are 0.281 and 0.922 respectively. Although scenario 2 is stable, it has an increased risk of instability as its index value is closer to 1.

The results of the Line Stability Factor (L_{qp}) calculation presented in figure 4-14 identified two transmission lines as the most critical in the NITS, in scenarios 2

and 3 respectively. Index values greater than the stability limit; 1.119 and 2.327 were calculated for the tie-line in S2 and S3, which are indicative of instability. An additional transmission line was identified critical in scenario 3 with an index value of 1.005. L_{qp} values calculated for the network in scenario 1 were all within the stability limit, with the highest being 0.223.

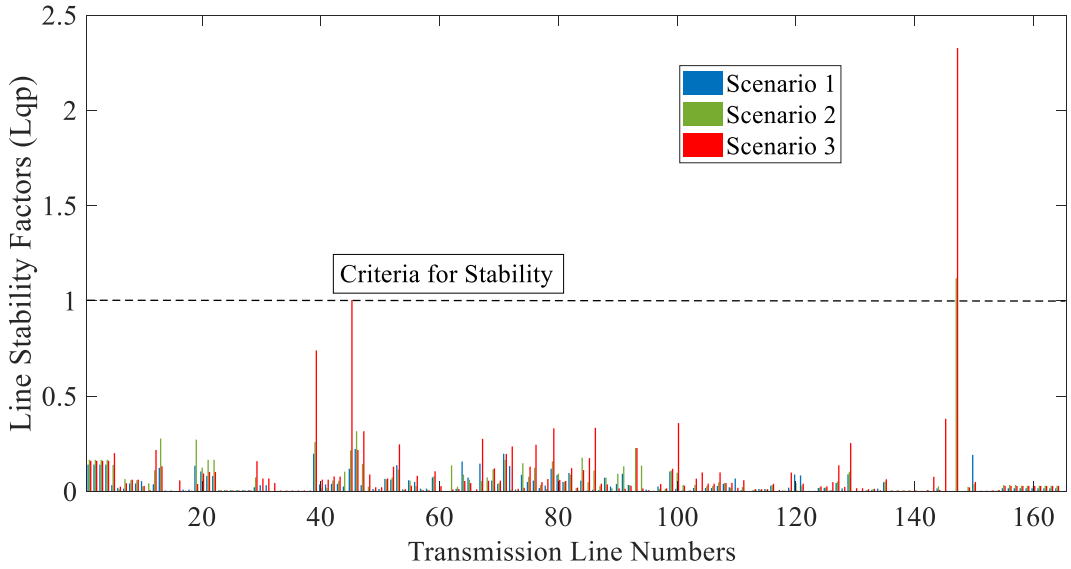

Figure 4-14: Line Stability Factor (Lqp) for the Transmission Lines in the NITS

Calculating the NVSI (see Figure 4-15) resulted in similar characteristics and confirmed the same transmission lines as being the most critical as with the previously calculated indices - FVSI and L_{qp}. The L_{qp} values for the critical transmission lines in scenarios 3 were 1.056 and 2.655, while that for scenario 2 was 2.274.

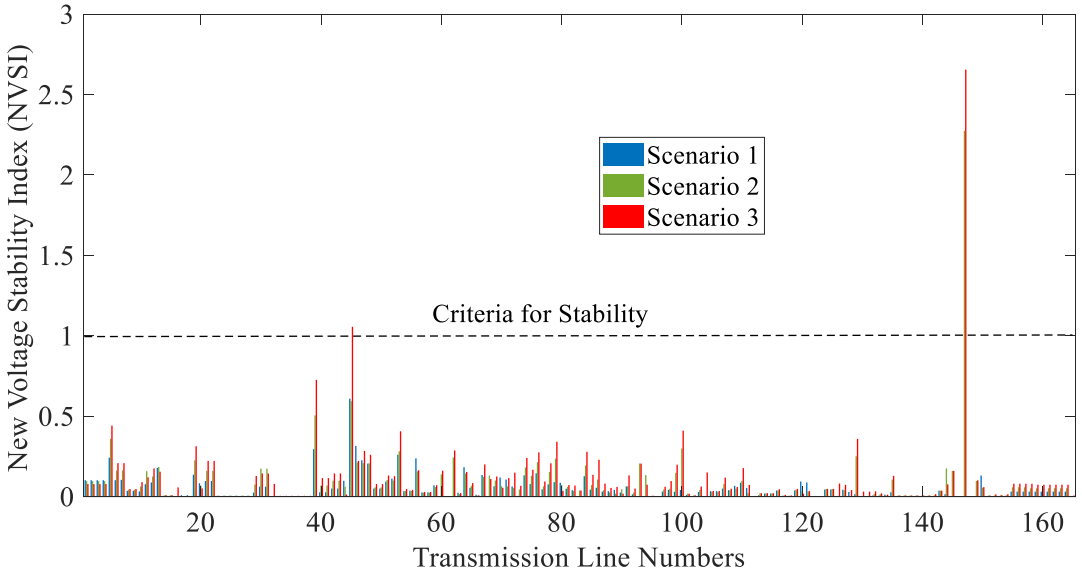

Figure 4-15: New Voltage Stability Index (NVSI) for the Transmission Lines in the NITS

The commissioning of the tie-line in scenario 2 influences the power flow dynamics in the entire network. The high demand on the line and the uncertainties in the parameters at the receiving end of the line (Burkina Faso) increases its risk of instability. Based on the very low voltage at the receiving end of the tie-line, it is confirmed that the loadability limit of the NITS is to some extent defined by this tie-line [29, 37].

Summary of Results

- Three different voltage stability indices – Fast Voltage Stability Index (FVSI), Line Stability Factor (L_{qp}) and New Voltage Stability Index (NVSI) were calculated for all transmission lines to identify the critical transmission lines necessary for the stability analysis.
- Although all three indices used in this thesis provide indication of the closeness of the network to the point of collapse, the FVSI and L_{qp} are extensively based on the reactive power variation while the NVSI considers the variation of both active and reactive power.
- The stability criteria of less than 1 (Index < 1) for all indices was satisfied in scenario 1, which indicates the stability of the NITS in scenario 1 (in other words no critical transmission line in that scenario). Scenarios 2 and 3 had transmission lines with index values violating the stability criteria, hence indicating instability or a higher risk of instability.
- The tie-line between Ghana and Burkina-Faso (L147) was identified as the most critical transmission line as it had the highest index values for all indices.

4.5 Contingency Analysis

The analysis of a power system to determine the severity of an outage to the whole system is known as contingency analysis. Abnormal network conditions, during which thermal overloads and voltage violations are evident in the power system are evaluated using contingency analysis. Typical contingencies include single contingencies (n-1 contingencies), which involve the loss of single elements like transmission line, transformer, generator, compensator, etc [96].

Contingency analysis is required for both short- and mid-term network expansion planning and is thus considered one of the methods of predicting the condition of the power system [114]. Conventional methods for performing contingency analysis involve load flow solutions, which are required to run for each contingency. Though results obtained from this method are accurate, the method tends to be very slow and tedious especially for large interconnected systems [91, 115]. It is thus essential to identify and investigate only the contingencies, which are very critical to system operation. The critical contingencies are identified in a process known as contingency selection [91, 95, 96, 114–116]. The critical transmission lines identified using the voltage stability index will form the basis of the critical contingencies in this thesis.

4.5.1 Transmission Line Contingency

For the transmission line contingency in the NITS, contingencies were defined for all transmission lines in order to validate the (N-1) reliability of the network. The voltage violations recorded during the contingencies indicate that the loss of the tie-line results in several violations in the network, and thus poses the highest risk to the network.

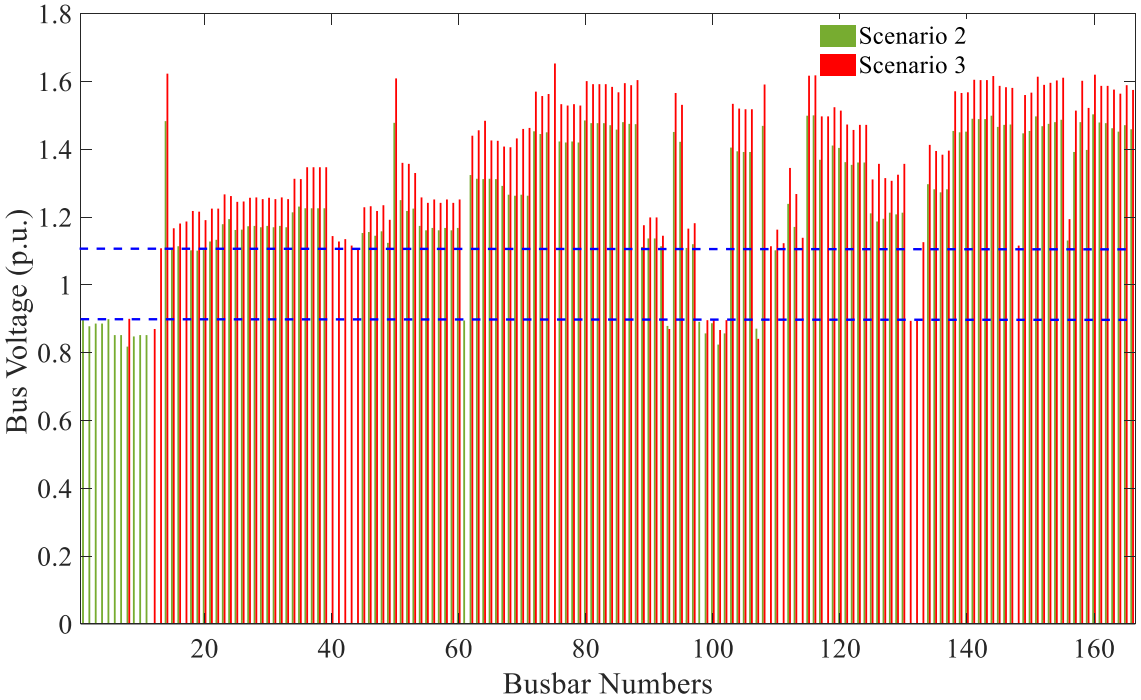

Figure 4-16: Voltage Violations during Contingency on the Tie-Line

The national grid code specifies 1.10 p.u. and 0.90 p.u. as the voltage limits (10% voltage stability margin) during contingencies in the NITS [50]. The voltage

stability margins are marked with broken lines in the figure. The figure shows that a contingency on the tie-line results in several violations of both the upper and lower voltage limit. Although system operations were maintained even with this contingency, several lines were overloaded (in addition to numerous voltage violations) causing the NITS to be vulnerable to system failure in the event of other faults.

Another important aspect here is that due to the large amount of power exported through the tie-line, this contingency leads to a greater change in the power flow, with corresponding grid losses. Table 4-4 compares the grid losses before and after the contingency on the tie-line.

Table 4-4: Comparison of Grid Losses before and after Contingency on the Tie-Line

Grid Losses	**Scenario 2**		**Scenario 3**	
	Pre-Cont.	Post-Contingency	Pre-Contingency	Post-Cont.
P (MW)	141.05	114.94	191.71	237.10
Q (MVAr)	128.08	-210.71	396.87	-553.74

Although grid losses generally increase with the contingency, a direct correlation between the contingency and losses could not be established for the active power loss in scenario 2 (see Table 4-4) as other factors like generation, load pattern and network topology, etc. also influence the grid losses.

4.5.2 Transformer Contingency

The transformer contingency was carried out by defining contingencies for all transformers in the NITS. Prior to the transformer contingencies, remedial measures for the transmission line contingencies were implemented in the network. No violations were recorded for scenarios 1 and 3 with one overloading recorded in scenario 2. The overloaded transformer is located at the receiving end of the tie-line to Togo and carries approximately 64% of the export demand. The appropriate remedial measures were implemented, which in addition to enhancing system reliability also improved voltages at the substations.

4.5.3 Renewable Generation Contingency

The concept of renewable generation contingency introduced here represents the variability in RE generation that may arise from the cloud cover on the PV units.

To simulate the effects of cloud cover on PV generation, the outputs of the PV units were reduced to 15%[23] [117–120] of the maximum output. An experiment carried out in [118] reveals that the output of the PV measures less than 25% of the rated power on very cloudy days.

Furthermore, the weather in northern Ghana can be very dry with increased dust accumulation, especially in the harmattan[24] period, which occurs during the dry season [121]. The location of the PV units in the north thus exposes the PV units to dust, whose accumulation on the PV modules when not cleaned on regular basis, leads to long-term reduction of the output power. The reduction in output power due to dust accumulation can be as low as 10% of the rated power [118] and depending on the weather and other factors, may lead to the loss of 18% and 78% of the output for monocrystalline and polycrystalline modules respectively over a one-year period [118].

The global solar irradiation, E_G made of two main components; the direct and diffuse irradiation [122, 123] is expressed by the following equation:

$$E_{G,hor} = E_{dir,hor} + E_{diff,hor} \tag{4.24}$$

The direct component, E_{dir} is more pronounced on a sunny day while the diffuse component, E_{diff} is prominent on a cloudy or dusty day, when the direct component is reduced. An index known as the clearness index, K_G is introduced to describe the relationship between the hourly and daily extraterrestrial irradiance (AM0) and the integrated energy density gathered from a horizontally mounted pyranometer [118]. It is used to express the ratio of the measured radiations and the energy density for extraterrestrial solar radiation in one day. The clearness index, K_G is directly related to the daily energy output of the PV units as shown in the formula, with H being the global horizontal radiation and H_0, the extra-terrestrial global radiation.

$$K_G = \frac{H}{H_0} \tag{4.25}$$

$$H_0 = \frac{1440}{\pi} * I_0 * \left[1 + 0.034 \cos\left(\frac{2\pi n}{365}\right)\right] * [\omega_0 \sin\varphi \cdot \sin\delta + \cos\varphi \cos\delta \sin\omega_0] \tag{4.26}$$

[23] Thick layered clouds reduce the PV output by about 80-90%, hence 15% output being the average of 10 and 20%.

[24] Harmattan is "a very dry, dusty easterly or north-easterly wind on the West African coast, occurring from December to February" - https://en.oxforddictionaries.com/definition/harmattan

I_0 is the solar constant equal to 0.0082 MJ/m^2/min.

A K_G value of 1 represents a very clear atmosphere, while a value of zero represents a cloudy atmosphere. Typical K_G values are in the range of 0.68 – 0.72 under cloudless conditions but reduces in the presence of clouds [124]. The lower clearness index recorded on cloudy days is as a result of the large amount of diffuse irradiation in the solar irradiation during cloud cover. On a very sunny day however, the direct irradiation becomes greater than the diffuse irradiation, which is about 10-20% [125].

The reduced direct component on cloudy days leads to reduced PV output, which is simulated by scaling down the PV generation to 15% of the maximum output. Three different combinations of wind and PV generations are thus investigated to determine the contingency with the worst impacts on the NITS. The investigated RE contingencies include:

- 15% PV + 100% Wind (effects of dust and cloud cover on the PV units with full wind generation)
- 15% PV + 0% Wind (effects of dust and cloud cover on the PV units with no wind generation)
- 100% PV + 0% Wind (maximum PV generation with no wind generation)

The outputs of the PV units and wind generators under these contingencies are summarised in the table below. Details of the generation schedules for the contingencies are provided in appendix C.

Table 4-5: RE Power Generation during the RE Contingency

RE Contingencies	***RE Power Generation (MW)***					
	S1 (2017)		S2 (2020)		S3 (2023)	
	PV	Wind	PV	Wind	PV	Wind
15% PV + 100% Wind	22 (150)[25]	90	49.5 (330)	200	76.5 (510)	275
15% PV + 0% Wind	22 (150)	0 (90)	49.5 (330)	0 (200)	76.5 (510)	0 (275)
100% PV + 0% Wind	150	0 (90)	330	0 (200)	510	0 (275

[25] The figures in bracket indicate the available maximum generation before the reduction.

15% PV + 100% Wind

The 85% reduction in PV generation translates into large power deficit in the NITS, which is balanced with the appropriate amount of conventional generation.

This contingency led to violations of the lower voltage limit (10% voltage stability margin) for contingencies [50]. Voltage variation during this contingency was highest in S3, with voltages ranging between 0.54 p.u. and 1.13 p.u. A few equipment overloads were also recorded in scenario 3, making it the worst scenario (largest voltage variation, highest equipment overload and branch flow) for this contingency.

15% PV + 0% Wind

In the absence of wind generation, this contingency represents the least RE generation in the NITS. The contingency alters the direction of power flow, which introduces new violations in voltage and loading limits. Furthermore, the NITS is operated with reduced operating reserve during this contingency.

Similar to the previous contingency, the 10% stability margin was violated in this contingency, with voltages ranging between 0.58 p.u. to 1.13 p.u. Equipment overloads recorded during this contingency worsened from S1 through to S3. Only one overload was recorded in S1 while three and seven violations were respectively recorded in scenarios 2 and 3. Conditions in the network were again worst in Scenario 3 (highest number of equipment overloads and worst voltage violations) during this contingency.

100% PV + 0% Wind

Unlike the other contingencies, where violations of the lower and upper voltage limits were recorded, only violations of the lower limit (0.90 p.u.) was recorded for this contingency. The number of equipment overloads recorded during this contingency was lower than in the other contingencies. While no overload was recorded in scenario 1, scenarios 3 and 2 had respectively one and two overloads.

It can be concluded that this contingency is less critical than the other RE contingencies, which have lesser RE power generation with more equipment overloads and larger voltage variations.

Figure 4-17 presents a summary of the voltage ranges during the contingencies. Details to the equipment loadings recorded in the contingencies are provided in appendix C.

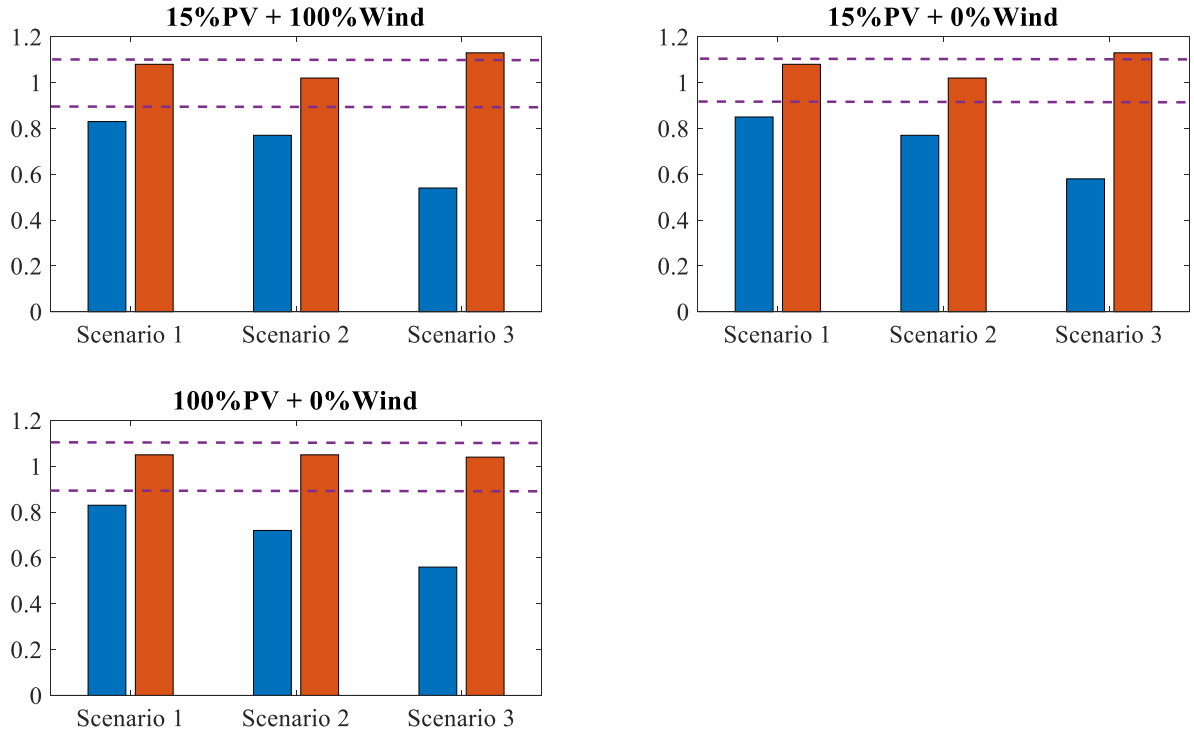

Figure 4-17: Voltage Variations during the RE Contingencies

Summary of Results

- ❖ Analysis of the line contingency in the NITS indicate that scenario 3 is the most critical during the transmission line contingency.
- ❖ A contingency on the tie-line between Ghana and Burkina Faso introduced the worst voltage violations and is thus the most critical transmission line, which makes the NITS vulnerable to other faults.
- ❖ Scenario 3 was greatly affected by the effects of the dust and cloud cover as simulated with the RE contingency. The highest number of equipment overloads and voltage violations were recorded during contingencies with reduced PV generation (15% PV + 100% Wind and 15%PV +0% Wind). The contingency with '100% PV + 0% Wind' recorded lesser overloads and no violations of the upper voltage limit, thus having the least impact in the NITS.

- Based on the results of the RE contingency, it can be concluded that reduced PV generation arising from cloud cover and dust have a greater impact on the bus voltages. The absence of wind generation in the NITS had less impact on the bus voltages, partly as a result of the location of the wind units in the network.

5 Stability Analysis of the NITS with RE Units

Having ascertained the readiness of the NITS to accommodate RE generation in the previous chapter, this chapter presents the stability analysis of the NITS with different percentages of RE. The main objective will be to evaluate the extent to which RE generation in the NITS affect system stability. Both static and dynamic stability analysis techniques are used for the evaluation.

5.1 Classification of Power System Stability

Power system stability is defined as the ability of a power system, for a given initial operating condition, to return to an equilibrium operating state after being subjected to a disturbance [126]. The complex processes that make up a power system depend on different operating conditions and network topologies, etc. and hence result in different forms of system instability. The non-linearity of the power system makes the dynamic performance dependent on the response rates and characteristics of various devices in the network [18]. As instability depends on several factors and takes different forms, it is important to appropriately classify the different forms of stability. The phenomenon of power system stability is thus categorized based on the size of disturbance, devices, processes and time span to be considered in assessing the stability, the physical nature of the resulting mode of instability and the most suitable method for calculating and predicting the stability [18, 126, 127]. Owing to the increased use of converter-interfaced-generation (CIG), five main forms of stability phenomena are identified. The forms of stability which include voltage, rotor angle, frequency, converter-driven and resonance stability are based on the parameter mostly affected by the disturbance. A pictorial description of the stability phenomenon, with the corresponding sub-categories is given in the figure below.

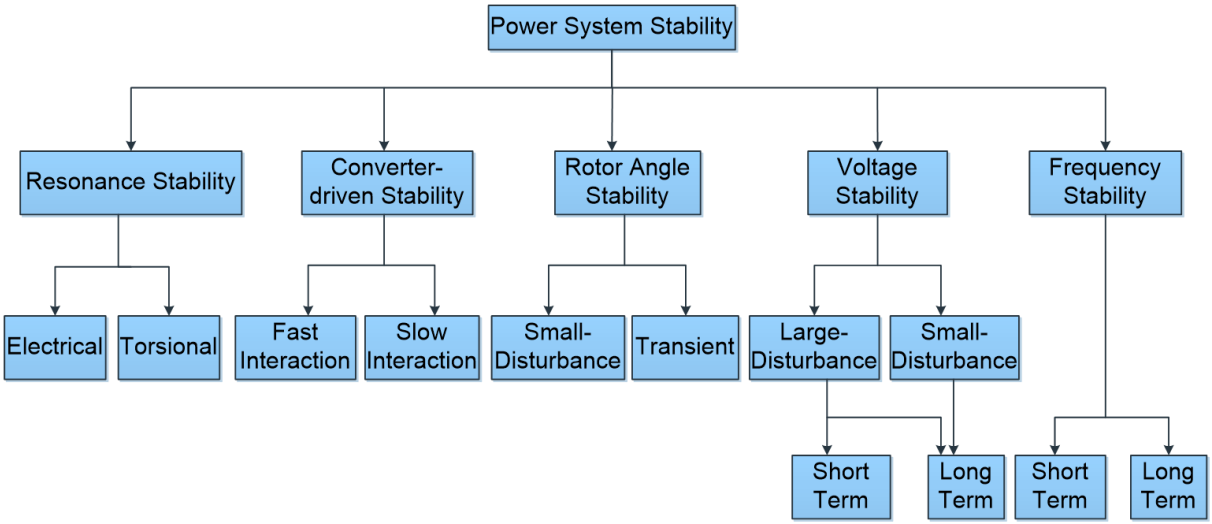

Figure 5-1: Classification of Power System Stability [126, 127]

5.1.1 Voltage Stability

Voltage stability refers to the ability of the power system to maintain steady acceptable voltages at all buses in the power system under normal operating conditions and after a disturbance. Voltage instability involves the progressive increase or decrease in voltages at some buses. The main cause of voltage instability is the power system's inability to meet the reactive power demand as a result of load demand increase and change in system conditions, etc [18, 126, 127]. Voltage stability is classified into small- and large-disturbance voltage stability based on the system's ability to control voltages following small disturbances (like small changes in loads) or large disturbances (like transmission system faults, loss of generation and contingencies) [18, 126, 127]. Voltage stability may span a few seconds to tens of minutes resulting in either short-term or long-term stability. Short-term voltage stability involves the dynamics of fast acting load components and is usually analysed within a few seconds with the appropriate differential equations, making it similar to rotor angle or converter-driven stability (slow interaction type) analysis [126, 127]. Long-term voltage stability on the other hand involves slower acting equipment such as generator current limiters and tap-changing transformers. The analysis span several minutes requiring long-term simulations for the analysis of system dynamic performance [126, 127].

5.1.2 Rotor Angle Stability

Rotor angle stability describes the ability of interconnected synchronous machines in a power system to remain in and regain synchronism after a

disturbance [18, 126, 127]. The resulting instability is characterised by increasing angular swings of generators, which may lead to the loss of synchronism [126]. For small disturbances such as small variations in loads and generation, the stability (known as small-disturbance or small-signal stability) is analysed using linearised system equations. Large-disturbance or transient stability involves large excursions of generator rotor angles and is influenced by the non-linear power angle relationship [18], [126]. Only transient stability will be considered in this thesis.

5.1.3 Frequency Stability

Frequency stability is the ability of the power system to maintain the frequency within an acceptable range after a disturbance, which results in a significant load and generation imbalance [18], [126]. Frequency instability may lead to the overloading of transmission lines, switching off generators with subsequent splitting of the system into subsystems. Frequency stability analysis will however not be considered within the scope of this thesis.

5.1.4 Converter-driven Stability

Converter-driven stability refers to the stability phenomenon arising from the increased use of converter-interface-generators (CIG) in the power system [127]. Owing to the wide time scale associated with the control of CIG (predominantly voltage-source converters, VSC), oscillations over a wide range of frequency are experienced which leads to two forms of converter-driven stability: slow and fast interactions. The fast-interaction stability deals with stability problems arising from the fast dynamic interactions of control systems of power electronic-based systems like HVDC, FACTS devices with fast-response components and CIG. Slow dynamic interactions of the control systems of power electronic-based devices with slow-response components classify the slow-interaction stability.

5.1.5 Resonance Stability

Resonance stability describes the subsynchronous resonance (SSR) of both electrical and electro-mechanical resonance [127].The subsynchronous resonance is exhibited either due to a resonance between series compensation and the electrical characteristics of the generator (purely electrical resonance) or due to a resonance between series compensation and the mechanical torsional frequencies of the turbine-generator shaft. The occurrence of the two-forms of resonance results in the sub-classification in the electrical and torsional stability.

5.2 Dynamics of Synchronous Machine Rotor

Power systems rely on synchronous machines for the generation of electrical power, as the adequate system operation depends on all synchronous machines remaining in synchronism. System stability is thus affected by the dynamics of synchronous generator rotor angles and the power-angle relationships [18]. Analysing the stability of a power system therefore requires the consideration of the synchronous machine rotor dynamics as presented below.

5.2.1 Swing Equation

The swing equation forms part of the equations of motion of a synchronous machine. The main equation that describes rotor motion is given by the net torque, which causes either acceleration or deceleration and is given as:

$$T_a = T_m - T_e \tag{5.1}$$

where T_a is the accelerating torque in N·m, T_m is the mechanical or shaft torque in N·m and T_e is the electromagnetic torque in N·m.

The motion of the synchronous machine rotor is governed by an equation based on the principle of dynamics that the accelerating torque is the product of the moment of inertia of the rotor and its angular acceleration [92] given as

$$T_a = T_m - T_e = J\frac{d^2\theta_m}{dt^2} \tag{5.2}$$

where J is the total moment of inertia of the rotor masses in kg·m^2, θ_m is the angular displacement of the rotor with respect to the stationary axis in mechanical radians (rad) and t is the time in seconds (s).

The machine is said to be working at synchronous speed or (in synchronism) if $T_a = 0$, i.e., $T_m = T_e$. The rotor angular displacement measured with respect to a reference axis which rotates at synchronous speed is given as

$$\theta_m = \omega_{sm} \cdot t + \delta_m \tag{5.3}$$

where ω_{sm} is the synchronous speed of the machine in mechanical radians per second and δ_m is the angular displacement of the rotor in mechanical radians with respect to the synchronously rotating reference axis.

The first and second derivative of equation 5.3 above are given as

$$\frac{d\theta_m}{dt} = \omega_{sm} + \frac{d\delta_m}{dt} \tag{5.4}$$

$$\frac{d^2\theta_m}{dt^2} = \frac{d^2\delta_m}{dt^2} \tag{5.5}$$

Substituting equation 5.5 in equation 5.2 results in

$$J\frac{d^2\delta_m}{dt^2} = T_a = T_m - T_e \tag{5.6}$$

Recalling that power (P) is the product of the torque (T) and the angular velocity (ω), introducing a new denotation for the rotor angular velocity (refer to equation 5.6) results in the following equation

$$\omega_m = \frac{d\theta_m}{dt} \tag{5.7}$$

$$J\omega_m\frac{d^2\delta_m}{dt^2} = P_a = P_m - P_e \tag{5.8}$$

where P_a, P_m *and* P_e are the accelerating, mechanical and electrical powers respectively. The coefficient $J\omega_m$ is the angular momentum of the rotor, which at synchronous speed is denoted by M, the inertia constant of the machine. The resulting equation 5.9 is further normalised in terms of the unit inertia constant H, defined as the stored kinetic energy at synchronous speed divided by the rated apparent power of the generator, S_{mach} [18, 92] as expressed in equation 5.10

$$M\frac{d^2\delta_m}{dt^2} = P_a = P_m - P_e \tag{5.9}$$

$$H = \frac{1}{2}\frac{J\omega^2{}_{sm}}{S_{mach}} = \frac{1}{2}\frac{M\omega_{sm}}{S_{mach}} \tag{5.10}$$

Substituting equation 5.9 into equation 5.8 yields

$$\frac{2H}{\omega_{sm}}\frac{d^2\delta_m}{dt^2} = \frac{P_a}{S_{mach}} = \frac{P_m - P_e}{S_{mach}} \tag{5.11}$$

Rewriting equation 5.11 and expressing in per unit (for unit consistency) results in

$$\frac{2H}{\omega_s}\frac{d^2\delta_m}{dt^2} = P_a = P_m - P_e \tag{5.12}$$

Equation 5.12 is known as the swing equation of the machine due to its representation of rotor angle swings during disturbances [18]. It is also a fundamental equation in stability studies that governs the rotational dynamics of a synchronous machine [92].

5.2.2 Power-Angle Equation

The power-angle equation is a useful expression that describes the relationship between the output power of a machine and its rotor angle [128]. It is a non-linear relationship, which is essential in system stability analysis [18]. The relationship is illustrated using the two-machine system below. The synchronous generator, GS is assumed to be connected to a motor (large load), M through a transmission line with inductive reactance X_L and negligible resistance and capacitance.

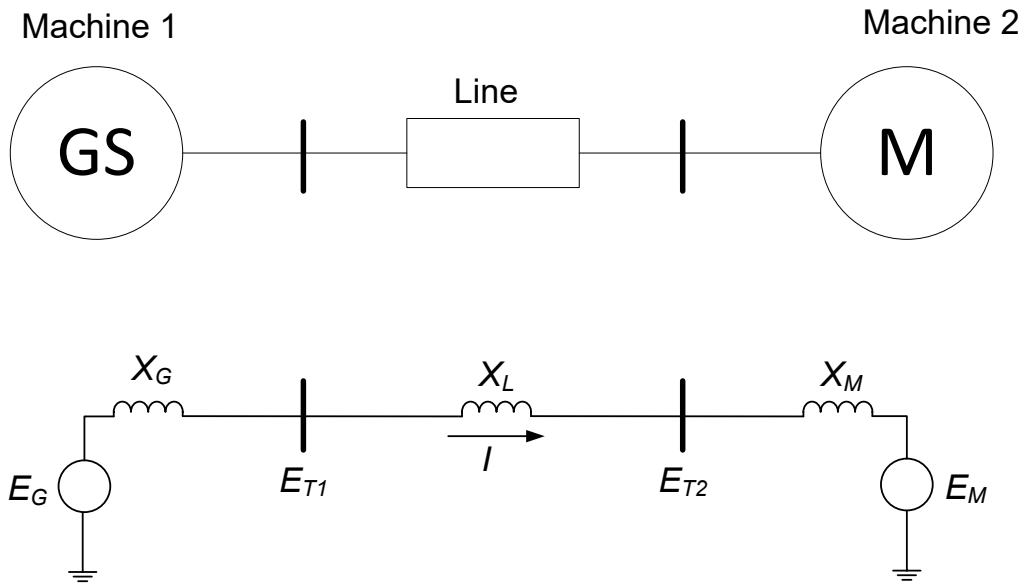

Figure 5-2: Single Line Diagram and Model of the Two Machine System [18]

The power transferred from the generator to the motor is a function of the angular separation between the two machines and is given by

$$P = \frac{E_G E_M}{X_T} \sin \delta \tag{5.13}$$

where $X_T = X_G + X_L + X_M$

Equation 5.13 is known as the power-angle equation, which is a sinusoidal relationship, implying no power transfer at angle zero. Increasing the angle results in a corresponding increase in power transfer till the maximum power is reached at angle 90º. A further increase in the angle beyond this point results in a decrease in the power transfer. The maximum power is thus directly proportional to the

internal voltages of the two machines and indirectly proportional to the collective reactance, which is the reactance of the transmission line and the machines.

5.2.3 Equal Area Criterion

The equal area criterion for stability is a graphical approach (see figure 5-3) used in analysing the stability of the two machine system [18], [93]. For this analysis, a three-phase short-circuit fault is assumed to occur at a bus, which is cleared after a certain period without disconnecting the transmission equipment.

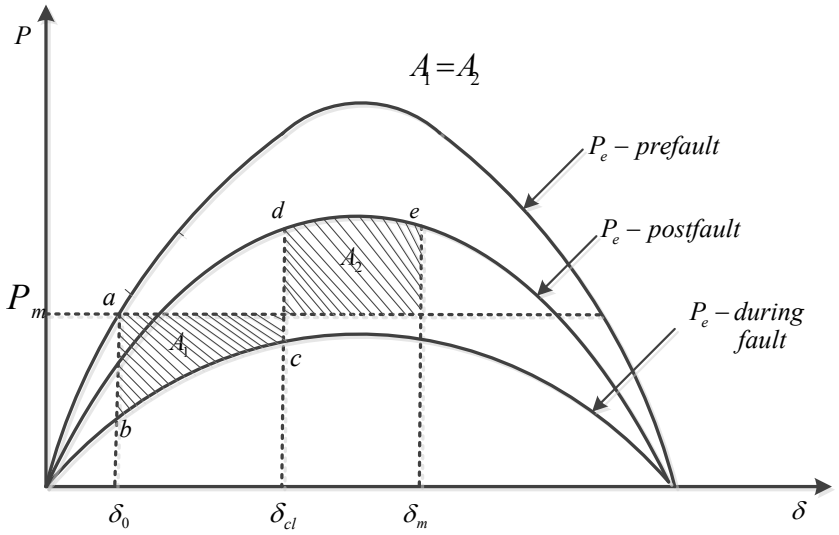

Figure 5-3: Equal-Area Criterion of a Power System [18, 93, 97]

As the power angle increases from its steady-state operating point past 90º to 180º, system voltage rapidly decreases. A power angle of 180º indicates the power system has lost synchronism and a total collapse has occurred. Reference can be made to [18, 93, 97] for details to the equal-area criterion.

5.3 Voltage Stability Analysis of the NITS

Voltage stability analysis has become an essential part of the routine planning and operation of a power system. The analysis of voltage stability is performed using static and dynamic stability analysis methods. Conventional load flow methods and algebraic equations are used in static analysis while time-domain simulations are used to solve non-linear equations of the system in dynamic analysis [129]. Using both voltage stability methods is essential in identifying the right balance between the static and dynamic reactive power sources as the dynamic reactive sources have the capability of acting to avert the risk of voltage collapse in

instances where the static reactive sources are not fast enough to intervene [106]. The use of both methods additionally provides an overall and accurate assessment of the voltage stability of the entire system as presented below.

5.3.1 Static Voltage Stability Analysis: P-V Curves

Steady-state voltage stability analysis utilizes power flow equations to identify the equilibrium points of the network. It is the most common means of assessing the static voltage stability [106], which also provides additional information on the sensitivities and the degree of instability.

As part of the main instruments for analysing static voltage stability, P-V curves use load flows to determine the maximum power that can be transmitted to a chosen load or group of loads. Figure 5-4 present a typical P-V curve, which provides information on the voltage variation (decreases) with changes in active power transfer.

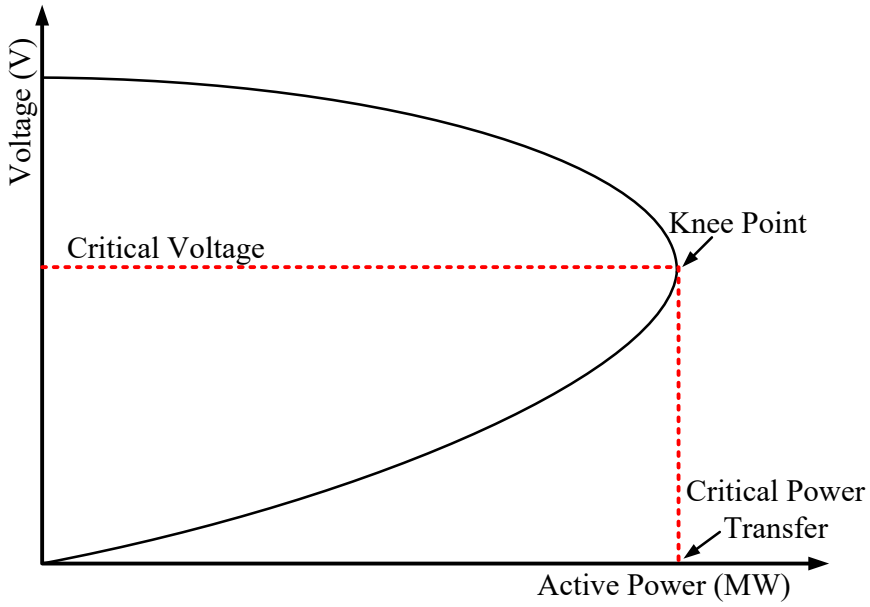

Figure 5-4: Typical P-V Curve of a Power System [18, 106]

The P-V curves, also known as nose curves are used to identify the static stability margin of a part of or the entire power system. The curves are obtained by incrementally varying the power flow to a bus and recording the corresponding bus voltage until the load flow does not converge [106]. This point is known as the 'knee-point' of the curve (critical power transfer), beyond which any further increase in power results in voltage reduction. The 'knee-point' of the curve also serves as the boundary between the stable and unstable operating regions. Operating points above the knee-point represent the stable region while points beneath the knee-point are the unstable operating points. The critical bus in the

network, which is most vulnerable to voltage instability is also identified with the P-V curves.

The *critical power transfer* is used as an indicator in the static voltage stability analysis using P-V curves. This is defined as the maximum power transfer in the network, beyond which an increase in power leads to voltage instability. Larger critical power transfers are indicative of a stable network. P-V curves developed for the critical buses in the NITS for all scenarios are shown in Figure 5-5 below.

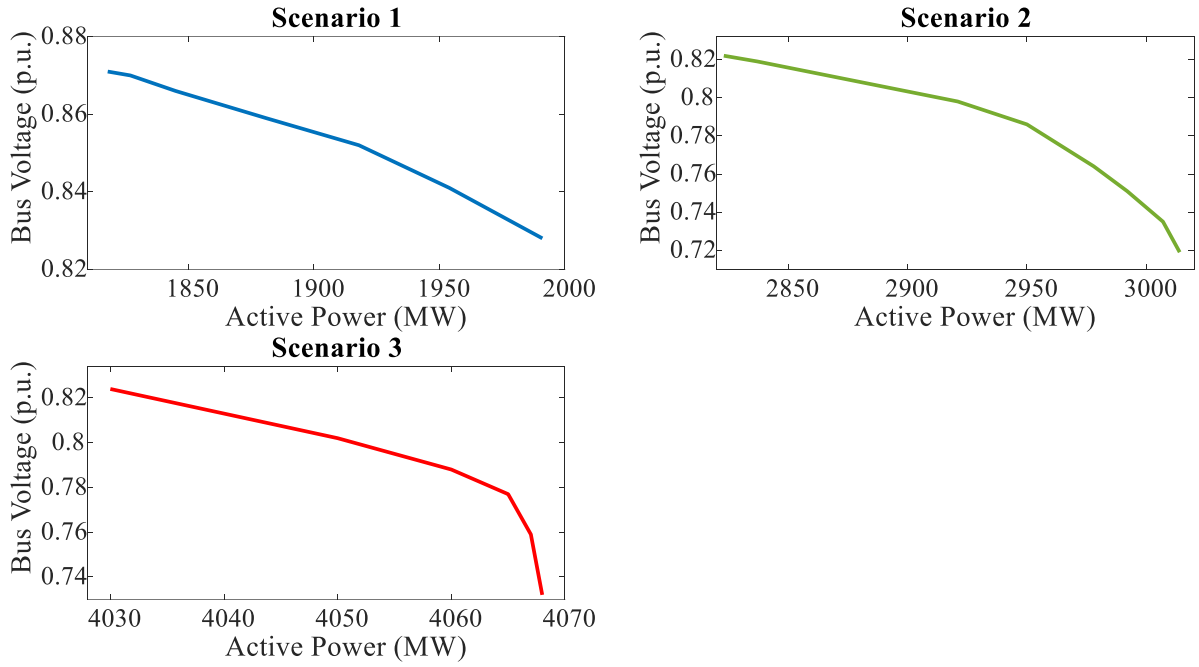

Figure 5-5: P-V Curves of the Critical Bus in the NITS – All Scenarios

The figure shows an improvement in the load transfer capability of the NITS across the scenarios despite the reduction in the bus voltage of the critical busbar. Critical power transfers of 1,991 MW, 3,014 MW and 4,068 MW were recorded respectively for the three scenarios, beyond which the system's risk of voltage instability increased with a potential voltage collapse. Although increasing critical power transfer is indicative of an improved voltage stability of the NITS, the actual point of instability of the network could be hidden by the installation of additional shunt capacitors [97] as was done in these scenarios. Operating the power system near the critical demand thus leads to a decrease in system voltage even with a small increase in demand.

Although the loading limits in the NITS improved, grid losses and line charging (charging currents) increased as seen in Table 5-1.

Table 5-1: Summary - Static Voltage Stability Analysis using P-V Curves

Scenarios	Critical Power Transfer (MW)	Grid Losses		Line Charging (MVAr)
		P (MW)	Q (MVAr)	
S1	1,991	86.50	68.48	-677.09
S2	3,014	179.79	519.59	-1,017.27
S3	4,068	303.13	1,536.42	-1,028.42

The increasing line charging are indicative of increasing transmission losses in the NITS, as the loadability of the NITS improves.

5.3.2 Static Voltage Stability Analysis: Q-V Curves

Q-V curves are also used in voltage stability analysis to determine the sensitivity and variation of bus voltage caused by changes in reactive power (injection and absorption). The curves are developed for the critical buses in the network [97] and are used to identify their respective reactive power margins to voltage stability [106, 130], i.e. the amount of reactive power required to maintain the bus voltage at the specified level. Below is a typical Q-V curve which shows the reactive power margin (RPM) and nose point. Operation to the right of the nose point represents stable operation as increase in reactive power results in a corresponding increase in voltage. Operation to the left of the nose point represents unstable operation as voltage reduces with increasing reactive power [18, 130]. The nose point, which represents the minimum reactive power required for stable operation also indicates the voltage stability limit of the network.

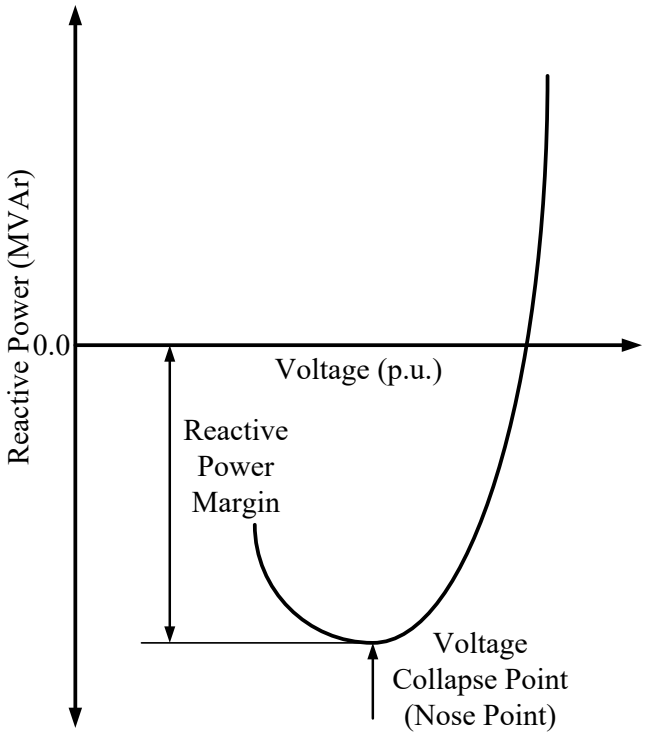

Figure 5-6: Typical Q-V Curve [131]

The reactive power margin (RPM) is used as an indicator in the static voltage analysis using Q-V curves. The RPM is defined as the amount of reactive power required (or available) to maintain voltage stability in the network. It is the negative value of the reactive power output at the nose point [106]. A positive RPM value is thus indicative of a stable system while a negative RPM indicates an unstable system. A system with the nose point above the horizontal axis is reactive power deficient and may require additional reactive power to maintain system security and reliability in order to prevent voltage collapse. On the other hand, if the nose point is below the horizontal axis, the system has some reactive power margin (equal the distance to the axis). Nonetheless, a system with some margin may still be reactive power deficient depending on the desired margin [131] set by the system operator. The nose point, which is the minimum point of the Q-V curve (where $dQ/dV = 0$) is also known as the critical point.

Figure 5-7 shows the Q-V curves developed for the critical buses in the NITS.

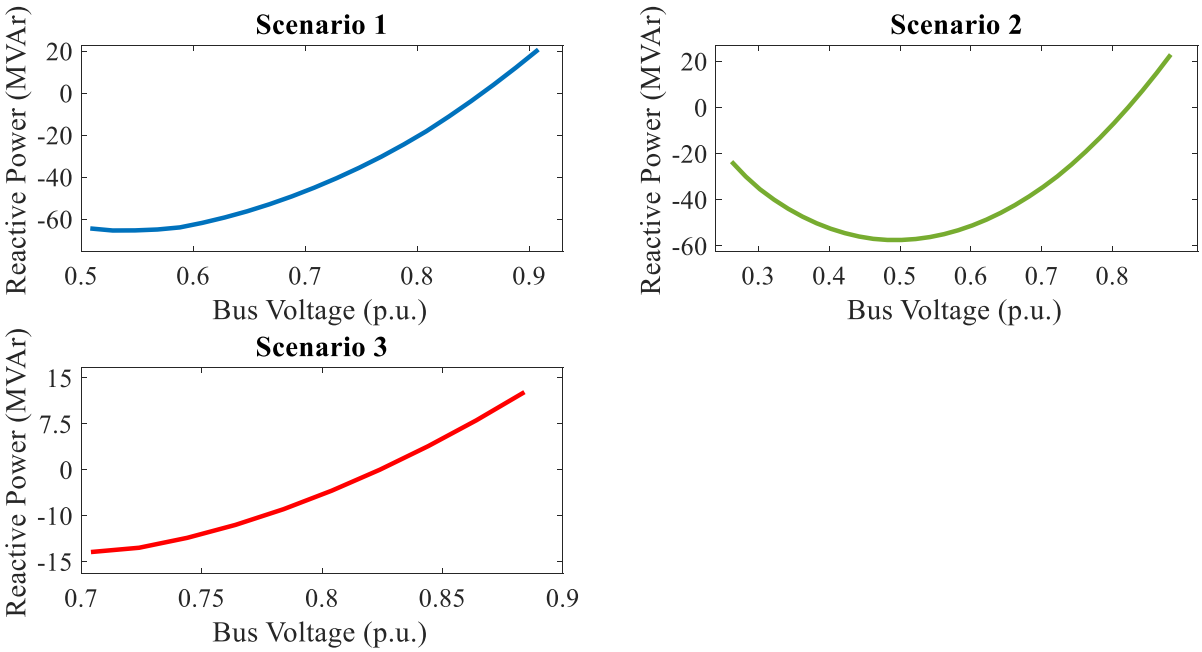

Figure 5-7: Q-V Curves of the Critical Bus in the NITS – All Scenarios

RPM values of 65.43 MVAr, 57.50 MVAr and 13.45 MVAr were recorded respectively for scenarios 1, 2 and 3. Adequate reactive power margin is however required to account for variations in network conditions. The figure shows a reduction in the RPM, which is indicative of an increased risk of voltage collapse in the NITS in the latter scenarios. The busbar in scenario 3 with the lowest RPM is considered the weakest amongst the critical busbars. The corresponding critical voltages is presented in the table as follows:

Table 5-2: Summary - Static Voltage Stability Analysis using Q-V Curves

Scenarios	Critical Voltage (p.u.)	Reactive Power (MVAr)
S1	0.528	-65.43
S2	0.502	-57.50
S3	0.704	-13.45

As lower voltages are indicative of the reactive power need of the network, the table shows that even with the existing RPM in the NITS (refer to figure 5-7), the NITS is still reactive power deficient.

5.3.3 Dynamic Voltage Stability Analysis

Dynamic voltage stability analysis is a time-domain analysis used to show the trajectory and behaviour of the power system after a disturbance. Disturbances such as loss of generators and transmission lines as well as system faults like

short-circuits are used to assess the voltage stability of the network. Dynamic voltage stability analysis reveals the transient and/or long-term stability of the network and is performed within a few seconds to tens of minutes to allow adequate time for the reaction of the necessary controllers. A system is thus considered stable if the time-domain simulations reach an equilibrium after the disturbance (post-contingency after a finite time period) [132].

In this thesis, the dynamic voltage stability of the NITS was evaluated by simulating the loss of load and transmission lines and investigating their respective effects. The duration and amplitude of the oscillation were used as indicators for the stability analysis. The duration of oscillation describes the length of time between the periods the fault occurred and when the voltage or rotor speed is damped (begins to settle into steady state). The amplitude of oscillation also describes the largest magnitude attained during the oscillation.

The stability criterion for this indicator is that the longer the rotor speed/voltage oscillates around the steady-state value during a disturbance, the more unstable the system is. Larger oscillation amplitudes (larger deviations from the steady-state value) are also indicative of instability. These imply that a system is considered stable when the steady-state value is reached in a shorter time or when the deviation of the oscillation from the steady-state value is the least.

Loss of Load

To simulate the effects of the loss of load on the voltage stability of the NITS, the ten largest loads making a total of about 360 MW (single largest load being 145 MW) were taken out of service at time = 1 s during a simulation period of 15 s. The figure shows a snippet of the NITS with the locations of five of the largest loads in the network.

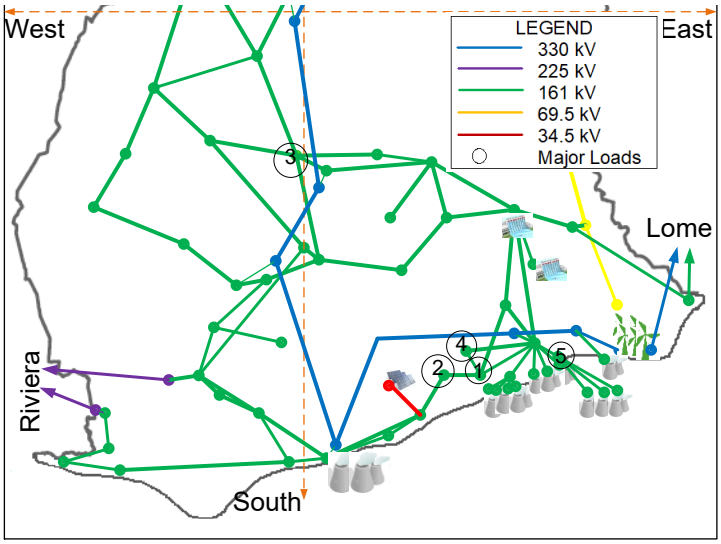

Figure 5-8: Overview of the Five Largest Loads in the NITS

Figures 5-9 to 5-12 show the resulting bus voltages and generator frequency during the loss of the largest single load (load 1 in Figure 5-8) in the NITS.

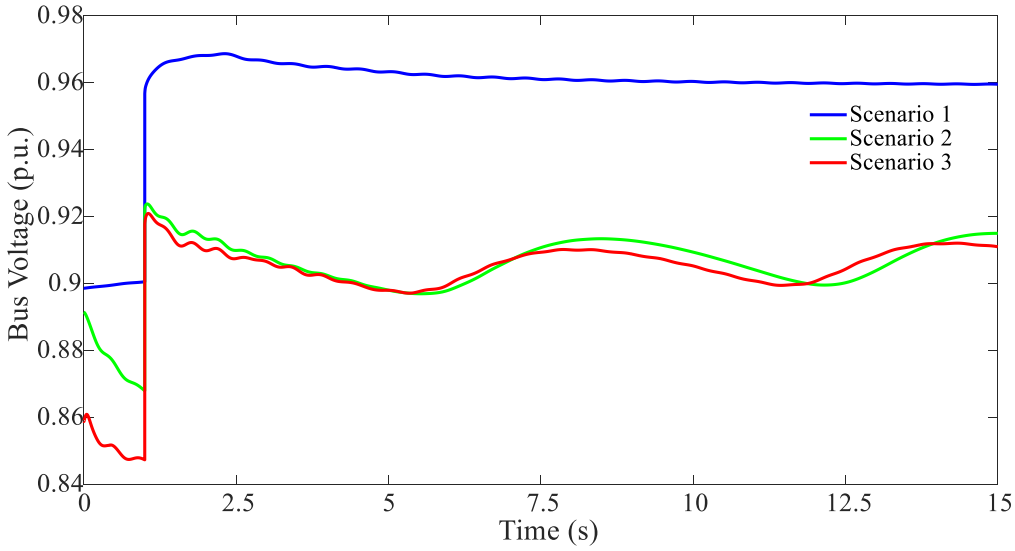

Figure 5-9: Bus Voltage of Load Bus during Loss of Load

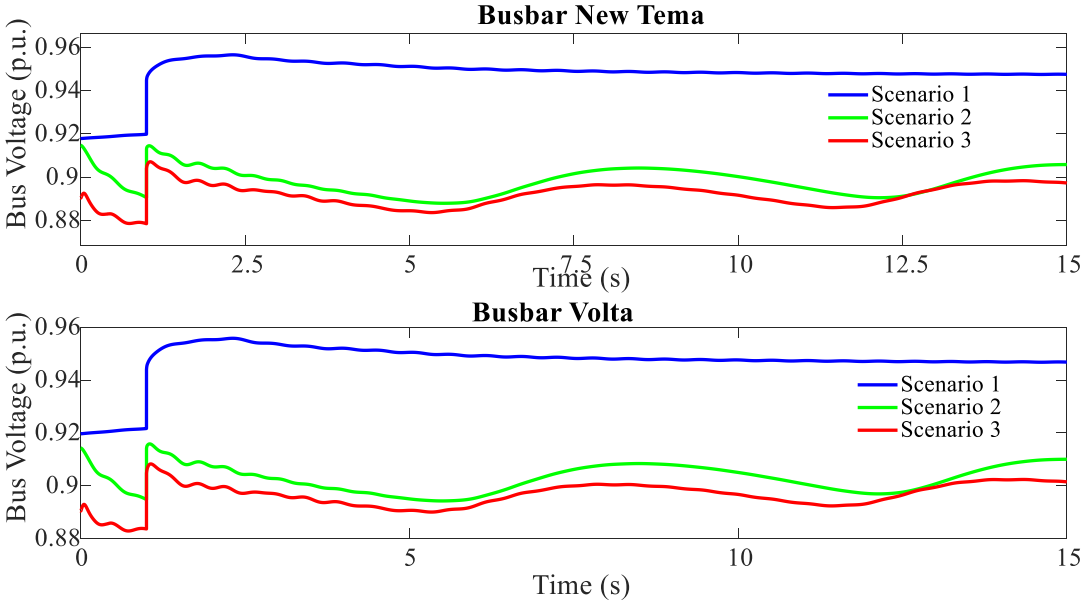

Figure 5-10: Bus Voltage of 161 kV Connected to the Load Buses during Loss of Load

The sudden loss of load in the network results in the short-term over-production of power from the generators, which lead to a temporary rise in generator speed and system voltage. The generator excitation reacts within a few seconds following the loss to restore the voltage by regulating the field current to its excitation system. The generator excitation responded to the change in voltage by decreasing its excitation current to stabilize the voltage. The voltage increase is then sensed by the AVR, which causes a reduction in the excitation voltage (current) in an attempt to restore the voltage to the initial value. The decrease in excitation current in response to the voltage increase from the load loss was sustained throughout the simulation period as long as the voltage was higher than the initial voltage.

The figure indicates a non-oscillatory profile in scenario 1, while the voltages in scenarios 2 and 3 are oscillatory with lower amplitude as was shown with the steady state analysis in chapter 4. Due to the size of the loads lost, the busbar voltages in scenarios 2 and 3 kept oscillating after the voltage rise and did not settle to steady-state within the 15 s simulation period. Increased RE penetration in these scenarios also led to a reduction in system inertia, which accounts for the oscillatory voltage profiles. The reduced inertia thus makes the network prone to instability as seen from the inability of the bus voltages to attain steady-state within the simulation period. The resulting frequency of the generators is as follows:

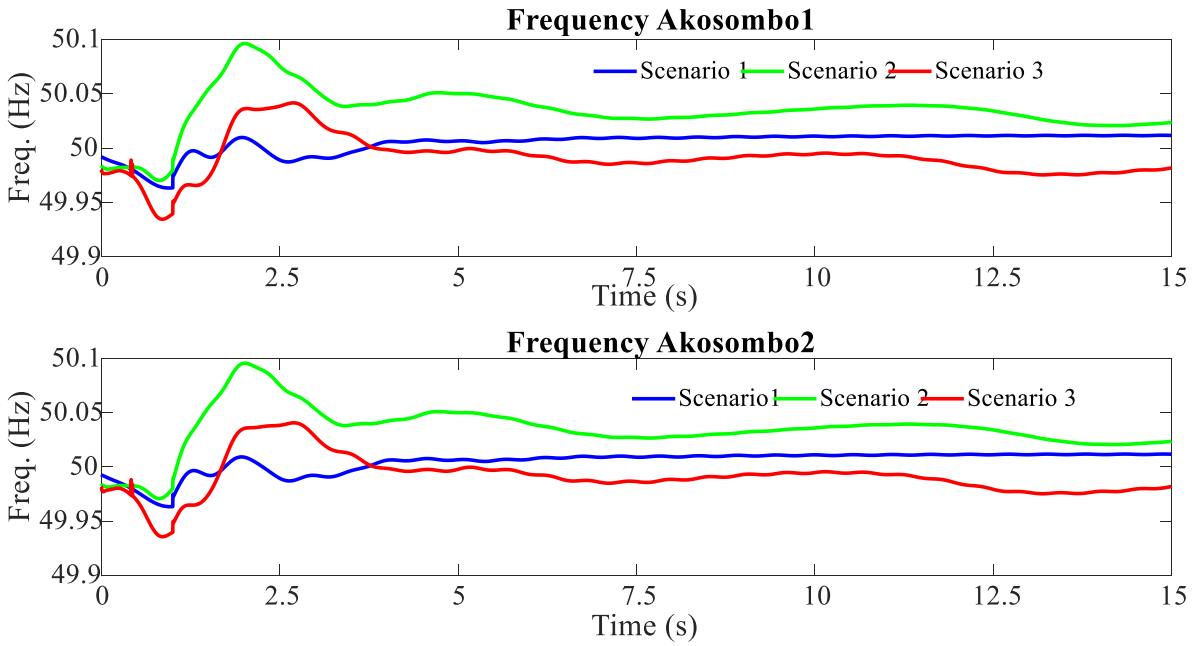

Figure 5-11: Frequency of Slack Generator during Loss of Load

Figure 5-11 shows that the behaviour of the slack generator in response to the load loss was poor in scenario 2. As previously seen, scenario 2 has the least conventional generation to RE generation ratio, translating into a reduced response from the conventional generation units during system faults. Due to the reduced number of conventional generating units in this scenario, the slack frequency increased to approximately 50.1 Hz to accommodate the frequency excursions in the network. The corresponding frequency profile of the generator connected to the load bus is presented in figure 5-12. This generator was not in operation in scenario 1 and thus the frequency profile will be shown for only scenarios 2 and 3.

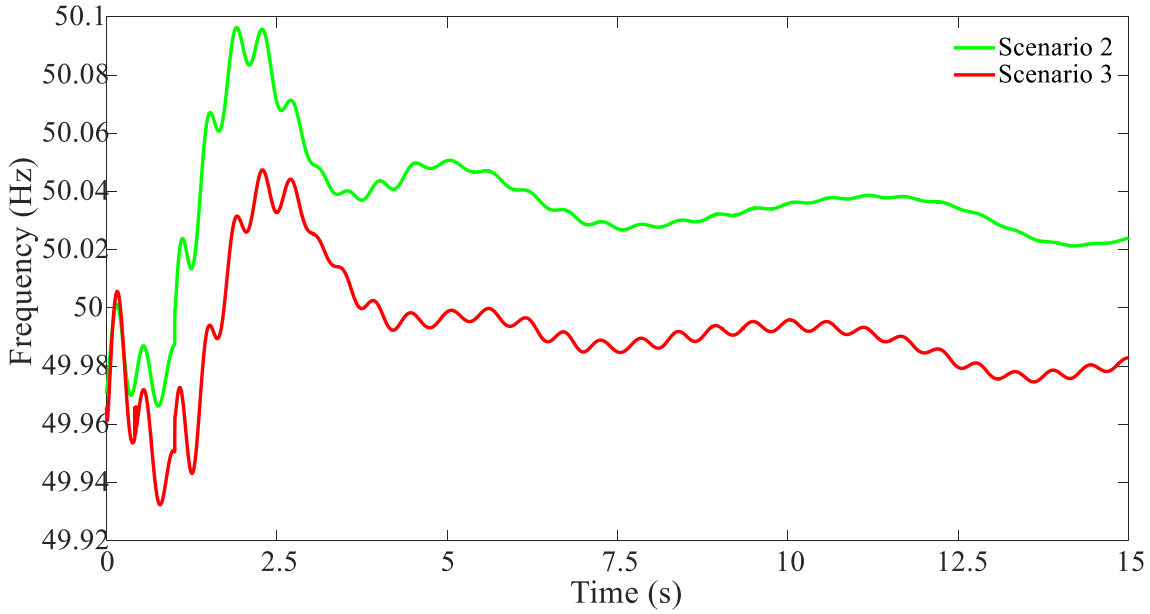

Figure 5-12: Frequency of Generator connected to the Load Bus during Loss of Load

The figure shows oscillatory frequency profiles in both scenarios with a higher frequency amplitude in scenario 3 due to the load size. Notwithstanding, the frequency margin for normal operation in the NITS ($48.75 \leq f \leq 51.25$ Hz) was not violated in any of the scenarios.

Transmission Line Loss

A three-phase short-circuit fault on the critical transmission lines cleared after 150 ms (by isolating the line) was used to simulate the line loss in the NITS. The simulated short-circuit fault occurred at 1 s for a simulation period of 15 s. Sample results of busbar voltages and generator rotor angles examined during the line loss are presented as follows. The critical transmission line was not in operation in scenario 1, hence results for scenarios 2 and 3 will be presented.

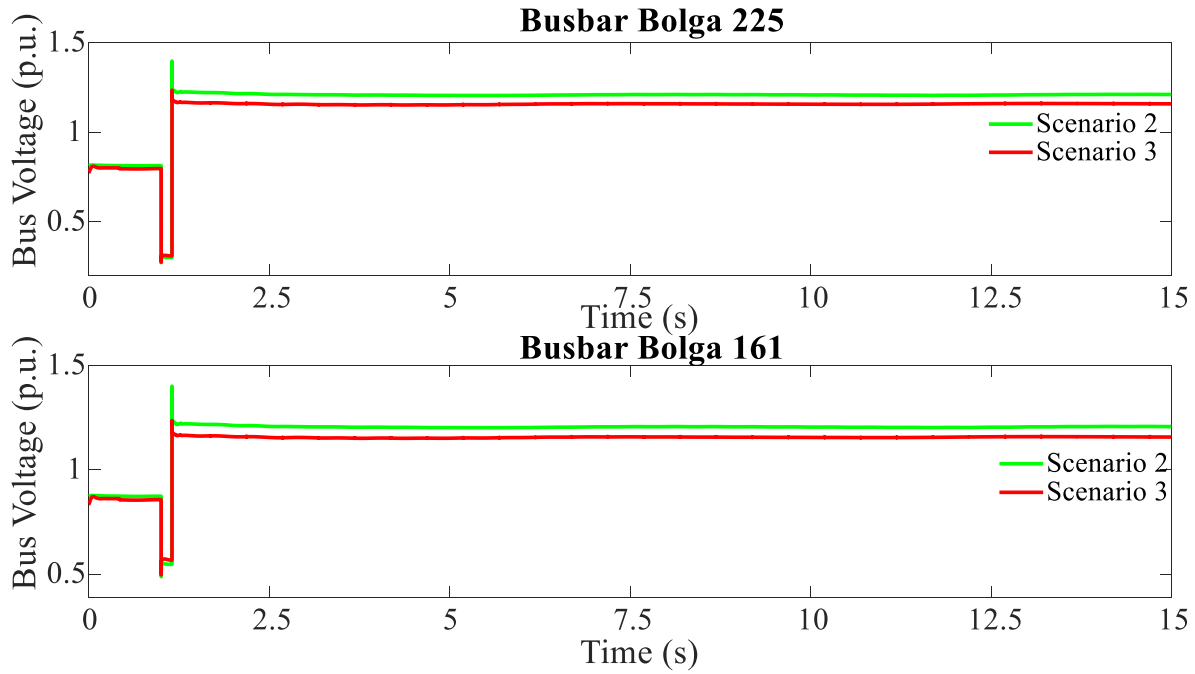

Figure 5-13: Voltage Profile at the Sending End of the Line during a Transmission Line Loss

Following the line outage, adjacent transmission lines became overloaded, which increased the reactive power losses, leading to a sudden reduction of voltage. In response to this, the generator excitation signalled an increase in the field current, which led to a temporary increase in reactive power to support the system voltage. This however is not sustained for a long period as the generator protective systems like the over-excitation limiters act to force the generators back within their limits, especially to prevent an overproduction of the field (excitation) current when the voltage is extremely low. While the generator increases reactive power production to restore the voltage, additional reactive power flows through the generator transformers, which increases the line loss and leads to a reduction in voltage, hence the unequal pre-fault and post-fault (steady-state) voltages. The corresponding rotor angles of selected generators in response to the loss of the critical line is shown in Figure 5-14.

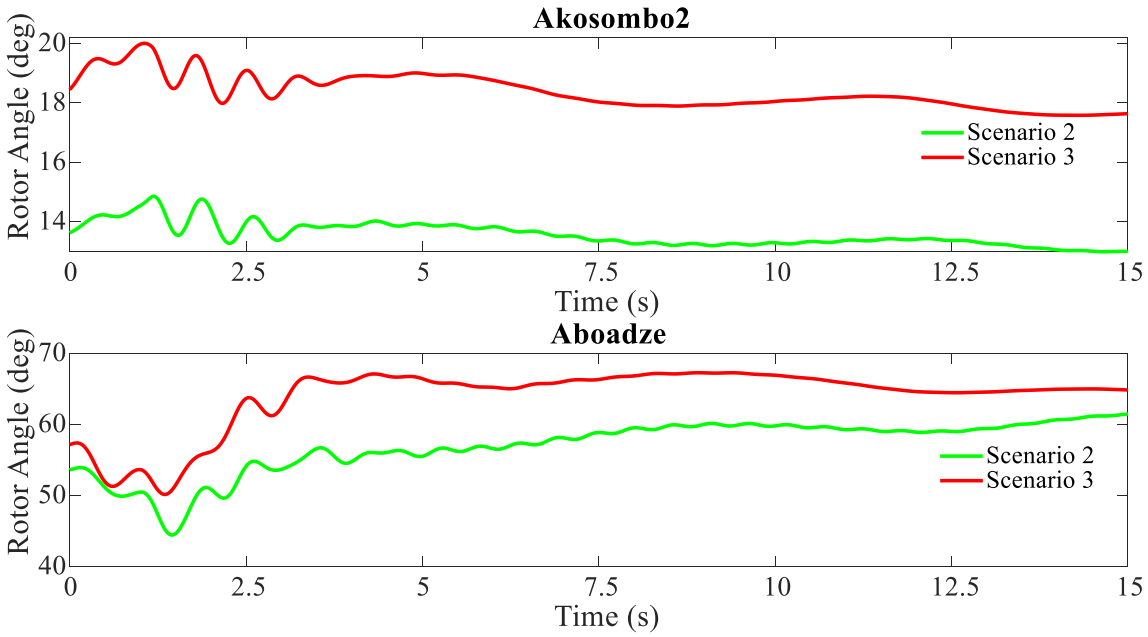

Figure 5-14: Rotor Angle of Selected Generators during the Transmission Line Loss

The figure shows the rotor angle of the generator with respect to the local reference generator. It is observed that the rotor angles of generators in Scenario 3 deviated more from the reference generator than in Scenario 2. The rotor angles oscillated shortly after the fault, but the oscillation got damped and finally settled to steady-state within the 15 s simulation period. The behaviour of the PV units in response to the transmission line loss was also investigated. The resulting reactive power profiles of PV units in the vicinity of the critical transmission line is presented in Figure 5-15.

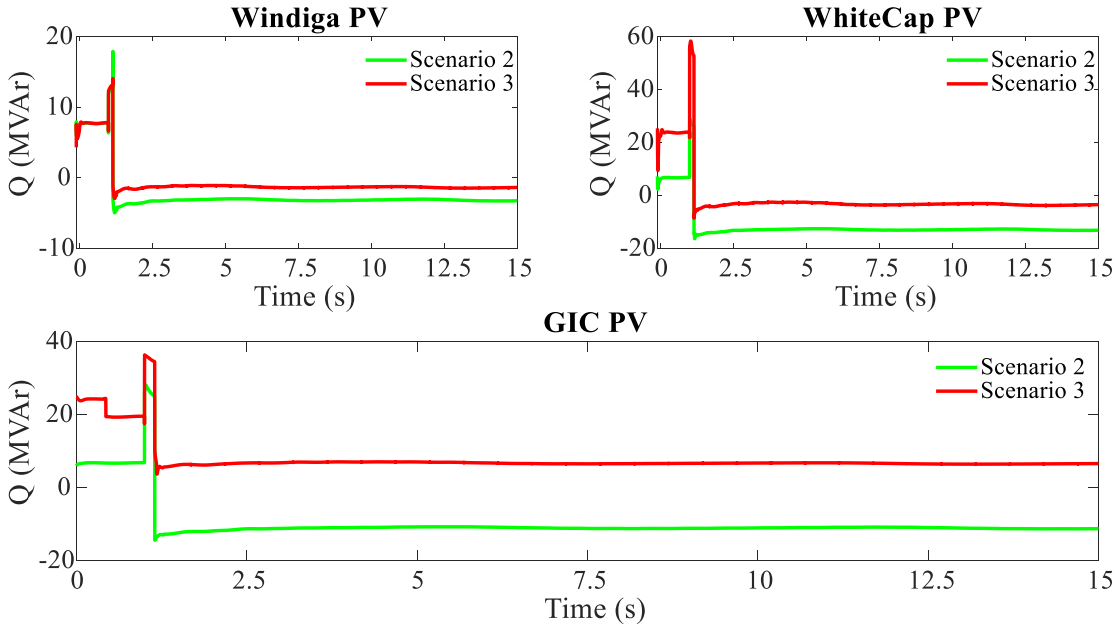

Figure 5-15: Reactive Power Profiles of PV Units within the Vicinity of the Critical Transmission Line

The figure confirms the response of the PV units during the loss of the critical transmission line in the NITS. The increased values in scenario 3 is associated with the larger amount of power transmitted (increased power export) with that transmission line.

5.4 Transient Stability Analysis

Transient stability is the ability of the power system to maintain synchronism during large disturbances, such as equipment and line outages, bus faults and cloud cover in case of PV generation. The time frame of interest is 3–5 s following a disturbance, which might be extended to 10–20 s depending on the system [18]. The severity of transient instability depends on network properties (such as the size of existing generators and available system inertia) and the nature (type, duration and location) of the disturbance. The reduction in system inertia due to increased PV generation in the NITS makes the rotor angle stability analysis vital in the operation of the network.

The transient stability of the NITS was investigated by applying a three-phase short-circuit fault to the critical transmission lines. The short-circuit fault, which occurred at 1 s was cleared after 150 ms for a simulation duration of 15 s. In addition to the critical clearing time (CCT), the maximum deviation of rotor speed (similar to the amplitude of oscillation, but specifically for rotor-angle) will be used as indicators for the assessment.

The CCT is defined for a given fault as the maximum fault clearing time within which the system remains transient stable. For a power system to remain stable, the given fault must be cleared or isolated from the system within the CCT. A system is considered unstable if for a given fault, the fault clearing time is longer than the CCT. The maximum deviation of rotor speed describes the largest deviation of the rotor speed during or after fault. Larger deviations for a given clearing time indicates a lower stability margin.

For the transient stability analysis in the NITS, a fault clearing time of 150 ms was used, which implies that for the network to be transient stable, all faults must be cleared within the fault clearing time. The resulting CCT for the NITS is summarised in table 5-3 as follows:

Table 5-3: Critical Clearing Times of the Scenarios

Scenarios	Critical Clearing Time (CCT)
S1	0.377
S2	0.124
S3	0.132

In addition to several transmission line overloads recorded, the least CCT recorded for scenario 1 was 0.377 s, 0.124 s for scenario 2 and 0.132 s for scenario 3. It is concluded that scenarios 2 & 3 are transient instable for the given lines as the CCTs are lesser than the 150 ms fault clearing time used. Based on the calculated CCTs, scenario 1 is considered transient stable as its least CCT is the longest among the other scenarios. Sample profiles of the generator rotor angle are shown in figures 5-16 and 5-17.

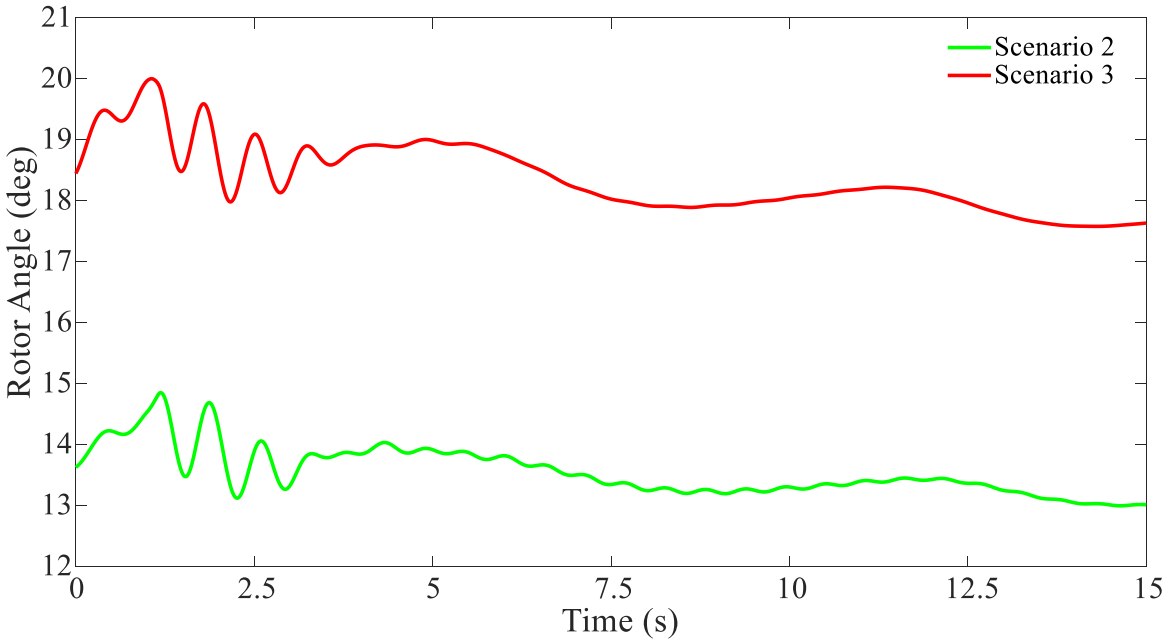

Figure 5-16: Generator Rotor Angle during a Three-Phase Short-Circuit Fault

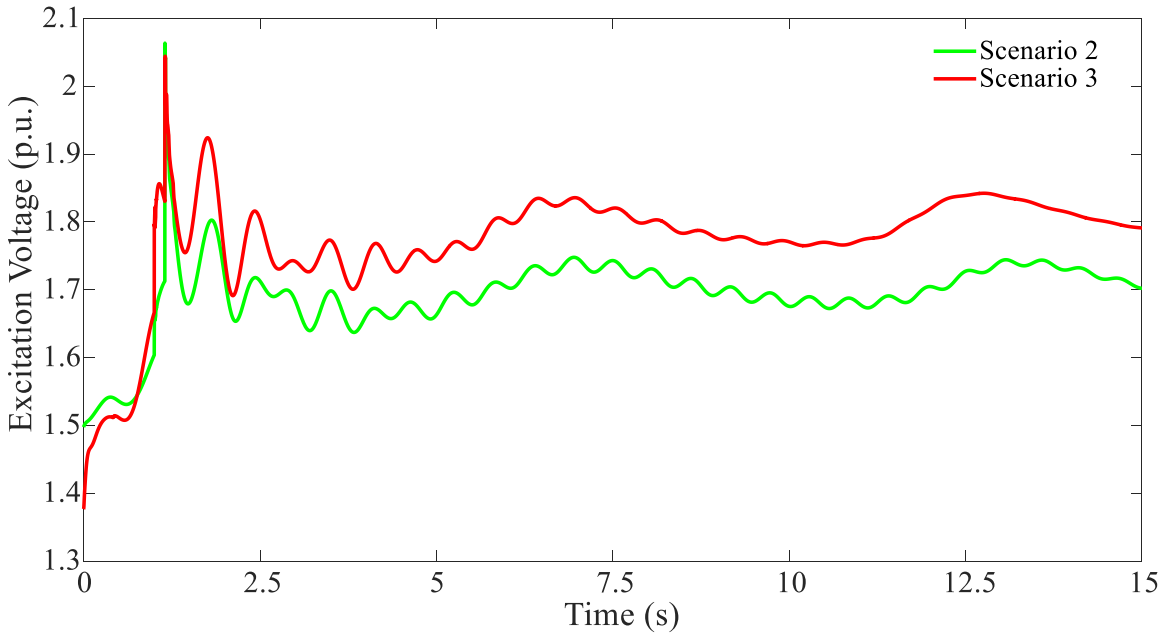

Figure 5-17: Generator Excitation Voltage during a Three-Phase Short-Circuit Fault

Figure 5-16 shows an oscillatory rotor angle profile, which gets damped in scenario 3. This is as a result of the increased number of conventional generating units in scenario 3, which contribute to a higher system inertia in scenario 3. With a good amount of inertia in the network, the network is sustained during faults. With reduced inertia however, the same fault becomes critical as system frequency drops below the 49.5 Hz band before the primary frequency control fully sets in.

Summary of Results

- The voltage and transient stability of the NITS have been analysed using P-V and Q-V curves (for static voltage stability) and time-domain simulations (for dynamic voltage and transient stability).
- The critical power transfer used as indicator in the analysis (P-V curve) increased from scenario 1 to scenario 3, which is indicative of an improvement of the loadability margin and the static voltage stability in the NITS. The enhanced static voltage stability could however deviate from the reality as the real point of instability may be altered by the installation of reactive compensation devices. Despite the improvement in the loading limits, grid losses and line charging increased.
- The static voltage analysis using the Q-V curves showed a reduction in the reactive power margin (RPM) over the years. The NITS in scenario 3

was identified as the most vulnerable to voltage instability as a lower RPM is indicative of an increased risk of voltage collapse. This implies that the reactive power demand of the NITS should be balanced as demand increases over the years.

- The dynamic voltage stability of the NITS was assessed by simulating the loss of load and transmission line. The loss of load in the NITS revealed scenarios 2 and 3 to have oscillatory voltage profiles during the loss of load, which is attributed to the reduction in system inertia due to the increased RE penetration. The reduced inertia especially in scenario 2 (least system inertia) resulted in higher frequency amplitude of the slack generator during the load loss.

- The rotor angles of generators in scenario 3 deviated more from the reference generator than in scenario 2 during the transmission line loss.

- The transient stability of the NITS was analysed using the critical clearing time (CCT) and the maximum deviation of rotor speed for a three-phase short-circuit fault. CCTs of 0.377 s, 0.124 s and 0.132 s were recorded respectively for scenarios 1, 2 and 3. Only the CCT for scenario 1 was higher than the 150 ms fault clearing time used for the simulation, making scenario 2 and 3 transient instable.

- Based on the network development plans and infrastructural changes associated with the RE integration in the NITS, scenario 2 is estimated to be the most vulnerable scenario. This is due to its largest inertia deficit as a result of the lower number of conventional generators providing inertia in the network.

6 Stability Enhancement Measures

Results of the stability analysis, which identify different forms of instability for different conditions in the NITS confirm that a power system may be stable for a particular disturbance but unstable for the other as was presented in [126]. Based on this, it becomes 'impractical and uneconomical to design power systems to be stable for every possible disturbance' [126]. With regards to the stability analysis presented in the previous chapter, methods for enhancing the voltage and transient stability in the NITS will be discussed here. As no one stability improvement measure is adequate for the network, it is necessary to recommend a combination of different methods for effectively maintaining the stability of the network under different conditions. Taking into consideration existing technical and economic constraints in the NITS, only measures that are economical and robust and are suitable for Ghana's network will be considered.

6.1 Power System Stabilizers

The power system stabilizer (PSS) is a supplementary control and protective feature of the excitation system which uses auxiliary stabilizing signals in its controls [18, 52]. It supplies additional input signals such as frequency, power and shaft speed [57] to the regulator to improve oscillation damping so as to enhance the dynamic performance of the network. The auxiliary signals are used to produce a damping torque in phase with the rotor speed deviation (oscillations), which are added to the generator rotor. The PSS also provides supplementary control to both the automatic voltage regulator (AVR) and the turbine-governor of the generating unit [52]. A signal sensor, low- and high-pass filters, phase compensation, gain and limiter form the main components of the PSS.

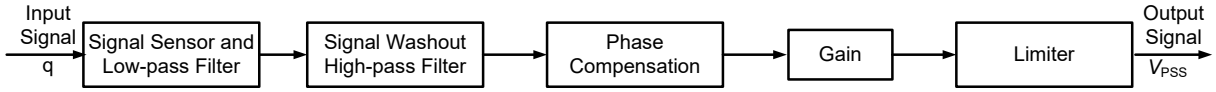

Figure 6-1: Major Components of the Power System Stabilizer (PSS) [52]

The input signal to the PSS could be the active power output of the generator, generator output frequency or rotor (shaft) speed deviation [52], [54]. The output signal which is fed into the AVR as the auxiliary signal is the V_{PSS}. A block diagram with the transfer functions of the individual blocks is shown in Figure 6-2 below:

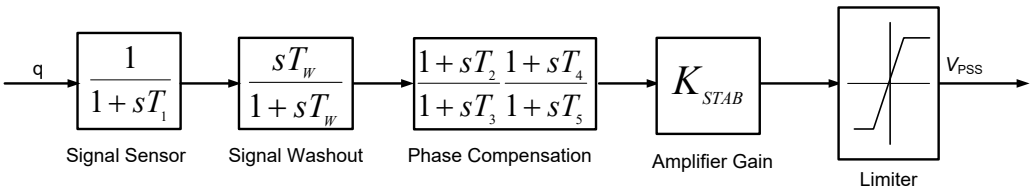

Figure 6-2: Functional Block Diagram of the Power System Stabilizer [18, 52, 133]

The *signal sensor block*, also a first-order low-pass filter is used to filter the input signal to the PSS.

The *signal washout block* is a high-pass filter which eliminates low frequencies in the signals, allowing the PSS to respond to the appropriate changes. It has a time constant T_W, which is required to be long enough (between 1s and 20s) to allow the signals to pass through unchanged. A washout time constant of 10s is however considered for an optimal improvement in system stability [133]. T_w values should however not be extremely long to cause undesirable excursions of the generator voltage during islanding [18].

The *phase compensation circuit*, usually made of a phase-lead compensation is used to compensate for the lag between the generator electrical torque and the exciter input [18, 133]. Two or more first-order blocks are often used in practice for the appropriate compensation, although a first order block is sometimes used.

The *gain block*, which comprises the stabilizer gain determines the amount of damping to be produced by the PSS [18, 133]. The gain of the PSS ranges between 1 and 50 [134] and should be set to a value that corresponds to the maximum damping, although sometimes limited by other considerations [18].

The *limiter* proportionally reduces the output signal when the prescribed magnitude is exceeded [52].

Although the use of the PSS in enhancing system stability has been proven to be a cost-effective method [52], few generators in the NITS are equipped with PSS, most of which are currently not in use. Despite, based on the objective of this thesis, all generators will be equipped with the STAB2A PSS model to evaluate their impacts on system stability. The STAB2A model is a power sensitive stabilizer, which produces a supplementary signal by introducing a phase-lead into a signal, which is proportional to the power output measured at the generator terminals [56]. This model is a dual-input stabilizer which derives the stabilizing signal using a combination of the power and speed. Details of the STAB2A PSS model can be found in [54, 57].

With the PSS in operation, a three-phase short-circuit fault on the critical line was simulated at time t = 1s for a period of 15 s.

The resulting rotor angle of a sample generator is presented in Figures 6-3 and 6-4.

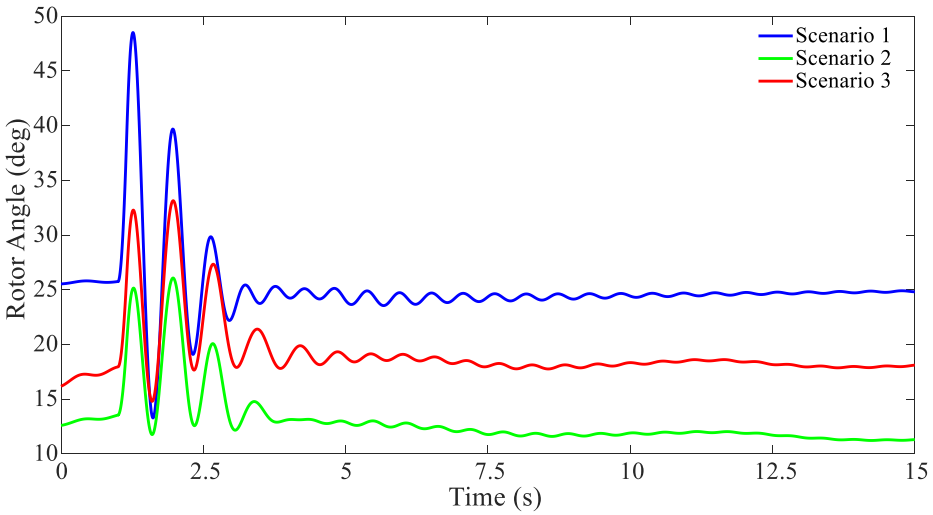

Figure 6-3: Generator Rotor Angle with PSS

The generator rotor angle during a three-phase fault is as follows:

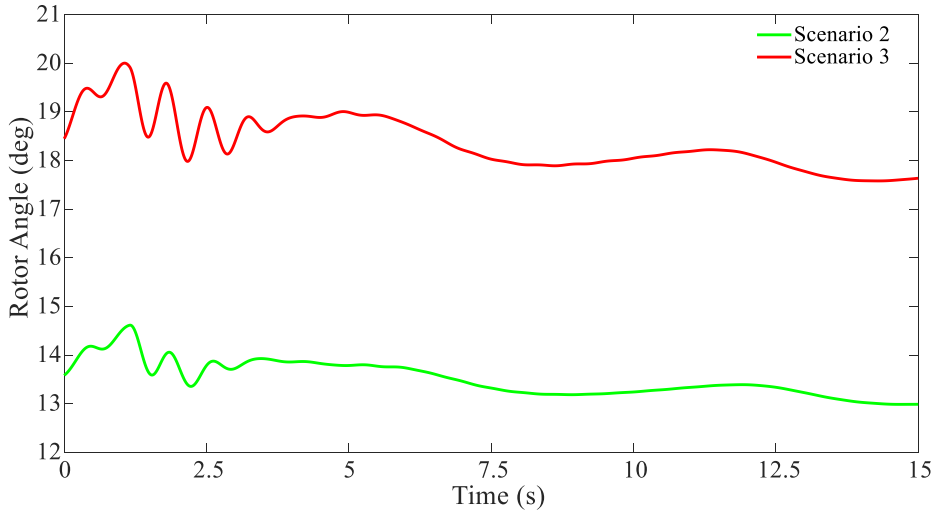

Figure 6-4: Generator Rotor Angle during a Three-Phase Short-Circuit Fault - with PSS

The figure shows that the generator rotor angle swings are well damped by the PSS in operation, which is also evident from the reduced settling times of the rotor angles. A comparison of the settling times with and without the use of the PSS is summarised in the table below:

Table 6-1: Comparison of Settling Times With and Without PSS

Scenarios	Settling Times (s)	
	Without PSS	With PSS
S1	11.46	8.78
S2	10.78	7.21
S3	13.42	8.21

6.2 FACTS Devices

Flexible AC transmission system (FACTS) devices are among the main devices used in enhancing power system stability (damping power oscillation and improving transient stability) in addition to their major function of controlling the flow of power in a power system [74, 135]. FACTS devices are mainly power electronic based and static devices that offer additional control of certain power system parameters [135]. FACTS devices are grouped into the series connected, shunt connected, combined series-series and combined shunt-series devices. Examples of the FACTS devices include among others the Static Var Compensator (SVC), Thyristor Controlled Series Compensator (TCSC), Static synchronous Compensator (STATCOM), Static Synchronous Series Compensator (SSSC) and Unified Power Flow Controller (UPFC). FACTS devices provide fast active and reactive power compensation in the power system and are thus used to provide voltage support, control power flow and increase the transient stability and oscillation damping in the network [39]. The STATCOM and SVC whose primary mode of voltage control are at the (critical) buses in the network will be considered further in this thesis. Although FACTS devices can be capital intensive, their capital investment and operating costs (maintenance and losses) are often offset by the benefits they offer [135]. The optimum location of the FACTS devices in the power system is very essential in the efficient utilization of particularly the existing network [39]. The genetic algorithm method of solving optimization will be used to determine the most reactive power deficient nodes in the NITS. The defined nodes will serve as the basis for the placement of the FACTS devices in the network.

6.2.1 Static Var Compensator (SVC)

The SVC is a shunt-connected FACTS device, which works as a static generator or absorber whose output is varied to control specific system parameters [18]. The

absence of rotating main parts and inertia in the SVC results in the term ‘static’ [18, 135] in its name. SVCs have fast responses (within 2-3 cycles), which enable the fast control of reactive power [135, 136]. It is used to control voltage either directly at the connected busbar or at a remote busbar. An aggregation of SVCs and mechanically switched reactors or capacitors whose output is coordinated is known as a static var system (SVS) [18]. The schematic diagram of a typical SVS is shown in Figure 6-5.

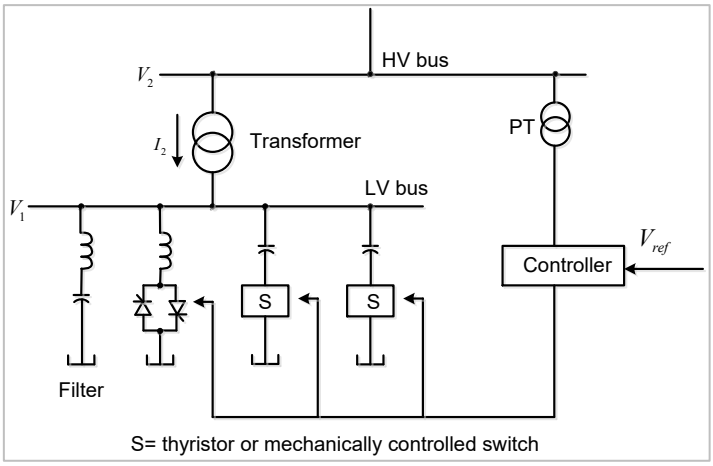

Figure 6-5: Schematic Diagram of a Static Var System (SVS) [18]

The capacitors in the SVS may be turned on or off in response to changes in reactive power demand based on the loading condition in the network. The thyristor-controlled reactor (TCR) has the function of fine-tuning the reactive power produced by the SVS [137]. Several basic types of SVC exist – saturated reactor (SR), thyristor-controlled reactor (TCR), thyristor-switched capacitor (TSC) and thyristor-switched reactor (TSR), etc. which are combined differently to form various compensation configurations used in the transmission network [18]. Details on the working principle of the SVC can be found in [18, 135–137].

6.2.2 Static Synchronous Compensator

The static synchronous compensator (STATCOM), also known as the improved SVC is a FACTS device, which utilizes a voltage-source (VSC) or current-source converter (often a VSC) to provide shunt compensation [39, 52, 59, 138]. The STATCOM is widely used for providing both steady-state and transient voltage control at different points in the power system. The schematic of a typical STATCOM is shown in Figure 6-6.

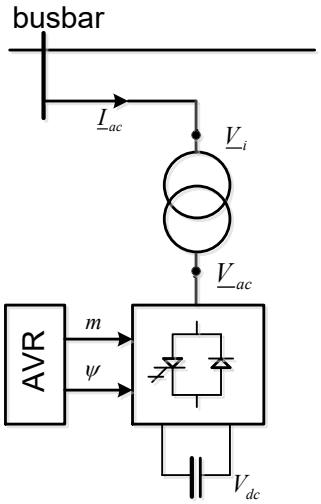

Figure 6-6: Schematic of a STATCOM based on a Voltage Source Converter [52, 138]

The VSC has only a capacitor on its DC side. The VSC seen in the schematic uses a pulse-width modulation (PWM) controller with two control parameters m and ψ, for the magnitude and phase of the AC voltage respectively. The AVR is included in the STATCOM to compensate the reactive power in the network. Its aim is to act on the control parameters (m and ψ) to ensure an accurate change in reactive power. The compensator acts like a capacitor and supplies reactive power when $V_{ac} > V_i$ (in that case the I_{ac} leads V_i). The compensator behaves like a reactor and absorbs reactive power when when $V_{ac} < V_i$ in which case I_{ac} lags behind V_i). The AC voltage and current are defined by the following equations:

$$\underline{V_{ac}} = mk\underline{V_{dc}}(\cos\psi + j\cos\psi) \tag{6.1}$$

$$\underline{I_{ac}} = \frac{\underline{V_i} - \underline{V_{ac}}}{jX} \tag{6.2}$$

As a voltage regulator in transmission networks, an additional PSS is required to effectively damp power oscillations [52]. The STATCOM has been proven to be more effective (provides better response)at low voltages than its static counterpart the SVC [74].

6.2.3 Optimum Location and Size of FACTS Devices

Similar to the optimization problem presented in section 4.3, this section aims at identifying the best five locations for reactive compensation devices (in this case the FACTS devices) in the NITS and their respective sizes. The genetic algorithm (GA) method of solving constrained and unconstrained optimization problems is used. The objective is to minimise grid losses and ensure that busbar voltages and equipment loadings are within defined limits at all times. The decision/control

variables of the optimization are the MVAr outputs and locations of the FACTS devices.

The objective function for minimizing grid losses is expressed in (6.3) as

$$S = I^2 \cdot Z \tag{6.3}$$

The constraints based on the bus voltage and thermal ratings of the transmission lines are given as

$$V_i^{min} \leq V_i \leq V_i^{max} \tag{6.4}$$

$$S_i = S_{rating} \tag{6.5}$$

The GA starts by randomly selecting the initial values of the control variables (MVAr output) which are within the maximum and minimum values as shown in Table 6-2. The table shows the possible maximum sizes of reactive power compensation in the NITS based on Ghana's network database. The locations of the devices are limited to only the 161 kV and 69 kV busbars in the NITS.

Table 6-2: Sizes of Reactive Power Compensation Devices in the NITS

Reactive Power Devices	**Reactive Power, Q (MVAr)**	
	Minimum	Maximum
1	0	30
2	0	30
3	0	30
4	0	30
5	0	30

A Newton Raphson load flow is carried out to determine the total system loss, which is followed by a thorough check of the optimization constraints (bus voltages and transmission line ratings) to ensure that they are all within the grid code stipulated range. The process is repeated until all constraints are met and a minimum value of the grid losses is obtained. The optimization process is described by the flow chart presented in Figure 6-7.

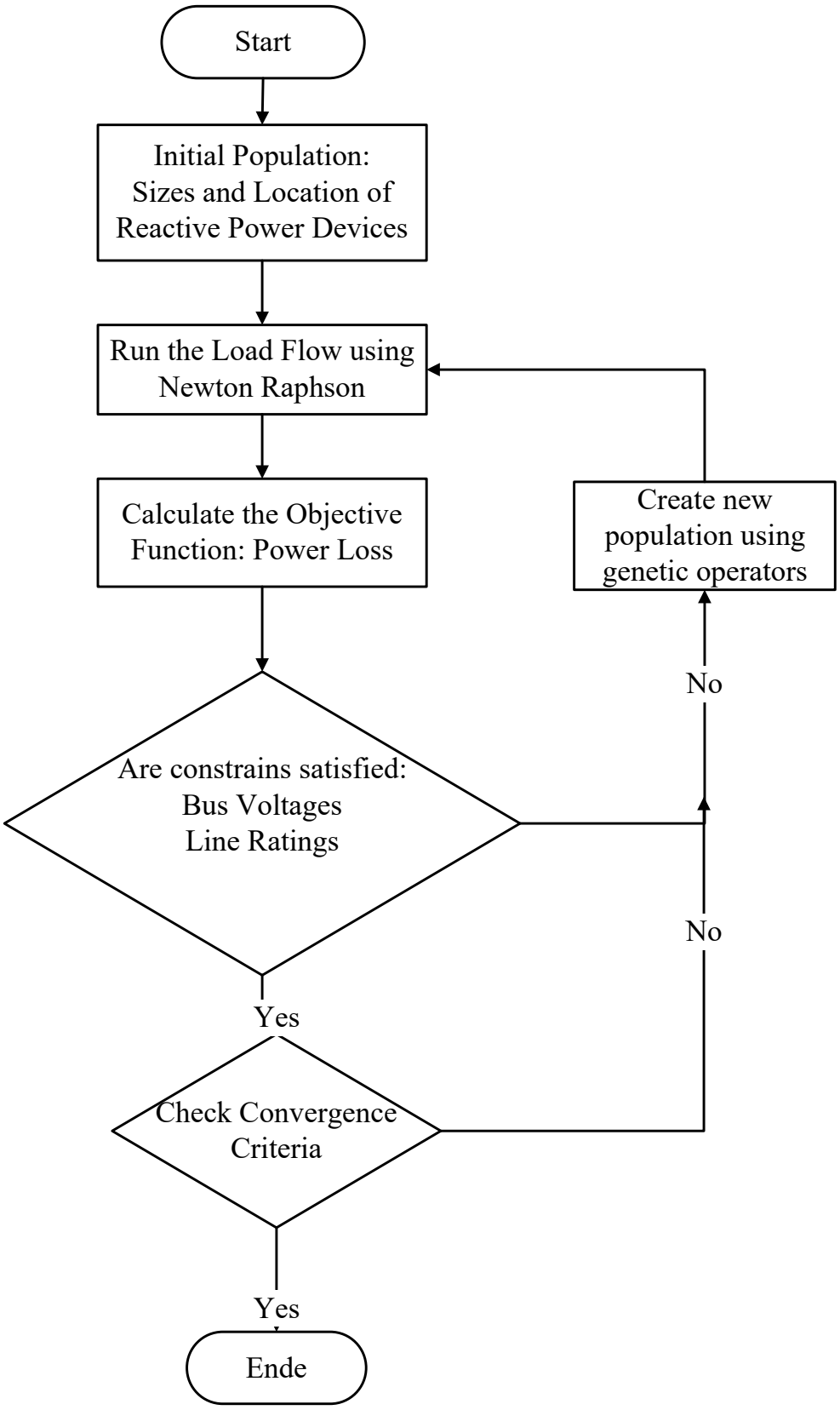

Figure 6-7: Flowchart for the Optimization Algorithm

Sample results of the optimization for scenario 1 is presented as follows: Results for Scenarios 2 and 3 are provided in table 0-10 in appendix E.

Table 6-3: Reactive Power Deficient Buses in the NITS - Scenario 1

	Scenario 1 (S1)			
	Simulation 1		*Simulation 2*	
	Bus ID	*Size (MVAr)*	*Bus ID*	*Size (MVAr)*
Q1	1201	0.67	1003	24.52
Q2	1309	0.13	1007	5.45
Q3	1066	23.75	1309	5.08
Q4	1077	25.90	1042	0.61
Q5	1004	28.33	1004	28.03

The table provides the five most reactive power deficient busbars in the NITS and the amount of reactive power required to maintain bus voltages and transmission line loadings within the given limits. These busbars will subsequently be the locations of the FACTS devices in the NITS. Busbar 1004 (Q5 in Figure 6-8) will be thence considered since it is also the busbar with the largest load in the NITS.

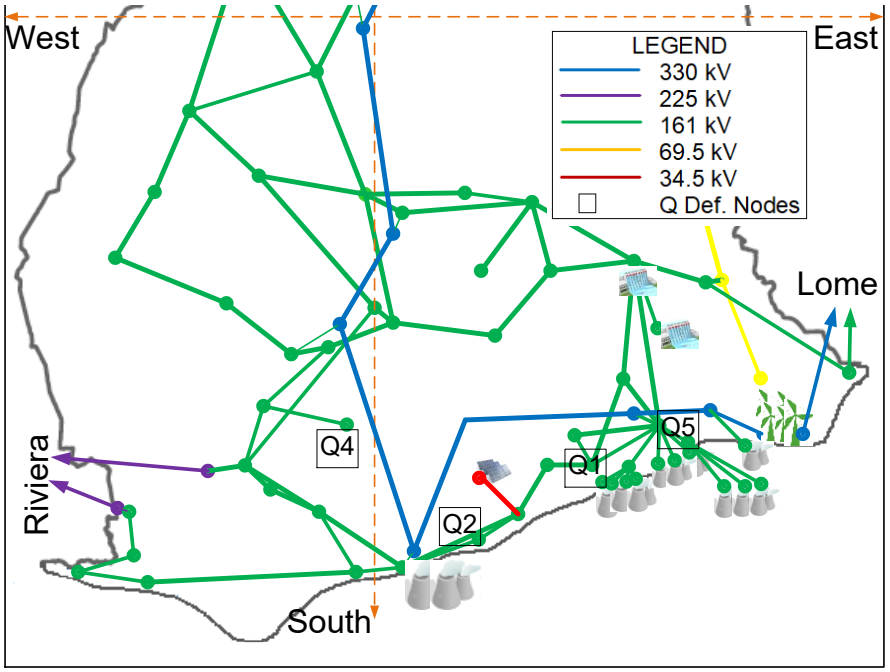

Figure 6-8: Reactive Power Deficient Busbars in the NITS

Four of the five reactive power deficient buses are located in the south (see Figure 6-8), with only one in the north. This optimization results confirms the voltage vulnerability of the busbars in the south of the NITS.

6.2.4 FACTS Devices in the NITS

This section presents the effects of installing FACTS devices in the NITS. The characteristic feature of the SVC for instance (which allows the capacitors to be

turned on and off the capacitor in response to reactive power changes) makes the SVC appropriate for use in the NITS.

SVC

With the FACTS devices in place, static voltage stability analysis using P-V and Q-V curves was performed to verify the effects of the FACTS devices in the network. The following figures show the P-V and Q-V curves with and without the SVC.

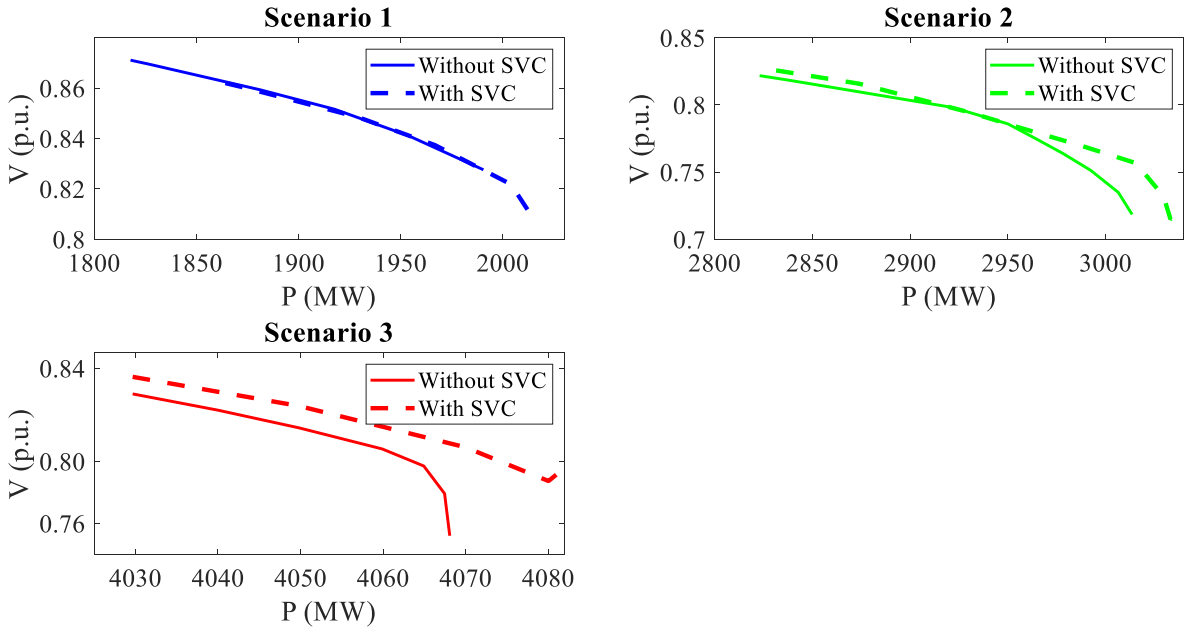

Figure 6-9: P-V Curves for with and without SVC - All Scenarios

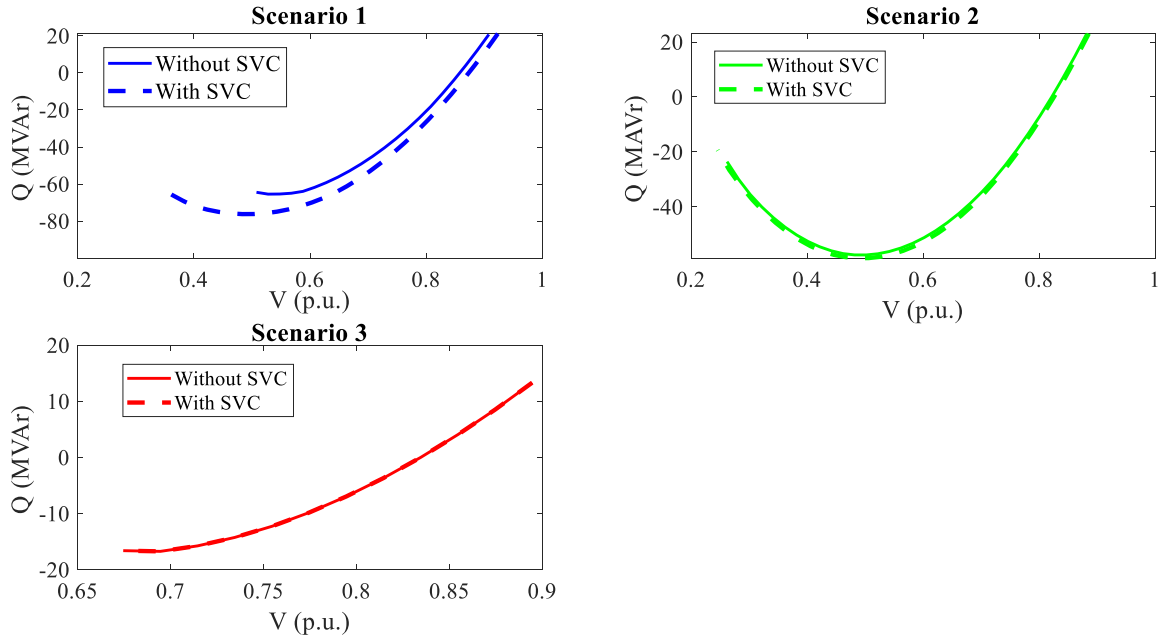

Figure 6-10: Q-V Curves for with and without SVC - All Scenarios

The critical power transfers increased with the SVC in the NITS and were better than in the case without the SVC (see Figure 6-9). This confirms the function of the SVC in improving the power transfer capability of the network. The Q-V curves with the SVC showed better RPM than without the SVC. With the SVC in the NITS, the network could withstand higher loading and maintain system operation at even lower voltages as seen in the summary in Table 6-4.

Table 6-4: Summary - Static Voltage Stability Analysis using P-V and Q-V Curves with SVC

Scenarios	Critical Power Transfer (MW)	Critical Voltage (p.u.)	Reactive Power (MVAr)
S1	2,013	0.483	-76.21
S2	3,036	0.486	-58.68
S3	4,082	0.694	-16.73

The installation of the SVC in the NITS increased the loadability of the network, which confirms the results in the research of [37]. Given this, the implementation of SVC offers the possibility to utilize more of the available power capacity and sustain stable operation even at lower voltages.

The impact of the SVC on the dynamic voltage stability was assessed using the loss of load and transmission line (similar to the case without SVC). Sample results of the busbar voltage and generator rotor angle for the load loss are presented in Figures 6-11 to 6-13.

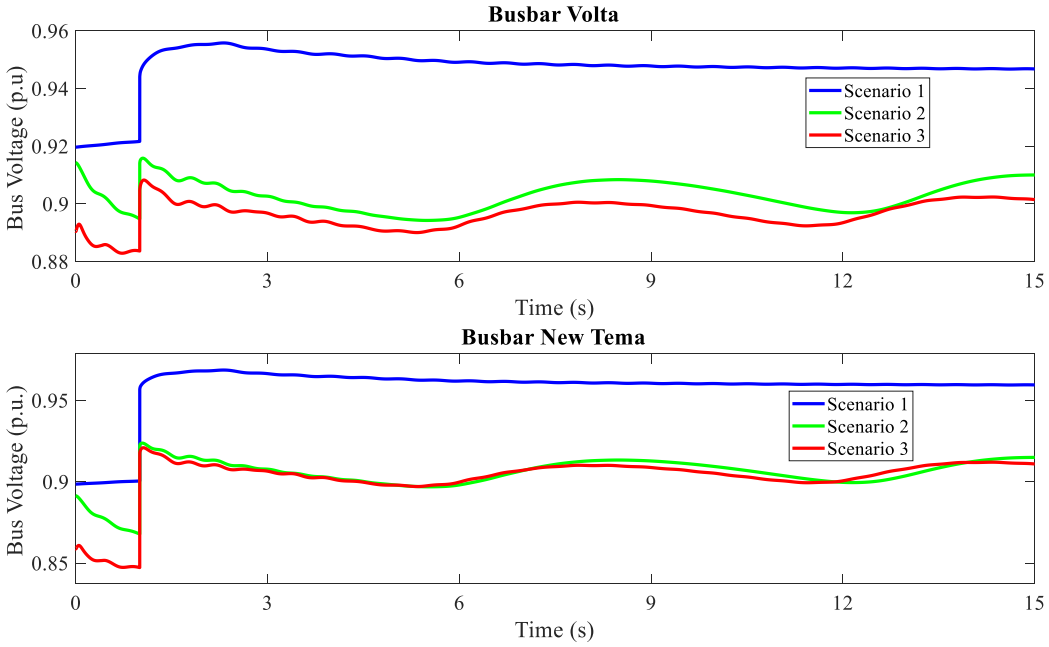

Figure 6-11: Busbar Voltages during Loss of Load - with SVC

The figure shows oscillatory bus voltages in scenarios 2 and 3 and a well damped voltage profile in scenario 1. The voltage of the busbar closer to the SVC (busbar New Tema) showed improved oscillation damping, which also confirms the importance of the optimum location of the SVC in providing an effective oscillation damping. The corresponding generator frequency profiles are shown below:

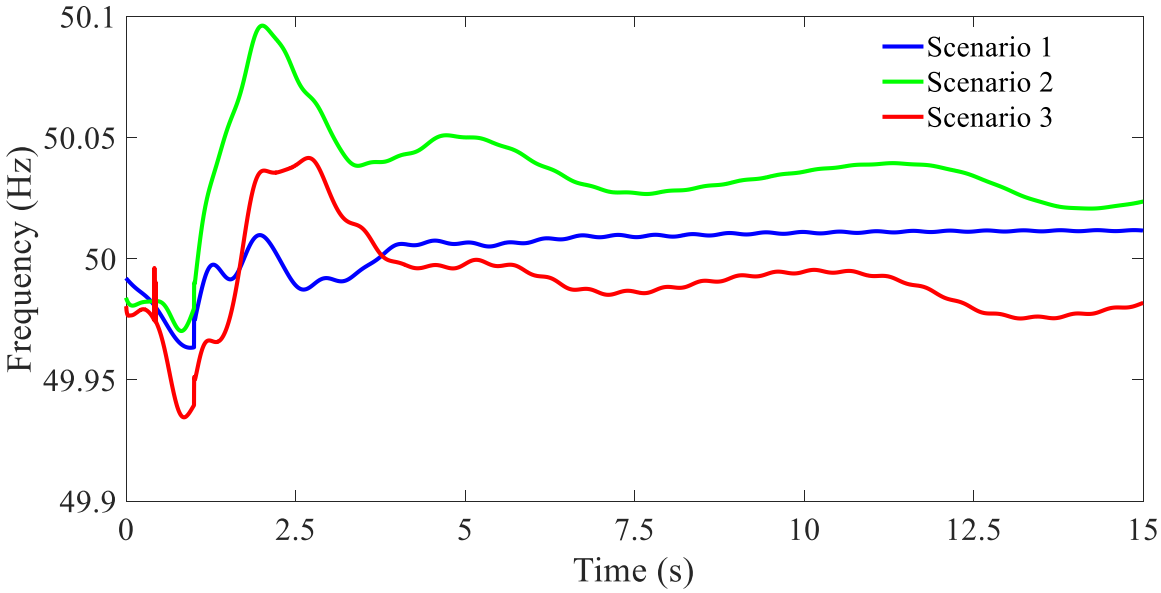

Figure 6-12: Generator Frequency (Slack Gen) during Loss of Load - with SVC

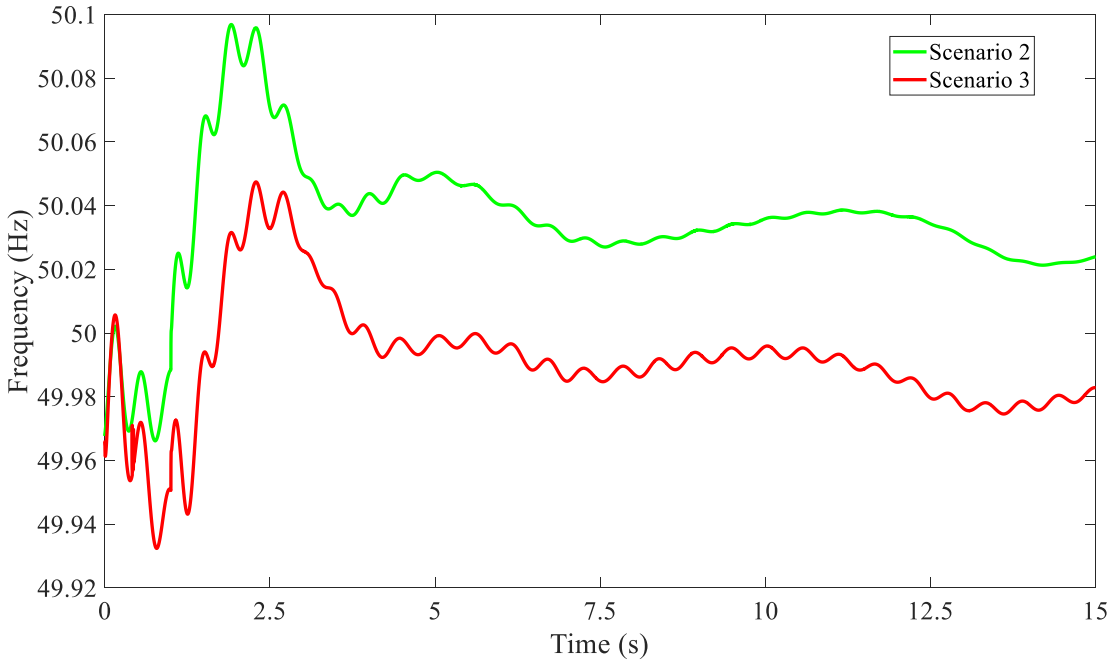

Figure 6-13: Generator Frequency (Closer Gen) during Loss of Load - with SVC

Figure 6-12 reveals a well-damped frequency oscillations at the slack during the loss of load with the SVC than without the SVC, which was more oscillatory with

higher frequency excursions. The improvement in oscillation damping confirms the effectiveness of the SVC in the NITS.

STATCOM

Similar to the SVC, the effects of the STATCOM in the NITS was assessed using static and dynamic voltage stability analysis techniques. Figures 6-14 and 6-15 present the results of the analysis using P-V and Q-V curves.

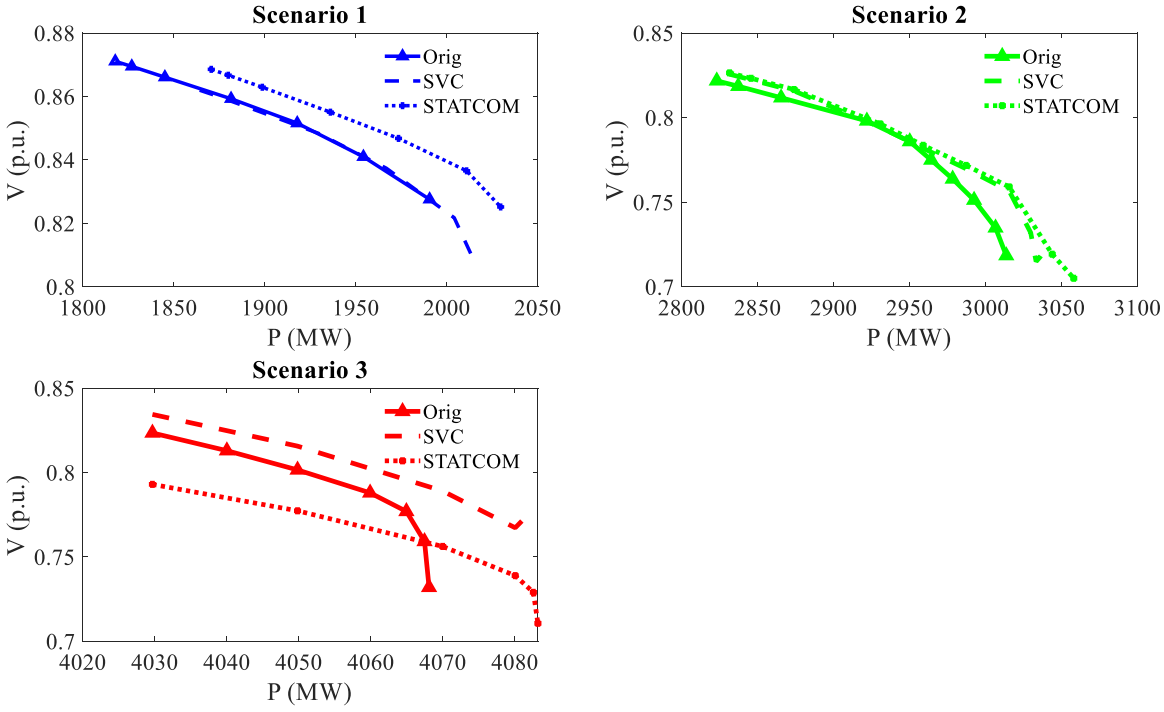

Figure 6-14: Comparison of P-V Curves - With and Without FACTS Devices

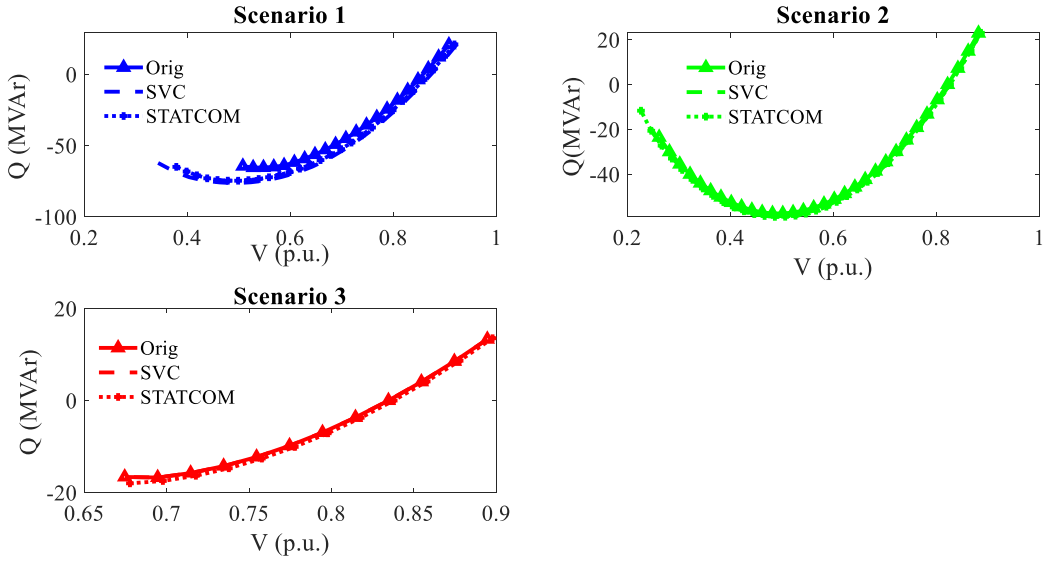

Figure 6-15: Comparison of Q-V Curves - With and Without FACTS Devices

While both the STATCOM and SVC improved the static stability of the NITS, the performance with the STATCOM was better than with the SVC. It is observed from Figure 6-15 that the RPM in the NITS improved only slightly with the installation of the FACTS devices, which makes a lot of difference in a sensitive network like Ghana's. Table 6-5 summarises the critical power transfers in the network without FACTS (original) and with the FACTS devices (SVC and STATCOM).

Table 6-5: Comparison of the Critical Power Transfer in the NITS

Scenarios	**Critical Power Transfer (MW)**		
	Original	With SVC	With STATCOM
S1	1,991	2,013	2,030
S2	3,014	3,036	3,072
S3	4,068	4,082	4,093

Corresponding frequency profiles of the slack and the generator closer to the load bus are shown in Figures 6-16 and 6-17.

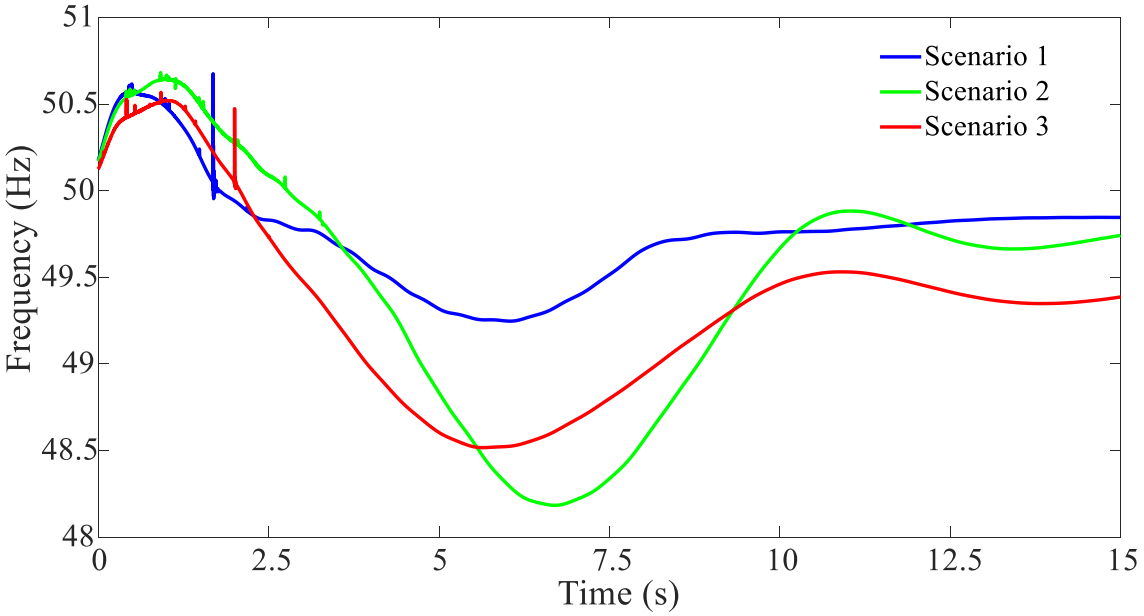

Figure 6-16: Generator Frequency (Slack Gen) during Loss of Load - with STATCOM

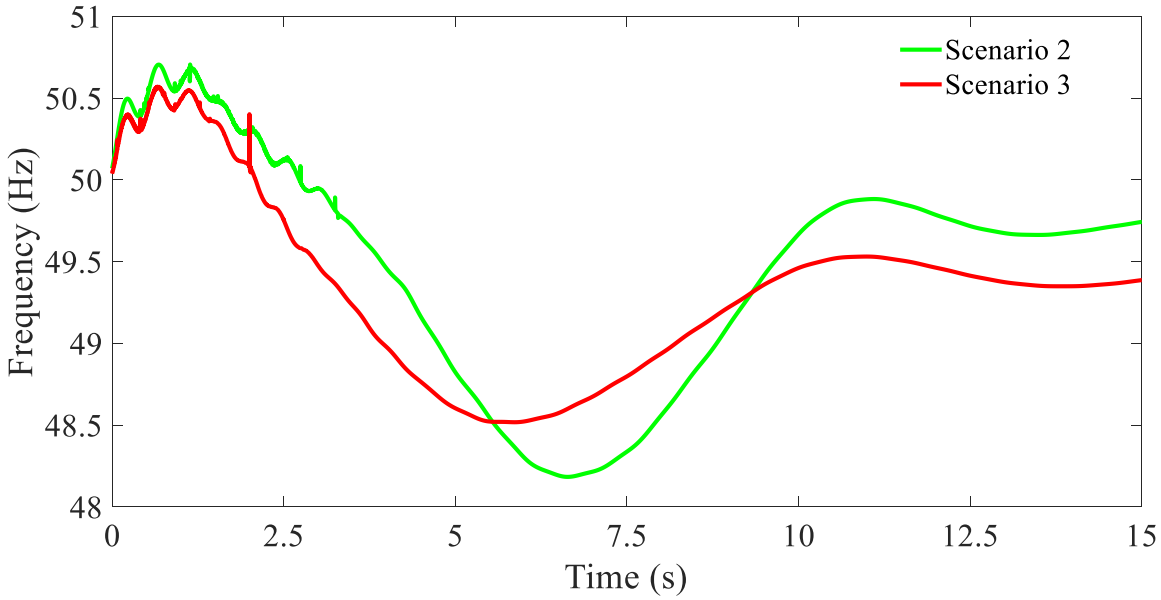

Figure 6-17: Generator Frequency (Closer Gen) during Loss of Load - with STATCOM

Figure 6-17 shows only scenarios 2 and 3 because the generator under consideration was not in operation in scenario but from scenario 2 onwards.

The rotor angle profile indicates an improvement in the oscillation dampings, which confirms the effectiveness of the STATCOM in the NITS. The oscillations were well damped with the STATCOM than without the STATCOM for all three scenarios.

Summary of Results

- Two main measures to improve system stability; the use of power system stabilizers (PSS) and flexible AC transmission system (FACTS) were proposed to enhance the stability of the NITS.
- The use of the PSS in combination with AVR improved the transient stability of the NITS as the settling times were drastically reduced. In contrast to the original case without PSS, the longest settling time recorded was 8.78s as against 13.42 s for the case without PSS.
- The genetic algorithm method of solving optimization was used to determine the optimum location of reactive compensation devices in the NITS. Using voltage and loading limit as the constraints, the method of optimization was used to identify the reactive power deficient nodes. These nodes became the installation points for the FACTS devices.

- SVC and STATCOM were subsequently installed on the identified reactive power deficient nodes and the simulation results showed improvement in the overall stability of the NITS. Oscillations in the network were well damped with the SVC and STATCOM.

7 Conclusions and Outlook

The final chapter of this thesis is made of three parts. The first part provides the conclusion remarks by summarising the analysis carried out in the thesis with the respective simulation results. Conclusions drawn from the research findings and results are also presented. The limitations that were encountered during the research (and measures taken to overcome the limitations) are provided in the second part. The chapter ends with the outlook for further research and suggestions for consideration in future research.

7.1 Conclusion

This research focussed on analysing the current state of the Ghanaian NITS and investigating the effects of the grid integration of RE on the stability of the NITS. A model of Ghana's transmission network was initially developed and used to model scenarios to consider changes (infrastructural and operational) in the network for three different years – 2017 (base case), 2020 (target case) and 2023 (post-target) scenarios, which are subsequently known as scenarios 1, 2 and 3 respectively. The thesis therefore provided detailed and adequate knowledge on network modelling, particularly for Ghana's national interconnected transmission system.

In modelling the Ghanaian transmission network in this research, system demand and all other components in the distribution network were aggregated and modelled as loads (with the necessary parameters). Power factor correction measures being implemented in the network were also considered. The 10% annual demand growth in the NITS was incorporated in the modelling. The generators (synchronous, PV and wind generators) were also modelled taking into consideration their characteristics, ratings and technical properties.

To commence the simulations, the period for the analysis was determined to be the 'off-peak' period in the network, with a subsequent adjustment of the system demand to the off-peak demand. Steady-state analysis (load flow and contingency analysis) were carried out to determine the state of the NITS and also identify the critical transmission lines using voltage stability indices.

The assessment of the current state of the NITS, which was one of the objectives of the research was carried out using steady-state analysis. Through this it was determined that the NITS suffers low voltages, especially on the heavily loaded busbars in the south. Voltages of busbars here violated the 5% voltage limit for normal operation, with several buses recording voltages lower than the 0.95 p.u. lower limit. The simulation results also revealed an increased number of transmission line overloads in the network. This led to the conclusion that the NITS is in a 'critical' state which requires urgent measures to maintain and improve both the reliability and security of the network. Implementing the necessary measures also enhances and prepares the network to accommodate RE generation. The integration of RE in the NITS thus provides generation in the north, contributes to reducing the high voltages recorded in the north and at the same time eases the transmission burden and reduces transmission losses.

Although the NITS in its current state (reactive compensation, generation and load) can accommodate approximately 5% RE with an amount of reinforcement, the bidirectional power flow driven by the RE generation in the north introduces additional operational changes in the network. Measures to manage the existing bottlenecks in the NITS such as the use of the reactive capability of synchronous generators, installation of reactive compensation devices, increasing the current carrying capacity of transmission lines and transformers, construction of new transmission corridors and the integration of the optimum amount of RE in the network were proposed. Implementing the proposed measures, improved the current state of the NITS and also increased the network's capacity to accommodate additional RE generation. As part of the steady-state analysis, voltage stability indices were further used to identify the critical transmission lines in the NITS, which indicated that the tie-line between Ghana and Burkina Faso is the most critical line in the network. The identified critical lines were used as basis for subsequent analysis in the research.

Contingency analysis of the network was performed to identify the vulnerable equipment in the NITS and also validate the (N-1) reliability of the network. The transmission line contingency revealed that although system operation could be maintained during the contingency of the tie-line, network losses increased drastically post-contingency. The transformer contingency on the other hand did not affect the NITS negatively. The effect of the loss of RE generation was also simulated with different RE contingencies (15% PV + 100% Wind, 15% PV + 0% Wind, 100% PV + 0% Wind) which suggested scenario 3 (post-target scenario) to be the most affected by the RE contingencies owing to the larger share

of RE in that scenario. The RE contingency '100% PV + 0% Wind' however had less effect on the NITS (lesser overloads and voltage violations) and led to the conclusion that the loss of wind generation in the NITS is not as detrimental as the loss of PV generation due to its size and location in the network.

Investigating the effects of the RE on the stability of the NITS was the second focus of this research. Here both static and dynamic voltage stability analysis techniques as well as transient stability analysis techniques were utilized. P-V and Q-V curves were the main tools in determining the critical power transfer and reactive power margin of the NITS. It was found that the critical power transfer of the network improved across the scenarios while the reactive power margin (RPM) decreased, which was indicative of the reactive power deficiency in the network. On the contrary, the dynamic voltage stability analysis showed the NITS was at a higher risk of instability in scenarios 2 and 3. Higher voltage oscillations (with longer durations) were recorded in these two scenarios, though scenario 3 was often better. The transient stability analysis also revealed a reduction in the critical clearing time (CCT) from scenarios 1 to 3. The CCT obtained for scenarios 2 and 3 were lower than the used fault clearing time, indicating transient instability in these scenarios. Scenario 2 was however considered the worst as larger oscillations with longer settling times were present.

An important consideration in this thesis is that the scenarios were developed not only based on increasing RE penetration but also with other network changes (such as increased demand, generation, different reactive compensation strategies and new infrastructure). These other factors also affect the dynamics of the stability of the network. Thus scenario 2 being the worst does not fully imply the effects of the RE units as these other factors also play a part. Despite, a major observation was that transmission line overloads in the south and high voltages in the north improved with increasing RE penetration in the NITS.

As part of efforts to improve the stability of the NITS, measures which suit the specific needs of the Ghanaian power system were proposed. The use of PSS (in combination with the AVR) and FACTS devices such as SVC and STATCOM were explored in this research. The simulation results showed that the use of the PSS enhances the transient stability as the settling times (duration of oscillations) were reduced. The genetic algorithm method for solving optimization problems was used to determine the optimum location of the FACTS devices in the NITS. Reactive power deficient nodes in the NITS were identified, which served as the points for installing the FACTS devices. The installation of the SVC and

STATCOM on these buses improved the overall stability, as power transfer capability and reactive power margin were enhanced. Voltage and frequency oscillations were similarly damped with the SVC and STATCOM.

Results of the analysis presented in this research indicate that the integration of RE in the NITS is 'technically' feasible and possible as long as measures are taken to ensure system operation within the required limits. The integration of RE was found to have both positive and detrimental effects on the stability of the NITS. The identification of the optimum RE penetration level in the NITS showed that most RE units are currently oversized (in relation to the approved capacities in the RE development licenses) leading to violations of the voltage and loading limits. Furthermore, the NITS showed different responses to different forms of stability, which confirms that a power system may be stable for one stability phenomenon but unstable for the other phenomenon.

The integration of RE in Ghana had both positive and negative impacts on the NITS depending on factors such as the penetration levels, type of disturbance, fault location, total system inertia (reduces with increasing RE penetration), location and loading direction of the PV units. These are important factors that influence the dynamics and hence the stability of the network. The research concludes that the reduced system inertia, which makes the system more prone to transient instability is compensated for by the reduction in active power flow, which in effect leads to a stable performance.

This research conceptually contributed to the analysis of the integration of RE in a power system with peculiarities inherent in Ghana as well as the effect of the RE integration on system stability. Through this research, it is made clear that the investigation of the concepts of system stability and RE integration is possible as the Ghanaian NITS, with its peculiarities is carefully investigated with different percentages of RE generation. The research findings however indicate that the integration of RE helps improve the stability of the NITS.

This research contributed to the methods of power system analysis using a combination of simulation and computing tools. While authors in several researches have employed tools such as MATLAB and PSSE, this research used the DIgSILENT PowerFactory simulation tool to perform both steady-state and dynamic simulations of a power network. In addition to this, MATPOWER and MATLAB were respectively used for static analysis and the analysis of the data and simulation results. The use of these tools offered the avenue to carefully

consider the real conditions of the NITS and to also use generic data (models and data) based on information from literature where there were no real data available.

While most research consider the individual effects of different stability phenomenon, this research simultaneously considered two main stability phenomenon – voltage and transient stability. The requirement for the consideration of different forms of stability became necessary as a power system may be stable for one stability phenomenon but unstable for another stability phenomenon. P-V and Q-V curves were used to determine the critical power transfer and reactive power margin in the analysis of the static voltage stability. The duration and amplitude of oscillation were used to analyse the dynamic voltage stability. In contrast to several literature that use only the critical clearing time (CCT) to assess the transient stability of a network, this research further used the maximum deviation of the rotor speed and duration of oscillation to analyse the transient stability of the NITS.

Measures to improve the stability of the NITS, which are suitable for the peculiarities of the Ghanaian power system were further proposed in this research. The use of the PSS improved the transient stability of the NITS with less settling times as compared to the case without PSS. The use of the FACTS devices - SVC and STATCOM increased the loadability of the network. The static and dynamic voltage as well as the transient stability of the NITS were enhanced with the FACTS devices, confirming their effectiveness in the NITS.

7.2 Limitations

Despite the analysis carried out in this thesis, the research work had the following limitations: geographic range, data availability and collection and the methods of stability analysis. Geographically, this research focussed on Ghana, which is only one country in Africa and as such does not lend itself to the generalizability of the research results for the African continent. Notwithstanding, countries with similar network structure, conditions and constraints could benefit from the analysis and results. Ghana was chosen because of its RE objective of increasing the share of RE in the generation mix amidst the constraints (technical and economic) and peculiarities of the network (location of generation and demand, length of transmission lines, etc).

Another major limitation of this thesis was access to data. Due to the focus on a real network, the availability and access to data was challenging and in most cases

difficult to come by due to the sensitivity of the data. There were instances where data received were outdated and could thus not be used. Data collection for that matter was cumbersome since not all requested information were available or could be accessed. Generic data and models from literature were subsequently used in such instance to enhance the simulation and analysis in this thesis.

The methods of analysing the stability of the NITS was another limitation to this research. Voltage stability was considered in this research using both static and dynamic voltage stability analysis techniques. Rotor angle stability was limited to transient stability without the consideration of the small-signal stability analysis. Due to the scope of this research, the phenomena of frequency stability and resonance stability due to the installation of FACTS devices were not considered. Although the main objective of the thesis was to analyse system stability, this was limited to only voltage and transient stability due to the inherent voltage issues in Ghana's power system.

7.3 Outlook

A major outlook of this thesis is to extend the research to the power systems of other African countries, especially those in the early stages of the RE development. For instance, the West African Power Pool (WAPP), which is the interconnection of the power systems of the West-African countries offers the platform for the investigation of the effects of RE integration on the interconnected network of west-African countries. This could be further developed to consider other power pools such as the East-African Power Pool (EAPP). A similar structure to the European Network of Transmission System Operators (ENTSO-E) is under consideration in the African context to enable the analysis of several national power systems as well as power trade among all African countries.

Further research could consider the use of the extended reactive capability (ERC) of the DFIG wind power plant to improve stability and overall system performance. The ERC of DFIG wind plants offers a flexible and increased power factor range compared to the conventional fixed power factor range of operation (between 0.95 leading and 0.95 lagging) for most power systems. The wind plants, which are strategically located in the NITS could be utilized to improve system stability.

Based on the results of the optimization to identify the optimum RE share in NITS, most RE units are currently oversized in the network leading to numerous violations of voltage and loading limits. To this, further research on investigating the effects of RE generation could consider the identified optimum RE share for the analysis rather than the RE percentage shares proposed by the Energy Commission. Results could be compared to confirm the effects of the optimum RE share in the NITS.

Further research could consider the use of high-voltage direct-current (HVDC) transmission to improve the stability of the NITS. Existing tie-lines in the interconnected network could be replaced with HVDC lines for improved operation.

8 References

[1] Ghana Grid Company, G. Energy Commission, Bui Power Authority, Electricity Company of Ghana Ltd., Northern Electricity Company, and Ghana National Petroleum Company, "2020 Electricity Supply Plan for Ghana: An Outlook of the Power Supply Situation for 2020 and Highlights of Medium Term Power Requirements," Accra, Ghana. Accessed: Apr. 1 2020. [Online]. Available: http://www.gridcogh.com/electricitysupplyplan

[2] Government of Ghana (Energy Commission), "2018 Electricity Supply Plan for Ghana: An Outlook of the Power Supply Situation for 2018 and Highlights of Medium Term Power Requirements," Accra, Ghana, 2018. Accessed: Aug. 28 2018. [Online]. Available: http://www.energycom.gov.gh/files/2018_Electricity_Supply_Plan.pdf

[3] Energy Commission *et al.,* "2019 Electricty Supply Plan for Ghana: An Outlook of the Power Supply Situation for 2019 and Highlights of Medium Term Power Requirements," Accra, Ghana. Accessed: Feb. 6 2020. [Online]. Available: http://www.energycom.gov.gh/files/2019%20Electricity%20Supply%20Plan.pdf

[4] Ghana Grid Company *et al.,* "2020 Electricity Supply Plan for Ghana: An Outlook of the Power Supply Situation for 2020 and Highlights of Medium Term Power Requirements," Accra, Ghana, 2020. [Online]. Available: http://www.gridcogh.com/electricitysupplyplan

[5] Statista, *Country Outlook - Economy of Ghana.* [Online]. Available: https://www.statista.com/outlook/998/226/economy/ghana (accessed: Apr. 2 2020).

[6] Trading Economics, *Ghana GDP 1960 - 2019 Data.* [Online]. Available: https://tradingeconomics.com/ghana/gdp (accessed: Apr. 2 2020).

[7] Energy Commission of Ghana, "2018 Energy (Supply and Demand) Outlook for Ghana," Accra, Ghana, Apr. 2018. Accessed: Aug. 27 2018. [Online]. Available: http://www.energycom.gov.gh/planning/data-center/energy-outlook-for-ghana

[8] E. N. Kumi, "The Electricity Situation in Ghana: Challenges and Opportunity," CGD Policy Paper., Center for Global Development, Washington DC. [Online]. Available: https://www.cgdev.org/sites/default/files/electricity-situation-ghana-challenges-and-opportunities.pdf

[9] Energy Commission, "2019 Energy (Supply and Demand) Outlook for Ghana," Accra, Ghana, Apr. 2019. Accessed: Feb. 6 2020. [Online]. Available: http://www.energycom.gov.gh/planning/data-center/energy-outlook-for-ghana

[10] *Renewable Energy Act, 2011 of the Republic of Ghana: Act 832*, 2011. Accessed: Feb. 20 2015. [Online]. Available: http://energycom.gov.gh/files/RENEWABLE%20ENERGY%20ACT%202011%20%28ACT%20832%29.pdf

[11] Ministry of Energy, Energy Commission, and National Development Planning Commission, "Ghana Renewable Energy Master Plan," Government of the Republic of Ghana, Accra, Ghana, Feb. 2019. Accessed: Feb. 6 2020. [Online]. Available: http://www.energycom.gov.gh/files/Renewable-Energy-Masterplan-February-2019.pdf

[12] Ministry of Energy, "Energy Sector Strategy and Development Plan," Ministry of Energy, Republic of Ghana, Feb. 2010. Accessed: Feb. 12 2015. [Online]. Available: https://ouroilmoney.s3.amazonaws.com/media/documents/2016/06/09/energy_strategy.pdf

[13] Ministry of Energy, Republic of Ghana, *Sector Overview: Overview of the Ghana Power Sector.* [Online]. Available: http://www.energymin.gov.gh/sector-overview (accessed: Sep. 5 2018).

[14] mfoss, "Microsoft Word - Guide to Electric Power - Final_3_ July 2005.doc,"

[15] Tractebel Engineering GDF SVEZ, "Generation Master Plan Study for Ghana," Tractebel Engineering GDF SVEZ GRIDCOG/4NT/224115/000/00, Nov. 2011.

[16] Economic Community of West African States (ECOWAS), *The West African Power Pool (WAPP).* [Online]. Available: http://www.ecowas.int/specialized-agencies/the-west-african-power-pool-wapp/ (accessed: Sep. 5 2018).

[17] West African Power Pool (WAPP), *Creation of WAPP.* [Online]. Available: http://www.ecowapp.org/en/content/creation-wapp (accessed: Sep. 5 2018).

[18] P. Kundur, *Power System Stability and Control*: McGraw-Hill, Inc., 1994.

[19] Enclave Power Company (EPC) Ghana, *About EPC* (accessed: Sep. 17 2018).

[20] Northern Electricty Distribution Company, *Profile of NEDCo.* [Online]. Available: http://www.nedcogh.com/profile.php (accessed: Apr. 2 2020).

[21] Energy Commission of Ghana, "Strategic National Energy Plan 2006 - 2020: Annex II of IV: Electricity," Energy Commission, Ghana, Accra, Ghana, Jul. 2006. Accessed: Feb. 15 2015. [Online]. Available: http://energycom.gov.gh/files/snep/electricity%20final%20PD.pdf

[22] Ministry of Energy, *About Us - Ministry of Energy of the Republic of Ghana.* [Online]. Available: https://www.energymin.gov.gh/about (accessed: Jan. 22 2018).

[23] Energy Commission, *About - Who we are.* [Online]. Available: http://www.energycom.gov.gh/about (accessed: Apr. 2 2020).

[24] RESOURCE CENTER FOR ENERGY ECONOMICS AND REGULATION, Ed., *Guide to Electric Power*. Accra, Ghana: Resource Center for Energy Economics and Regulation, 2005.

[25] Volta River Authority, *About Us - Profile of VRA.* [Online]. Available: https://www.vra.com/about_us/profile.php (accessed: Apr. 2 2020).

[26] Bui Power Authority, *About Bui.* [Online]. Available: https://buipower.com/about-us/ (accessed: Feb. 6 2020).

[27] Ghana Grid Company, *Overview.* [Online]. Available: http://www.gridcogh.com/overview (accessed: Apr. 2 2020).

[28] Volta River Authority, *Northern Electricity Distribution Company (NEDCo).* [Online]. Available: https://www.vra.com/subsidiaries/northern_electricity_distribution.php (accessed: Sep. 13 2018).

[29] J. E. Essilfie, Z. Muller, J. Svec, and J. Tlusty, "STATCOM effect on voltage stability in Ghanaian electrical grid," in *Electric Power Engineering (EPE), Proceedings of the 2014 15th International Scientific Conference on*, Brno-Bystrc, Czech Republic, May. 2014 - May. 2014, pp. 235–240. Accessed: Apr. 27 2020. [Online]. Available: https://ieeexplore.ieee.org/stamp/stamp.jsp?tp=&arnumber=6839445

[30] Moeller & Poeller Engineering (M.P.E.) GmbH, "Analysis of System Stability in Developing and Emerging Countries: Impact of Variable Renewable Energies on Power System Reliability and System Security," Eschborn, Germany, Aug. 2013. Accessed: Mar. 21 2016. [Online]. Available: https://www.giz.de/expertise/downloads/giz2013-en-power-system-stability-developing-emerging-countries.pdf

[31] A. I. Elombo, S. P. Chowdhury, S. Chowdhury, and H. J. Vermeulen, "Grid Integration of Wind Energy: A Case Study on a Typical Sub-transmission Network in Namibia," in *45th International Universities Power Engineering Conference UPEC2010*, pp. 1–6. Accessed: Feb. 3 2015. [Online]. Available: https://ieeexplore.ieee.org/stamp/stamp.jsp?tp=&arnumber=5649209

[32] A. I. Elombo, S. P. Chowdhury, S. Chowdhury, and H. J. Vermeulen, "Impacts of grid integration of wind energy in the Namibian power network," in *International Conference on Power System Technology (POWERCON), 2010: 24-28 Oct. 2010, Hangzhou, China*, Zhejiang,

Zhejiang, China, 2010, pp. 1–8. Accessed: Feb. 3 2015. [Online]. Available: https://ieeexplore.ieee.org/stamp/stamp.jsp?tp=&arnumber=5666087

[33] M. Bello, C. Carter-Brown, R. Smit, and I. E. Davidson, "Power Planning for renewable energy grid integration - Case Study of South Africa," in *2013 IEEE Power & Energy Society General Meeting*, pp. 1–5. Accessed: Feb. 3 2015. [Online]. Available: https://ieeexplore.ieee.org/stamp/stamp.jsp?tp=&arnumber=6672904

[34] B. M. Buchholz and Y. Sassnick, "The German experience of the grid integration of renewable energy sources," in *2005 IEEE Russia Power Tech*, pp. 1–5. Accessed: Mar. 11 2015. [Online]. Available: https://ieeexplore.ieee.org/document/4524786

[35] J. Cochran, L. Bird, J. Heeter, and D. J. Arent, "Integrating Variable Renewable Energy in Electric Power Markets: Best Practices from International Experience," NREL/TP-6A00-53732, Apr. 2012. Accessed: 8th Dec. 2016. [Online]. Available: http://www.nrel.gov/docs/fy12osti/53732.pdf

[36] J. Enslin, *Grid Impacts and Solutions of Renewables at High Penetration Levels.* [Online]. Available: https://quanta-technology.com/sites/default/files/doc-files/Grid-Impacts-and-Solutions-of-Renewables-Executive-Summary.pdf (accessed: Mar. 21 2016).

[37] J. E. Essilfie, J. Tlusty, and P. Santarius, "Using SVC to improve Voltage Stability of the Ghana Power Network," *Przegląd Elektrotechniczny (Electrotechnical Review)*, R. 89, nr 5, 033-2097, pp. 47–53, 2013. [Online]. Available: http://pe.org.pl/articles/2013/5/10.pdf

[38] Z. Fang, L. Zenghuang, and C. Liu, "Achievement and experience of improving power system stability by PSS/excitation control in China," in *2004 IEEE Power Engineering Society General Meeting*, Denver, CO, USA, 2004, pp. 1767–1771. Accessed: Apr. 29 2020. [Online]. Available: https://ieeexplore.ieee.org/stamp/stamp.jsp?tp=&arnumber=1373180

[39] W. Qiao, R. Harley, and G. Venayagamoorthy, "Effects of FACTS Devices on a Power System Which Includes a Large Wind Farm," in *2006 IEEE PES Power Systems Conference and Expositions, Atlanta, GA, USA*, pp. 2070–2076. Accessed: Apr. 12 2020. [Online]. Available: https://ieeexplore.ieee.org/stamp/stamp.jsp?tp=&arnumber=4076056

[40] S. Eftekharnejad, V. Vittal, Heydt, B. Keel, and J. Loehr, "Impact of increased penetration of photovoltaic generation on power systems," *IEEE Transactions on Power Systems*, vol. 28, no. 2, pp. 893–901, 2013, doi: 10.1109/TPWRS.2012.2216294.

[41] R. Toma and M. Gravilas, “The Impact on Voltage Stability of the Integration of Renewable Energy Sources into the Electricity Grid,” in *2014 International Conference and Exposition on Electrical and Power Engineering (EPE 2014)*.

[42] H. Pingping, D. Ming, and L. Binbin, “Study on transient stability of grid-connected large scale wind power system,” in *2010 2nd IEEE International Symposium on Power Electronics for Distributed Generation Systems*, Hefei, China, Jan. 2010, pp. 621–625. Accessed: Apr. 14 2020. [Online]. Available: https://ieeexplore.ieee.org/stamp/stamp.jsp?tp=&arnumber=5545847

[43] M. EL-Shimy, M.A.L. Badr, and O. M. Rassem, “Impact of large scale wind power on power system stability,” in *Power System Conference, 2008. MEPCON 2008, 12th International Middle-East*, Aswan, Egypt, 2008, pp. 630–636. Accessed: Apr. 21 2020. [Online]. Available: https://ieeexplore.ieee.org/stamp/stamp.jsp?tp=&arnumber=4562365

[44] P. G. Bueno, J. C. Hernández, and F. J. Ruiz-Rodriguez, “Stability assessment for transmission systems with large utility-scale photovoltaic units,” *IET Renewable Power Generation*, vol. 10, no. 5, pp. 584–597, 2016, doi: 10.1049/iet-rpg.2015.0331.

[45] R. Shah, N. Mithulananathan, R. Bansal, K. Y Lee, and A. Lomi, “Influence of Large-scale PV on Voltage Stability of Sub-transmission System,” *International Journal on Electrical Engineering and Informatics*, vol. 4, no. 1, pp. 148–161, 2012, doi: 10.15676/ijeei.2012.4.1.12.

[46] K. Akom, M. K. Joseph, and T. Shongwe, “Renewable Energy Sources and Grid Integration in Ghana: Issues, Challenges and Solutions,” in *2018 International Conference on Intelligent and Innovative Computing Applications (ICONIC)*, Plaine Magnien, Dec. 2018 - Dec. 2018, pp. 1–6.

[47] C. Kuamoah, “Renewable Energy Deployment in Ghana: The Hype, Hope and Reality,” *Insight on Africa*, vol. 12, no. 1, pp. 45–64, 2020, doi: 10.1177/0975087819898581.

[48] E. Mboumboue, M. M. Inoussah, and D. Njomo, “The Renewables" Development Constraints in Cameroon: Challenges and Future Prospects,” *International Journal of Science and Research (IJSR)*, vol. 10, no. 2, pp. 211–220, 2021. [Online]. Available: https://www.researchgate.net/publication/349108488_The_Renewables_Development_Constraints_in_Cameroon_Challenges_and_Future_Prospects

[49] I. D. Ibrahim *et al.,* “A review on Africa energy supply through renewable energy production: Nigeria, Cameroon, Ghana and South Africa as a case study,” *Energy Strategy Reviews*, vol. 38, p. 100740, 2021, doi: 10.1016/j.esr.2021.100740.

[50] Energy Commission of Ghana, "National Electricity Grid Code: Republic of Ghana," Oct. 2009.

[51] Tractebel Engineering GDF SVEZ, "Transmission System Master Plan for Ghana," GH-GRID/4NT/0195162/000/01, Feb. 2011.

[52] J. Machowski, J. W. Bialek, J. R. Bumby, *Power System Dynamics: Stability and Control*: John Wiley & Sons, Ltd.

[53] Ö. Usta, M. H. Musa, M. Bayrak, and M. A. Redfern, "A New Relaying Algorithm to Detect Loss of Excitation of Synchronous Generators," *Turkish Journal of Electrical Engineering*, vol. 15, no. 3, pp. 339–349, 2007. [Online]. Available: http://journals.tubitak.gov.tr/elektrik/issues/elk-07-15-3/elk-15-3-3-0610-2.pdf

[54] *IEEE Recommended Practice for Excitation System Models for Power System Stability Studies*, IEEE Std 421.5 - 2016, IEEE Standard Association, New York, USA.

[55] V. Jerkovic, K. Miklosevic, and Z. Spoljaric, "Excitation System Models of Synchronous Generator," in *28th International Conference Science in Practice.* Accessed: May 11 2020. [Online]. Available: https://bib.irb.hr/datoteka/475822.Final_paper_-_SiP2010_Jerkovic.pdf

[56] DIGSILENT GmbH, "DIgSILENT PowerFactory User Manual: Version 2016," DIGSILENT GmbH, Gomaringen, Germany r2648, Mar. 2016.

[57] *IEEE Recommended Practice for Excitation System Models for Power System Stability Studies*, IEEE Std 421.5-2005, IEEE, Apr. 2006.

[58] M. W. Asmah, "Comparison of the Behavior of the Different Voltage Control Systems for Synchronous Generators," Institute of Electrical Power Systems, Technical University of Darmstadt, Darmstadt, Germany 515, 09 March, 2014. Accessed: March 2014.

[59] G. Andersson, "Dynamics and Control of Electric Power Systems," Zurich, February, 2012.

[60] R. T. Byerly et al., "Dynamic Models for Steam and Hydro Turbines in Power System Studies: IEEE Committee Report," *IEEE Trans. on Power Apparatus and Syst.*, PAS-92, no. 6, pp. 1904–1915, 1973, doi: 10.1109/TPAS.1973.293570.

[61] Power System Dynamic Performance Committee and Power System Stability Subcommittee & Task Force on Turbine-Governor Modeling, "Dynamic Models for Turbine-Governors in Power System Studies," IEEE PES-TR1, Jan. 2013.

[62] P. Sorensen, B. Andresen, J. Fortmann & P. Pourbeik, Ed., *Modular structure of wind turbine models in IEC 61400-27-1*: IEEE, 2013.

[63] W. W. Price, J. J. Sanchez-Gasca, Ed., *Simplified wind turbine generator aerodynamic models for transient stability studies*: IEEE, 2006.

[64] M. Singh & S. Santoso, "Dynamic Models for Wind Turbines and Wind Power Plants," National Renewable Energy Laboratory (NREL), Golden, Colorado 80401 NREL/SR-5500-52780, Oct. 2011.

[65] T. Ackermann, Ed., *Wind power in power systems,* 2nd ed. Chichester: Wiley, 2012. [Online]. Available: http://site.ebrary.com/lib/alltitles/docDetail.action?docID=10560548

[66] M. Poeller and S. Achilles, "Aggregated Wind Park Models for Analysing Power System Dynamics," in *4th International Workshop on Large-Scale Integration of Wind Power and Transmission Networks for Offshore Wind Farms, Billund (Denmark), 20-21 Oct, 2003.* Accessed: May 1 2020. [Online]. Available: https://tarjomefa.com/wp-content/uploads/2017/04/6510-English-TarjomeFa.pdf

[67] J. J. Sanchez-Gasca, Ed., *Generic wind turbine generator models for WECC - a second status report*: IEEE, 2015.

[68] Australian Energy Market Operator, "Wind Turbine Plant Capabilities Report: 2013 Wind Integration Studies," Australian Energy Market Operator, AEMO ABN 94 072 010 327, 2013. Accessed: 09 August, 2017.

[69] P. Pourbeik et al, Ed., *Generic stability models for type 3 & 4 wind turbine generators for WECC*: IEEE, 2013.

[70] P. Sorensen et al., Ed., *Final Draft International Standard IEC 61400-27-1: Electrical simulation models of wind turbines*, 2014.

[71] P. Sorensen, B. Andresen, J. Fortmann, and P. Pourbeik, "Modular structure of wind turbine models in IEC 61400-27-1," in *Modular structure of wind turbine models in IEC 61400-27-1*, Vancouver, BC, 2013, pp. 1–5.

[72] Electric Power Research Institute, EPRI, "Specification of the Second Generation Generic Models for Wind Turbine Generators," Knoxville, TN, USA NFT-1-11342-01, 20th Sep. 2013. Accessed: 21st April, 2017.

[73] O. Goksu, M. Altin, J. Fortmann, and P. E. Sorensen, "Field Validation of IEC 61400-27-1 Wind Generation Type 3 Model With Plant Power Factor Controller," *IEEE Trans. Energy Convers.*, vol. 31, no. 3, pp. 1170–1178, 2016, doi: 10.1109/TEC.2016.2540006.

[74] M. J. Hossain, H. R. Pota, M. A. Mahmud, and R. A. Ramos, "Investigation of the Impacts of Large-Scale Wind Power Penetration on the Angle and Voltage Stability of Power Systems," *IEEE Systems Journal*, vol. 6, no. 1, pp. 76–84, 2012, doi: 10.1109/JSYST.2011.2162991.

[75] F. Wu, X.-P. Zhang, and P. Ju, “Impact of wind turbines on power system stability,” in *IREP Symposium Bulk Power System Dynamics and Control - VII: Revitalizing Operational Reliability, 2007: 19-24 Aug. 2007, Charleston, SC, USA*, Charleston, SC, USA, 2007, pp. 1–7. Accessed: Apr. 21 2020. [Online]. Available: https://ieeexplore.ieee.org/stamp/stamp.jsp?tp=&arnumber=4410535

[76] R. J. Konopinski, P. Vijayan, and V. Ajjarapu, “Extended Reactive Capability of DFIG Wind Parks for Enhanced System Performance,” *IEEE Trans. Power Syst.*, vol. 24, no. 3, pp. 1346–1355, 2009, doi: 10.1109/TPWRS.2009.2023260.

[77] J. G. Slootweg and W. L. Kling, “Aggregated modelling of wind parks in plower system dynamics simulations,” in *2003 IEEE Bologna PowerTech: Conference proceedings : June 23-26, 2003, Faculty of Engineering, University of Bologna, Bologna, Italy*, Bologna, Italy, 2004, pp. 626–631. Accessed: May 2 2020. [Online]. Available: https://ieeexplore.ieee.org/stamp/stamp.jsp?tp=&arnumber=1304458

[78] A. Ellis, “PV System Models for System Planning and Interconnection Studies,” Cedar Rapids, Iowa. Accessed: 24 May, 2016.

[79] Y. T. Tan, D. S. Kirschen, and N. Jenkins, “A Model of PV Generation Suitable for Stability Analysis,” *IEEE Trans. Energy Convers.*, vol. 19, no. 4, pp. 748–755, 2004, doi: 10.1109/TEC.2004.827707.

[80] L. Qu, D. Zhao, T. Shi, N. Chen, and J. Ding, “Photovoltaic Generation Model for Power System Transient Stability Analysis,” *IJCEE*, vol. 5, no. 3, pp. 297–300, 2013, doi: 10.7763/IJCEE.2013.V5.717.

[81] *Renewable Energy Sub-Code for NITS connected Variable Renewable Energy Power Plants in Ghana,* Energy Commission of Ghana, Accra, Ghana, Jan. 2015. [Online]. Available: http://www.energycom.gov.gh/files/Renewable%20Energy%20Code%20for%20the%20Transmission%20System,%202015.pdf

[82] H. W. K. M. Amarasekara, L. Meegahapola, A. P. Agalgaonkar, and S. Perera, “Impact of renewable power integration on VQ stability margin,” in *2013 Australasian Universities Power Engineering Conference (AUPEC)*, 2013, pp. 1–6. [Online]. Available: http://ieeexplore.ieee.org/stamp/stamp.jsp?arnumber=6725356

[83] S. Kabir, M. Nadarajah, and R. Bansal, “Impact of large scale photovoltaic system on static voltage stability in sub-transmission network,” in *2013 IEEE ECCE Asia Downunder*, 2013, pp. 468–473. [Online]. Available: http://ieeexplore.ieee.org/stamp/stamp.jsp?arnumber=6579138

[84] P. Lilienthal, "High Penetrations of Renewable Energy for Island Grids," in *Power Engineering.* Accessed: Jun. 3 2016. [Online]. Available: https://www.power-eng.com/2007/11/01/high-penetrations-of-renewable-energy-for-island-grids/

[85] Energy Commission of Ghana, Ghana Grid Company, Volta River Authority, Bui Power Authority, and Electricity Company of Ghana Ltd., "2017 Electricity Supply Plan for Ghana: An Outlook for the Power Supply Situation for 2017 and Highlights of Medium Term Power Requirements," Energy Commission of Ghana; Ghana Grid Company; Volta River Authority; Bui Power Authority; Electricity Company of Ghana Ltd., Accra, Ghana, 2017. Accessed: Dec. 14 2017. [Online]. Available: http://www.energycom.gov.gh/files/2017%20Electricity%20Supply%20Plan%20-%20Final%20Report.pdf

[86] IRENA - International Renewable Energy Agency, "Ghana Renewables Readiness Assessment," Nov. 2015. [Online]. Available: http://www.irena.org/DocumentDownloads/Publications/IRENA_RRA_Ghana_Nov_2015.pdf

[87] M. W. Asmah, R. Baisie, B. K. Ahunu, and J.M.A. Myrzik, Eds., *Assessment of the Steady State Voltage Stability of the Ghanaian Transmission System with the Integration of Renewable Energy Sources*, 2017.

[88] Energy Commission of Ghana, "National Renewable Energy Report," Accra, Ghana, Jan. 2005.

[89] Power Planet - Energy Management Systems, *Electrical Load Factor* (accessed: 15th May, 2018).

[90] Energy Commission of Ghana, "2016 Electricity Supply Plan for Ghana: An Outlook of the Power Supply Situation for 2016 and Highlights of Medium Term Power Requirements," Accra, Ghana, Feb. 2016.

[91] G. D. Rohini, B. Kantharaj, R. D. Satyanarayana Rao, "Transmission Line Contingency Analysis in Power system using Fast Decoupled Method for IEEE-14 bus Test system.," *IJISET - International Journal of Innovative Science, Engineering & Technology*, vol. 2, no. 4, pp. 991–994, 2015. [Online]. Available: http://ijiset.com/vol2/v2s4/IJISET_V2_I4_157.pdf

[92] J. J. Grainger & W. D. Stevenson, *Power System Analysis*. New York: McGraw-Hill, op. 1994.

[93] W. D. Stevenson [JR], *Elements of Power System Analysis,* 4th ed. Singapore: McGraw-Hill International Book Company, 1982.

[94] G. W. Stagg & A. El-ablad, *Computer Methods in Power System Analysis*. New York: McGraw-Hill Book Co, 1968.

[95] E. F. Dela Cruz et al., Ed., *Algorithm development for Power System Contingency screening and ranking using Voltage-Reactive Power Performance Index*: IEEE, 2016.

[96] S. Robak, J. Machowski, K. Gryspanowicz, Ed., *Contingency selection for power system stability analysis*: IEEE, 2017.

[97] Electric Power Research Institute, EPRI, "EPRI Power System Dynamics Tutorial," 1016042, Jul. 2009. Accessed: 5th December, 2014. [Online]. Available: https://www.epri.com/

[98] O. E. Oni, I. E. Davidson, and K. N. I. Mbangula, Eds., *Dynamic Voltage Stability Studies using a Modified IEEE 30-Bus System*. Piscataway, NJ: IEEE, 2016.

[99] I. Albizu, A. J. Mazon, and I. Zamora, "Methods for increasing the rating of overhead lines," pp. 1–6. [Online]. Available: http://ieeexplore.ieee.org/stamp/stamp.jsp?arnumber=4524481

[100] M. Ntuli, N. Mbuli, L. Motsoeneng, R. Xezile, and J. H. C. Pretorius, "Increasing the capacity of transmission lines via current uprating: An updated review of benefits, considerations and developments," in *2016 Australasian Universities Power Engineering Conference (AUPEC)*, 2016, pp. 1–6. [Online]. Available: http://ieeexplore.ieee.org/stamp/stamp.jsp?arnumber=7749338

[101] E. Mateescu, D. Marginean, G. Gheorghita, E. Dragan, I. A. St. Gal, and C. Matea, "Uprating a 220 kV double circuit transmission line in Romania; Study of the possible solutions, technical and economic comparison," in *2011 IEEE PES 12th International Conference on Transmission and Distribution Construction, Operation and Live-Line Maintenance (ESMO)*, 2011, pp. 1–7. [Online]. Available: http://ieeexplore.ieee.org/stamp/stamp.jsp?arnumber=5282152

[102] S. P. Hoffmann, A. M. Clarks, "The Approach to Thermal Uprating of Transmission Lines in the UK," in *Cigre Session 2004 B2-317.* [Online]. Available: https://e-cigre.org/publication/B2-317_2004-the-approach-to-thermal-uprating-of-transmission-lines-in-the-uk

[103] M. Reta-Hernandez, *Transmission Line Parameters.* [Online]. Available: https://www.unioviedo.es/pcasielles/uploads/proyectantes/cosas_lineas.pdf (accessed: 18th December, 2017).

[104] Eland Cables Ltd., *AAC, AAAC, ACSR Aluminium Conductors*.

[105] O. O. Obadina, G. J. Berg, "Identifying electrically weak and strong segments of a power system from a voltage stability viewpoint," *IEE Proceedings C - Generation, Transmission and Distribution*, vol. 137, no. 3,

pp. 202–217, 1990. [Online]. Available: https://ieeexplore.ieee.org/stamp/stamp.jsp?tp=&arnumber=48970

[106] Western Electricity Coordinating Council (WECC), "Guide to WECC/NERC Planning Standards I.D: Voltage Support and Reactive Power," Mar. 2006.

[107] N. A. M. Ismail, A. A. M. Zin, A. Khairuddin, and S. Khokhar, "A comparison of voltage stability indices," in *2014 IEEE 8th International Power Engineering and Optimization Conference (PEOCO2014)*, Langkawi, Malaysia, Mar. 2014 - Mar. 2014, pp. 30–34.

[108] C. Reis and F.P.M. Barbosa, "A Comparison of Voltage Stability Indices," in *MELECON 2006 - 2006 IEEE Mediterranean Electrotechnical Conference*, Benalmadena, Spain, May. 2006, pp. 1007–1010.

[109] J. Modarresi, E. Gholipour, and A. Khodabakhshian, "A comprehensive review of the voltage stability indices," *Renewable and Sustainable Energy Reviews*, vol. 63, pp. 1–12, 2016, doi: 10.1016/j.rser.2016.05.010.

[110] I. Musirin and T. K. Abdul Rahman, "Estimating Maximum Loadability for Weak Bus Identification Using FVSI," *IEEE Power Eng. Rev.*, vol. 22, no. 11, pp. 50–52, 2002, doi: 10.1109/MPER.2002.4311799.

[111] I. Musirin and T. K. Abdul Rahman, "Novel fast voltage stability index (FVSI) for voltage stability analysis in power transmission system," in *Student Conference on Research and Development*, Shah Alam, Malaysia, Jul. 2002, pp. 265–268.

[112] A. Mohamed, G. B. Jasmon, and S. Yusof, "A Static Voltage Collapse Indicator Using Line Stability Factors," *Journal of Industrial Technology*, vol. 7, no. 1, pp. 73–85, 1998. [Online]. Available: https://jit.sirim.my/Volume/Volume%207%20No.1%201998/a_static_voltage_collapse_indicator_using_line_stability_factors.pdf

[113] R. Kanimozhi and K. Selvi, "A Novel Line Stability Index for Voltage Stability Analysis and Contingency Ranking in Power System Using Fuzzy Based Load Flow," *Journal of Electrical Engineering and Technology*, vol. 8, no. 4, pp. 694–703, 2013, doi: 10.5370/JEET.2013.8.4.694.

[114] S. Burada, D. Joshi and K. D. Mistry, Ed., *Contingency Analysis of Power System by using Voltage and Active Power Performance Index*: IEEE Xplore, 2016.

[115] A. K. Roy, S. K. Jain, "Improved Transmission Line Contingency Analysis in Power System Using Fast Decoupled Load Flow," *International Journal of Advances in Engineering & Technology, IJAET*, vol. 6, no. 5, pp. 2159–2170, 2013. [Online]. Available: https://www.researchgate.net/profile/Amit_Roy/publication/258207126_Improved_Transmission_Line_

Contingency_Analysis_in_Power_System_using_Fast_Decoupled_Load_Flow/links/0c96052739097c69b9000000/Improved-Transmission-Line-Contingency-Analysis-in-Power-System-using-Fast-Decoupled-Load-Flow.pdf

[116] S. R. Gongada, T. Srinivasa Rao, P. Mallikarjuna Rao, and S. Salima, Eds., *Power system contingency ranking using fast decoupled load flow method*: IEEE, 2016.

[117] D. Matuszko, "Influence of the extent and genera of cloud cover on solar radiation intensity," *Int. J. Climatol.*, vol. 32, no. 15, pp. 2403–2414, 2012, doi: 10.1002/joc.2432.

[118] A. Bonkaney, S. Madougou, and R. Adamou, "Impacts of Cloud Cover and Dust on the Performance of Photovoltaic Module in Niamey," *Journal of Renewable Energy*, vol. 2017, pp. 1–8, 2017, doi: 10.1155/2017/9107502.

[119] Y. Abdellatif, A. Alsalaymeh, I. Muslih, and A. Alshduifat, "Cloud Effect on Power Generation of Grid Connected Small PV Systems," *World Academy of Science, Engineering and Technology, International Journal of Electrical, Computer, Energetic, Electronic and Communication Engineering*, vol. 9, no. 9, pp. 1054–1059, 2015.

[120] Suri M., Cebecauer T., Skoczek A., Meyer R., Marais R., Mushwana C., Reinecke J., Ed., *Cloud cover impact on photovoltaic power production in South Africa*, 2014.

[121] H. Breuning-Madsen and T. W. Awadzi, "Harmattan dust deposition and particle size in Ghana," *CATENA*, vol. 63, no. 1, pp. 23–38, 2005, doi: 10.1016/j.catena.2005.04.001.

[122] Konrad Mertens, *Photovoltaic: "Lehrbuch zu Grundlagen, Technologie und Praxis",* 3rd ed. Leipzig: Fachbuchverlag Leipzig im Carl Hanser Verlag, 2015.

[123] Volker Quaschning, *'Regenerative Energiesysteme' - Renewable Energy Systems: 'Technologie - Berechnung - Simulation',* 9th ed. Munich: Carl Hanser Verlag.

[124] J. Page, "The Role of Solar-Radiation Climatology in the Design of Photovoltaic Systems," in *McEvoy's Handbook of Photovoltaics*: Elsevier, 2018, pp. 601–670.

[125] National Renewable Energy Laboratory (NREL), "Shining On," National Renewable Energy Laboratory (NREL) NREL/TP-463-4856, May. 1992. Accessed: 12th March, 2008. [Online]. Available: file://H:/IE3_15022019/12%20Literature%20PhD%20Research/01%20Grundlagen/Solar%20Irradiaition%20-%20Diffuse%20Radiation.pdf

[126] P. Kundur et al., “Definition and Classification of Power System Stability IEEE/CIGRE Joint Task Force on Stability Terms and Definitions,” *IEEE Trans. Power Syst.*, vol. 19, no. 3, pp. 1387–1401, 2004, doi: 10.1109/TPWRS.2004.825981.

[127] IEEE Power & Energy Society, “Stability definitions and characterization of dynamic behavior in systems with high penetration of power electronic interfaced technologies,” IEEE, 2020.

[128] P. M. Anderson and A. A. Fouad, *Power System Control and Stability*. Hoboken: John Wiley & Sons, 2003.

[129] IEEE Power & Energy Society, “Voltage Stability Assessment: Concepts, Practices and Tools,” Institute for Electrical and Electronic Engineers, Inc. (IEEE) PES-TR9, Aug. 2002.

[130] A. C. Zambroni de Souza, F. W. Mohn, I. F. Borges, and T. R. Ocariz, “Using PV and QV curves with the meaning of static contingency screening and planning,” *Electric Power Systems Research*, vol. 81, no. 7, pp. 1491–1498, 2011, doi: 10.1016/j.epsr.2011.02.012.

[131] Western Electricity Coordinating Council (WECC), *Voltage Stability Criteria, Undervoltage Load Shedding Strategy and Reactive Power Reserve Monitoring Methodology*, 1998.

[132] B. Gao, G. K. Morison, and P. Kundur, “Towards the development of a systematic approach for voltage stability assessment of large-scale power systems,” *IEEE Trans. Power Syst.*, vol. 11, no. 3, pp. 1314–1324, 1996, doi: 10.1109/59.535672.

[133] P. Dey, A. Bhattacharya, and P. Das, “Tuning of power system stabilizer for small signal stability improvement of interconnected power system,” *Applied Computing and Informatics*, 2017, doi: 10.1016/j.aci.2017.12.004.

[134] S.-K. Wang, J.-P. Chiou, and C.-W. Liu, “Parameters tuning of power system stabilizers using improved ant direction hybrid differential evolution,” *International Journal of Electrical Power & Energy Systems*, vol. 31, no. 1, pp. 34–42, 2009, doi: 10.1016/j.ijepes.2008.10.003.

[135] K. R. Padiyar, *FACTS controllers in power transmission and distribution*. New Delhi: New Age International (P) Ltd., Publishers, 2007.

[136] M. P. Palsson, T. Toftevaag, K. Uhlen, and J.O.G. Tande, “Large-scale wind power integration and voltage stability limits in regional networks,” in *2002 Power Engineering Society summer meeting*, Chicago, IL, USA, Jul. 2002, pp. 762–769. Accessed: Apr. 17 2020. [Online]. Available: https://ieeexplore.ieee.org/stamp/stamp.jsp?tp=&arnumber=1043417

[137] DIGSILENT GmbH, *Technical Reference: Static Var Systems (SVS)*. Gomaringen, Germany, 2020.

[138] D. P. Kothari, I. J. Nagrath, *Modern Power System Analysis,* 3rd ed. New Delhi: Tata McGraw-Hill Pub. Co, 2003.

List of Abbreviations

Abbreviations

AC	Alternating Current
AO	Amplitude of Oscillation
AVR	Automatic Voltage Regulator
BPA	Bui Power Authority
BSP	Bulk Supply Point
CC	Combined Cycle
CIG	Converter-Interface-Generation
CCT	Critical Clearing Time
CPF	Continuous Power Flow
DC	Direct Current
DDSG	Direct-Driven Synchronous Generator
DEC	Discontinuous Excitation Control
DFIG	Doubly-Fed induction Generator
DFLR	Desensitized Four Loop Regulator
DG	Distributed Generation
DN	Distributed Network
DSM	Demand Side Management
EC	Energy Commission
ECG	Electricity Company of Ghana
ENTSO-E	European Network of Transmission System Operators
EPC	Enclave Power Company
ERC	Extended Reactive Capability
FACTS	Flexible AC Transmission System
FIT	Feed in Tarif
FVSI	Fast Voltage Stability Index
GDP	Gross Domestic Product

GridCo	Ghana Grid Company
GS	Generation Station
HFO	Heavy Fuel Oil
HRSG	Heat Recovery Steam Generator
HVDC	High-Voltage Direct Current
HVRT	High-Voltage Ride-Through
IEC	International Electrotechnical Commission
IEEE	Institute of Electrical/Electronic Engineering
IPP	Independent Power Producer
LCO	Light Crude Oil
LVRT	Low-Voltage Ride-Through
MoE	Ministry of Energy
MRSD	Maximum Rotor Speed Deviation
NEDCo	Northern Electricity Company
NITS	National Interconnected Transmission System
NVSI	New Voltage Stability Index
OD	Oscillation Duration
OPF	Optimum Power Flow
PCC	Point of Common Coupling
PID	Proportional-Integral-Derivative
PSS	Power System Stabilizer
PURC	Public Utility Regulatory Commission
PV	Photovoltaic
RCF	Rate of Change of Frequency
RE	Renewable Energy (Energies)
REPO	Renewable Energy Purchase Obligation
RMS	Root Mean Square
RPI	Reactive Power Injection
RPM	Reactive Power Margin

RSC	Rotor Side Converter
SG	Synchronous Generator
SLD	Single Line Diagram
SSSC	Static Synchronous Series Compensator
SSR	Sub-Synchronous Resonance
STATCOM	Static Synchronous Compensator
SVC	Static VAR Compensator
SVS	Static VAR System
S1	Scenario 1
S2	Scenario 2
S3	Scenario 3
TGR	Transient Gain Reduction
TSO	Transmission System Operator
UPF	Unity Power Factor
VALCO	Volta Aluminium Company
VDE	Verband der Elektrotechnik Elektronik Informationstechnik
VFC	Variable Frequency Converter
VRA	Volta River Authority
VRE	Variable Renewable Energy
VSC	Voltage Source Converter
VSI	Voltage Stability Index
WAPP	West African Power Pool
WFM	Wind Farm Management System
WTG	Wind Turbine Generator

List of Symbols

A	Line Ampacity (Thermal Limit or MVA Rating)
B_{ij}	Susceptance between Nodes *i* and *j*
$cos\Phi$, pf	Power Factor
D_{sh}	Damping Coefficient (Torsion Damping)
E'_d	Direct (*d*) Axis Transient Voltage
E'_q	Quadrature (*q*) Axis Transient Voltage
$E_{diff,hor}$	Diffuse Solar Irradiation (horizontal)
$E_{dir,hor}$	Direct Solar Irradiation (horizontal)
$E_{G,hor}$	Global Solar Irradiation (horizontal)
f	Frequency
G_{ij}	Conductance between nodes *i* and *j*
H	Global Horizontal Radiation
H	Inertia Constant
H_0	Extra-terrestrial Global Radiation
H_G	Generator Inertia Constant
H_T	Turbine Inertia Constant
I	Current
$I_{(hv)}$	Transformer Current (referred to the high voltage side)
I_0	Solar Constant
i_{ds}	*d* Axis Stator Current
I''_{kA}	Initial Short-circuit Current
i_{qs}	*q* Axis Stator Current
I_{rated}	Rated Current
J	Total Moment of Inertia of the Rotor Masses
K_G	Clearness Index
K_{sh}	Shaft Stiffness Coefficient (Torsion Stiffness)
L_m	Mutual Inductance

L_{QP}	Line Stability Factor
L_{rr}	Rotor Self-Inductance
M	Inertia Constant of the Machine
n	Number of Buses in the Network
N_L	Number of Transmission Lines in the Network
P	Active Power
P_a	Accelerating Power
P_e	Electrical Power
P_i	Active Power Flow in the Transmission Line
P_i^{max}	Maximum Active Power Flow in the Transmission Line
P_{IP}	Power Performance Index
P_{IV}	Voltage Performance Index
P_{MECH}, P_m	Mechanical Power
P_n	Rated Active Power
P_r	Receiving ending-end Active Power
P_s	Sending-end Active Power
Q	Reactive Power
Q_r	Receiving-end Reactive Power
Q_s	Sending-end Reactive Power
R	Resistance
S_k	Short-circuit Power
S''_{kN}	Initial Short-circuit Power
s_r	Rotor Slip
S_{rated}	Rated Ampacity
T'_0	Rotor Circuit Time Constant
T_a	Accelerating Torque
T_e	Electromechanical Torque
T_{EM}	Electromagnetic (electrical) Torque
t_f	Time of Fault Occurrence

T_m	Mechanical or Shaft Torque
t_{osc}	Oscillation Time
T_{sh}	Shaft Torque
T_{WM}	Wind Torque
U_n	Rated Voltage
V_{imax}	Voltage of the Measurement Transducer
V_{cmax}	Maximum Continuous Voltage
V_{cmin}	Minimum Continuous Voltage
v_{dr}	*d* Axis Rotor Voltage
V_i	Voltage Magnitude (Post-Contingency) of Bus *i*
V_{imax}	Maximum Limit of the Voltage at the *i*th bus
V_{imax}	Minimum Limit of the Voltage at the *i*th bus
V^i_{sp}	Specificed Voltage at the *i*th bus
V_j	Voltage Magnitude of Bus *j*
V_n	Rated Voltage
V_{PCC}	Voltage at PCC
v_{qr}	*q* Axis Rotor Voltage
V_{REF}	Reference Voltage
V_s	Sending-end Voltage
V_{SCL}	Voltage of the Stator Current Limiter
V_{ST}	Stabilizer Output Voltage
V_{UEL}	Voltage of the Underexcitation Limiter
V_{Wind}	Wind Speed
W	Weighting Factor
X	Line Reactance
X_s	Stator Reactance
X'_s	Stator Transient Reactance
Y	Admittance
Y_{ij}	Mutual Admittance between Two Nodes, *i* and *j*

Z	Line Impedance
z	Order of the Exponent (for the penalty function)
β	Blade Angle
ΔI_q	Change in Reactive Current
δ_m	Angular Displacment of the Rotor (from the synchronously rotating reference axis)
ΔV_t	Change in Terminal Voltage
θ_m	Rotor Angular Displacment (with respect to a reference axis which rotates at synchronous speed)
$\theta_{sh\ Tw}$	Shaft Twist (torsion) Angle
$\omega_{r,max}$	Maximum Rotor Speed the Generator
$\omega_{r,nom}$	Rated Rotor Speed the Generator
ω_s	Synchronous Angle Speed
ω_{sm}	Synchronous Speed of the Machine
ω_T	Turbine Angle speed
ω_{turb}	Rotational Speed
Φ_R	Generator Power Angle

Units

kA	Kiloamperes
km	Kilometers
kV	Kilovolts
MVA	Megavolt-amperes
MVAr	Megavars
MW	Megawatts
V	Volts

List of Figures

List of Tables

Appendix

A: Overview of the Locations and Sizes of Generating Units in the NITS

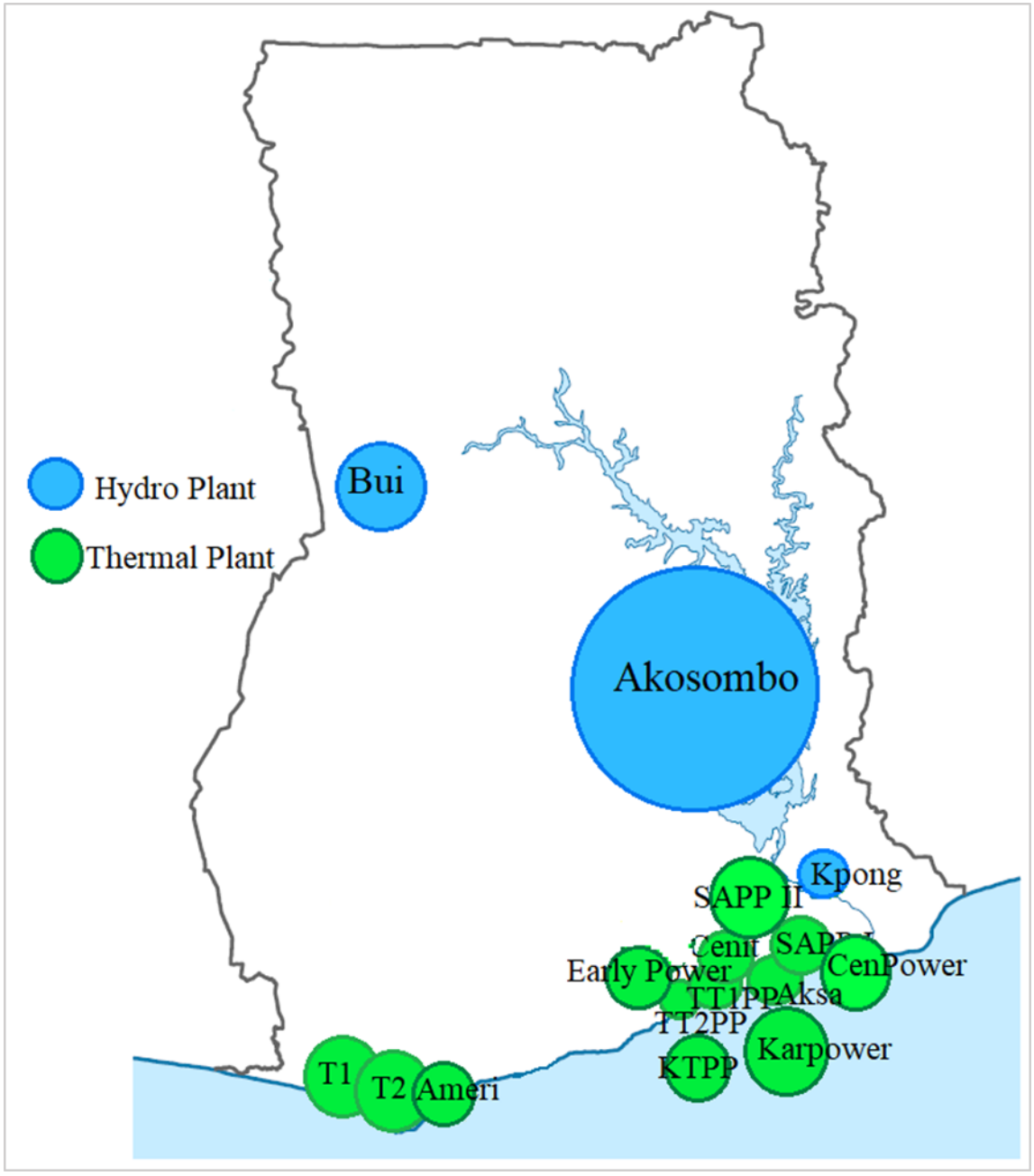

Figure 0 - 0-1: Overview of the Locations and Sizes of the Generating Units in the NITS

B: Synchronous Generator Parameters

Table 0-1: Sample Parameters of the Synchronous Generators used in the NITS Model

Parameter	*Sample Generator*	
	Salient Pole	*Round Rotor*
Nominal Power, S_n (MVA)	179.5	141.7
Power Factor, pf	0.95	0.85
Nominal Active Power, P_{nom} (MW)	170.525	120.4
Nominal Reactive Power, Q_{nom} (MVAr)	56.05	74.6
Maximum Reactive Power, Q_{max} (MVAr)	-	-
Minimum Reactive Power, Q_{min} (MVAr)	-	-
Nominal Voltage, U_n (kV)	14.4	13.8
Nominal Speed, N (tr/min)	115.4	3000
Moment of Inertia, PD2 (t/m^2)	173.4	
Inertia Constant, H (s)	2.97	7.78
Maximum Power, RGP_{max} (MW)	170.525	120
Short-Circuit Ratio, SCR	-	0.41
Unsaturated D-Axis Subtransient Reactance, X''_{du} (p.u.)	0.21	-
Saturated D-Axis Subtransient Reactance, X''_{di} (p.u.)	0.24	0.214
Unsaturated D-Axis Transient Reactance, X'_{du} (p.u.)	0.31	-
Saturated D-Axis Transient Reactance, X'_{d} (p.u.)	0.33	0.327
Unsaturated D-Axis Synchronous Reactance, X_{di} (p.u.)	1.26	-
Unsaturated Q-Axis Subtransient Reactance, X''_{qu} (p.u.)	0.35	2.426
Saturated Q-Axis Subtransient Reactance, X''_{qi} (p.u.)	0.32	0.212
Unsaturated Q-Axis Transient Reactance, X'_{q} (p.u.)	-	0.412
Saturated Q-Axis Synchronous Reactance, X_{qi} (p.u.)	0.76	2.344
Armature Resistance, R1 (p.u.)	-	0.005
Negative Sequence Resistance, R2 (p.u.)	-	0.018
Negative Sequence Reactance Saturated, X2v (p.u.)	0.29	0.159
Negative Sequence Reactance Unsaturated, X2i (p.u.)	0.29	0.205
Zero Sequence Reactance Saturated, Xov (p.u.)	0.096	0.104
D-Axis Subtransient Short Circuit Time Constant, T''_{do} (s)	0.036	0.015
D-Axis Subtransient Open Circuit Time Constant, T''_{d} (s)	0.048	0.022
D-Axis Transient Open Circuit Time Constant, T'_{do} (s)	6.64	7.642
D-Axis Transient Short Circuit Time Constant, T'_{d} (s)	1.66	-
Short Circuit Amarture Time Constant, T_a (s)	0.19	-

C: Generation Schedule for RE Contingency

Table 0-1: Generation Scheduling for RE Contingency – 15% PV + 100% Wind

Generating Unit	*Total Output (MW)*					
	S1		S2		S3	
Akosombo GS	520		520		520	
Kpong GS	80		120		120	
Takoradi Thermal	472.5		472.5		630	
Asogli 330	157.5		155		330	
Asogli	30.5		-		183.5	
Ameri	300		300		300	
Karpower	225		225		225	
CENIT	-		100		100	
Tema Thermal 1	-		100		100	
Collector	-		309		330	
KTPP	-		200		200	
Early Power	-		200		200	
TEI	-		-		100	
Aksa	-		-		80	
Total Conv. Generation	**1785.5**		**2701.5**		**3417.2**	
	Orig.	*15%*	*Orig*	*15%*	*Orig*	*15%*
GIC	20	3	50	7.5	50	7.5
Grn Ele	20	3	40	6	40	6
Sankana	20	3	50	7.5	100	15
Savanah	30	4.5	50	7.5	100	15
Signik	20	3	50	7.5	50	7.5
WhiteCap	20	3	50	7.5	100	15
Windiga	20	3	20	3	20	3
Ayitepa Solar	-	-	20	3	20	3
TFI Solar	-	-	-	-	30	4.5
Total Solar Generation	150	22.5	330	49.5	510	76.5
	Orig	*100%*	*Orig*	*100%*	*Orig*	*100%*
Ayitepa Wind	90	90	150	150	225	225
Ada Wind	-	-	50	50	50	50
Total Wind Generation	90	90	200	200	275	275
Total Generation		**1898**		**2951**		**3768.7**

Table 0-2: Generation Scheduling for RE Contingency – 15% PV + 0% Wind

Generating Unit	*Total Output (MW)*					
	Scenario 1		Scenario 2		Scenario 3	
Akosombo GS	520		520		520	
Kpong GS	80		120		120	
Takoradi Thermal	472.5		472.5		630	
Asogli 330	157.5		310		330	
Asogli	30.5		122.2		183.2	
Ameri	300		300		300	
Karpower	225		225		225	
CENIT	100		100		100	
Tema Thermal 1	-		100		100	
Collector	-		309		330	
KTPP	-		200		200	
Early Power	-		200		200	
TEI	-		-		100	
Aksa	-		-		370	
Total Conv. Generation	**1885.5**		**2978.7**		**3708.2**	
	Orig	*15%*	*Orig*	*15%*	*Orig*	*15%*
GIC	20	3	50	7.5	50	7.5
Grn Ele	20	3	40	6	40	6
Sankana	20	3	50	7.5	100	15
Savanah	30	4.5	50	7.5	100	15
Signik	20	3	50	7.5	50	7.5
WhiteCap	20	3	50	7.5	100	15
Windiga	20	3	20	3	20	3
Ayitepa Solar	-	-	20	3	20	3
TFI Solar	-	-	-	-	30	4.5
Total Solar Generation	150	22.5	330	49.5	510	76.5
	Orig	*0%*	*Orig*	*0%*	*Orig*	*0%*
Ayitepa Wind	90	0	150	0	225	0
Ada Wind	-	-	50	0	50	0
Total Wind Generation	90	0	200	0	275	0
Total Generation		**1908**		**3028.2**		**3784.7**

Table 0-3: Generation Scheduling for RE Contingency – 100% PV + 0% Wind

Generating Unit	*Total Output (MW)*					
	Scenario 1		Scenario 2		Scenario 3	
Akosombo GS	520		520		520	
Kpong GS	80		120		120	
Takoradi Thermal	472.5		472.5		472.5	
Asogli 330	157.5		310		330	
Asogli	-		-		183.2	
Ameri	300		300		300	
Karpower	225		225		225	
CENIT	-		100		100	
Tema Thermal 1	-		100		100	
Collector	-		309		330	
KTPP	-		200		200	
Early Power	-		-		200	
TEI	-		-		100	
Aksa	-		-		-	
Total Conv. Generation	**1755**		**2656.5**		**3180.7**	
	Orig	*100%*	*Orig*	*100%*	*Orig*	*100%*
GIC	20	20	50	50	50	50
Grn Ele	20	20	40	40	40	40
Sankana	20	20	50	50	100	100
Savanah	30	30	50	50	100	100
Signik	20	20	50	50	50	50
WhiteCap	20	20	50	50	100	100
Windiga	20	20	20	20	20	20
Ayitepa Solar	-	-	20	20	20	20
TFI Solar	-	-	-	-	30	30
Total Solar Generation	150	150	330	330	510	510
	Orig	*0%*	*Orig*	*0%*	*Orig*	*0%*
Ayitepa Wind	90	0	150	0	225	0
Ada Wind	-	-	50	0	50	0
Total Wind Generation	90	0	200	0	275	0
Total Generation		**1905**		**2986.5**		**3690.7**

D: Equipment Loading and Branch Flows - Contingency

Table 0-1: Equipment Loading in the Pre- and Post-Contingency States – 15% PV + 100% Wind

	Equipment Loading (%)					
Transmission Line	Scenario 1		Scenario 2		Scenario 3	
	Pre-Cont.	Post-Cont.	Pre-Cont.	Post-Cont.	Pre-Cont.	Post-Cont.
lne_1008_1009_1	74.78	83.35	N.A.[26]	N.A.	61.55	85.59
trf_1028_10281_1	N.A.	N.A.	N.A.	N.A.	7.72	85.88
lne_1002_1075_1	N.A.	N.A.	N.A.	N.A.	37.13	86.20
lne_1002_1075_2	N.A.	N.A.	N.A.	N.A.	37.13	86.20
trf_1043_10431_1	N.A.	N.A.	N.A.	N.A.	55.85	123.70
trf_1043_10431_2	N.A.	N.A.	N.A.	N.A.	55.85	123.70

Table 0-2: Branch Flows in the Pre- and Post-Contingency States – 15% PV + 100% Wind

	Branch (Active Power) Flow (MW)					
Transmission Line	Scenario 1		Scenario 2		Scenario 3	
	Pre-Cont.	Post-Cont.	Pre-Cont.	Post-Cont.	Pre-Cont.	Post-Cont.
lne_1008_1009_1	-109.28	-124.56	N.A.	N.A.	-114.63	-151.77
trf_1028_10281_1	N.A.	N.A.	N.A.	N.A.	0.00	0.00
lne_1002_1075_1	N.A.	N.A.	N.A.	N.A.	109.70	255.82
lne_1002_1075_2	N.A.	N.A.	N.A.	N.A.	109.70	255.82
trf_1043_10431_1	N.A.	N.A.	N.A.	N.A.	-28.10	-28.10
trf_1043_10431_2	N.A.	N.A.	N.A.	N.A.	-28.10	-28.10

Table 0-3: Equipment Loading in the Pre- and Post-Contingency States – 15% PV + 0% Wind

	Equipment Loading (%)					
Transmission Line	Scenario 1		Scenario 2		Scenario 3	
	Pre-Cont.	Post-Cont.	Pre-Cont.	Post-Cont.	Pre-Cont.	Post-Cont.
trf_1004_10471_1	92.50	93.15	N.A.	N.A.	N.A.	N.A.

[26] N.A.: Non-Applicable

trf_30101_30101_1	N.A.	N.A.	79.39	90.22	N.A.	N.A.
trf_1023_10231_1	N.A.	N.A.	49.93	98.73	N.A.	N.A.
lne_1001_1022_2	N.A.	N.A.	87.05	105.36	47.08	103.71
lne_1002_1075_1	N.A.	N.A.	N.A.	N.A.	37.13	85.48
lne_1002_1075_2	N.A.	N.A.	N.A.	N.A.	37.13	85.48
trf_1028_10281_1	N.A.	N.A.	N.A.	N.A.	7.72	85.93
lne_1014_1015_1	N.A.	N.A.	N.A.	N.A.	56.12	86.60
trf_1043_10431_1	N.A.	N.A.	N.A.	N.A.	55.85	122.92
trf_1043_10431_2	N.A.	N.A.	N.A.	N.A.	55.85	122.92

Table 0-4: Branch Flow in the Pre- and Post-Contingency States – 15% PV + 0% Wind

	Branch (Active Power) Flow (MW)					
Transmission Line	Scenario 1		Scenario 2		Scenario 3	
	Pre-Cont.	Post-Cont.	Pre-Cont.	Post-Cont.	Pre-Cont.	Post-Cont.
trf_1004_10471_1	100.00	100.00	N.A.	N.A.	N.A.	N.A.
trf_30101_30101_1	N.A.	N.A.	-103.48	-124.19	N.A.	N.A.
trf_1023_10231_1	N.A.	N.A.	-2.41	-2.41	N.A.	N.A.
lne_1001_1022_2	N.A.	N.A.	-98.42	-125.94	-60.10	-111.58
lne_1002_1075_1	N.A.	N.A.	N.A.	N.A.	109.70	255.84
lne_1002_1075_2	N.A.	N.A.	N.A.	N.A.	109.70	255.84
trf_1028_10281_1	N.A.	N.A.	N.A.	N.A.	0.00	0.00
lne_1014_1015_1	N.A.	N.A.	N.A.	N.A.	87.85	132.58
trf_1043_10431_1	N.A.	N.A.	N.A.	N.A.	-28.10	-28.10
trf_1043_10431_2	N.A.	N.A.	N.A.	N.A.	-28.10	-28.10

Table 0-5: Equipment Loading in the Pre- and Post-Contingency States – 0% PV +100% Wind

	Equipment Loading (%)					
Equipment	Scenario 1		Scenario 2		Scenario 3	
	Pre-Cont.	Post-Cont.	Pre-Cont.	Post-Cont.	Pre-Cont.	Post-Cont.
trf_30101_30101_1	N.A.	N.A.	79.39	89.94	N.A.	N.A.
lne_1001_1022_2	N.A.	N.A.	87.05	103.89	47.08	99.32

Table 0-6: Branch Flow in the Pre- and Post-Contingency States – 0% PV +100% Wind

Transmission Line	*Branch (Active Power) Flow (MW)*					
	Scenario 1		Scenario 2		Scenario 3	
	Pre-Cont.	Post-Cont.	Pre-Cont.	Post-Cont.	Pre-Cont.	Post-Cont.
trf_30101_30101_1	N.A.	N.A.	-103.48	-126.78	N.A.	N.A.
lne_1001_1022_2	N.A.	N.A.	-98.42	-123.13	-60.10	-108.06

E: Reactive Power Deficient Buses for All Scenarios

Table 0-1: Reactive Power Deficient Buses in the NITS - All Scenarios

Scenario 1 (S1)			
Simulation 1		*Simulation 2*	
Bus ID	*Size (MVAr)*	*Bus ID*	*Size (MVAr)*
1201	0.67	1003	24.52
1309	0.13	1007	5.45
1066	23.75	1309	5.08
1077	25.90	1042	0.61
1004	28.33	1004	28.03
Scenario 2 (S2)			
Simulation 1		*Simulation 2*	
Bus ID	*Size (MVAr)*	*Bus ID*	*Size (MVAr)*
1053	27.18	1056	16.40
1035	26.18	1029	24.21
1069	21.23	1053	21.03
1305	24.91	1035	27.77
1303	25.36	1051	9.15
Scenario 3 (S3)			
Simulation 1		*Simulation 2*	
Bus ID	*Size (MVAr)*	*Bus ID*	*Size (MVAr)*
111	12.957	27	0.46
105	1.84	125	27.10
125	24.72	167	1.47
41	25.49	102	27.82
37	5.88	46	2.28

Publications

[MWA 1] H. Zimmer, M. W. Asmah, J. Hanson, "Influence of Excitation Systems on the Dynamic Voltage Behavior of Power System" In *11th International Conference on Power System Transients*, Cavtat, Croatia, June, 2015

[MWA 2] M. W. Asmah, B. K. Ahunu, J. Myrzik, "Power System Expansion using Renewable Energy Sources in Ghana", In *50th Universities Power Engineering Conference (UPEC)*, Stoke-on-Trent, England, Sept., 2015

[MWA 3] M. W. Asmah, B. K. Ahunu, J. Myrzik, "Challenges in the Ghanaian power system: the prospects of renewable energy sources", In *12th IEEE AFRICON Conference*, Addis-Ababa, Ethiopia, Sept., 2015

[MWA 4] M. W. Asmah, B. K. Ahunu, R. Baisie, J. Myrzik, "Strengthening the Ghanaian Power System to Accommodate Variable Renewable Energies", In *IEEE PowerAfrica Conference*, Accra, Ghana, June, 2017

[MWA 5] J. Amanor-Boadu, M. W. Asmah, E. Sanchez-Sinencio, "A Universal Fast Battery Charging and Management Solution for Stand-alone Solar Photovoltaic Home Systems in Sub-Saharan Africa", In *IEEE PowerAfrica Conference*, Accra, Ghana, June, 2017

[MWA 6] M. W. Asmah, R. Baisie, B. K. Ahunu, J. Myrzik, "Assessment of the Steady State Voltage Stability of the Ghanaian Transmission System with the Integration of Renewable Energy Sources", In *12th International Conference on Power System Transients*, Seoul, South Korea, June, 2017

[MWA 7] Y. Zhou, C. Rehtanz, K. Sebaa, P. Luo, Y. Li, M. W. Asmah, "A Dynamic Corrective Control Method for Congestion Mitigation of Hybrid AC/DC Power Systems", In *International Journal of Electrical Power and Energy Systems, Volume 134, January 2022*

[MWA 8] D. O. Ampofo, A. Abdelsamad, M. W. Asmah, J. Myrzik, "A Strategy to Parameterize Q(U) Control to Enhance Voltage Stability using a Centralized Based Method", In *NEIS 2020; Conference on Sustainable Energy Supply and Energy Storage Systems, Hamburg, Germany, Sept., 2020*

[MWA 9] D. O. Ampofo, A. Abdelsamad, M. W. Asmah, J. Myrzik, “Adaptive Q(U) Control using combined Genetic Algorithm and Artificial Neural Network”, In *2020 IEEE Electric Power and Energy Conference (EPEC), Edmonton, Canada, Nov., 2020*

Supervised Master Thesis

[MT 1] A. Aajour „Dynamische Modellierung zur transienten Stabilitätsanalyse des Übertragungsnetzes von Ghana“, ie3-17.050, Master Thesis. Technische Universität Dortmund, Sept. 2017

[MT 2] P. Beckmann, „Voltage Control in the National Interconnected Transmission System (NITS) of Ghana “, ie3-18.024, Master Thesis. Technische Universität Dortmund, May 2018